



University of Cagliari

PhD DEGREE

Life, Environmental and Drug Sciences

Biomedical Curriculum

Cycle XXXIII

**BIOLOGICAL ACTIVITIES AND PHENOLIC
COMPOSITION OF *WASHINGTONIA FILIFERA* SEEDS**

Scientific Disciplinary Sector BIO/10

PhD Student:

Sonia Floris

Coordinator of the PhD Programme

Prof. Simona Distinto

Supervisor

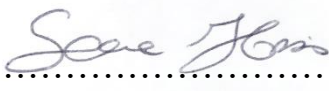
Prof. Antonella Fais

Final exam. Academic Year 2019 – 2020

Thesis defence: April 2021 Session

Declaration

I declare that this thesis represents my own work, except where due acknowledgement is made, and that it has not been previously included in a thesis, dissertation or report submitted to this University or to any other institution for a degree, diploma or other qualifications.

Signed 

Sonia Floris

TABLE OF CONTENTS

<i>Declaration</i>	2
<i>Acknowledgements</i>	7
<i>Abstract</i>	8
<i>List of publications</i>	9
<i>Articles</i>	9
<i>Conference paper</i>	10
<i>List of abbreviations</i>	12
CHAPTER 1: Introduction	15
1.1 Natural bioactive compounds	15
1.1.1 Antioxidants	17
1.1.2 Polyphenols	23
1.2 Alzheimer's disease	29
1.3 Diabetes mellitus	33
1.4 Enzyme inhibition	35
1.4.1 Competitive inhibition	36
1.4.2 Mixed and non-competitive inhibition	36
1.4.3 Uncompetitive inhibition	37

1.4.4 Graphic determination of inhibition type	37
1.5 <i>Washingtonia filifera</i>	42
1.6 Objective of this thesis	44
CHAPTER 2: Material and Methods	46
2.1 Chemicals	46
2.2 Plant material	46
2.3 Fatty acid analysis of <i>n</i> -hexane extracts	47
2.4 Total polyphenols content	49
2.5 Total flavonoids content	49
2.6 HPLC–DAD–ESI/MS analyses	50
2.7 UHPLC-ESI-QqTOF-MS analyses	51
2.8 Biological activities	52
2.8.1 ABTS ^{•+} radical scavenging activity	52
2.8.2 Xanthine oxidase assay	53
2.8.3 Tyrosinase assay	54
2.8.4 Elastase assay	54
2.8.5 Collagenase assay	55
2.8.6 <i>In Vitro</i> Determination of Sun Protection Factor	55

2.8.7 Cholinesterase assays	56
2.8.8 α -Amylase assay	57
2.8.9 α -Glucosidase assay	57
2.8.10 ThT binding assay	59
2.8.11 Congo red stain	60
2.8.12 Negative stain	60
2.9 Cell culture	61
2.9.1 Cell viability	61
2.9.2 Intracellular ROS levels	62
2.10 Data analysis	62
2.11 Molecular docking	63
CHAPTER 3: Results and Discussion	65
3.1 Fatty acid analysis of <i>n</i> -hexane extracts	65
3.2 Total polyphenols, total flavonoids content and antioxidant activity	68
3.3 HPLC/UHPLC–DAD–ESI/MS analyses	71
3.4 Biological Activities	75
3.4.1 Xanthine oxidase inhibition	75
3.4.2 Tyrosinase, elastase and collagenase inhibition	79

3.4.3 Sun Protection Factor	87
3.4.4 Cholinesterase inhibition	88
3.4.5 α -Amylase and α -Glucosidase inhibition	90
3.4.6 Inhibition of IAPP aggregate formation	99
3.4.7 Cell viability and intracellular ROS level	102
3.5 Molecular docking	104
CHAPTER 4: Conclusions	112
References	114

Acknowledgements

This thesis was supported by the following people, who provided insight and expertise that greatly assisted the research. My sincere thanks go to all of them.



UNIVERSITY
OF CAGLIARI

Prof. Antonella Fais
Prof. Rosaria Medda
Dr. Francesca Pintus
Dr. Benedetta Era
Dr. Amit Kumar
Dr. Alessandra Piras
Prof. Valeria Sogos
Dr. Antonella Rosa



Dr. Piotr Kuś



Prof. Celestino Santos-Buelga
Prof. Ana M. González-Paramás



Prof. Gunilla T. Westermark
Xiaohong Gu



Dr. Marzouki Hanene

Abstract

Plant materials represent a great source of antioxidant and bioactive compounds which are different in their chemical composition and biological properties. There has been a remarkable increment on research of antioxidant molecules because of their protective action against oxidative stress. It causes serious cell and tissue damage leading it to be the major cause of aging process and the pathogenesis of several diseases like diabetes and neurodegenerative diseases. The chemical composition and the biological properties of fruits of the palm *Washingtonia filifera* (Lindl.) H.Wendl. is poorly studied. Therefore, the aim of this thesis was to investigate the potential bioactivity of *W. filifera* fruit extracts and relate them with the phenolic profile. The phenolic composition, antioxidant capacity and the inhibitory activity on different enzymes implicate in several disease were evaluated. In particular, *W. filifera* seed extracts appeared to be a good source of phenolics and showed a significant antioxidant activity. The phenolic composition mainly consisted of procyanidin dimers B1–B4. Alcoholic seed extracts displayed interesting xanthine oxidase, butyrylcholinesterase, elastase, collagenase, α -amylase and α -glucosidase inhibitory activity. Docking studies were also performed to predict the binding sites of the main compounds identified within enzymes structure. All in all, *W. filifera* seeds appear as a promising natural source for the purification of bioactive compounds with antioxidant and biological properties.

List of Publications

Articles

1. B. Era[#], **S. Floris**[#], V. Sogos, C. Porcedda, A. Piras, R. Medda, A. Fais, F. Pintus. Anti-aging potential of extracts from *Washingtonia filifera* seeds. [#]Co-authorship. *Plants* 2021 Jan; 10(1):151. doi: 10.3390/plants10010151.
2. **S. Floris**, A. Fais, R. Medda, F. Pintus, A. Piras, A. Kumar, P. M. Kuś, G. T. Westermark, B. Era. *Washingtonia filifera* seed extracts inhibit the islet amyloid polypeptide fibrils formations and α -amylase and α -glucosidase activity. *J. Enzyme Inhib. Med. Chem.* 2021. Vol. 36, No. 1, 517–524. doi.org/10.1080/14756366.2021.1874945.
3. G. L. Delogu, B. Era, **S. Floris**, R. Medda, V. Sogos, F. Pintus, G. Gatto, A. Kumar, G.T. Westermark, A. Fais. A new biological prospective for the 2-phenylbenzofurans as inhibitors of α -glucosidase and of the islet amyloid polypeptide formation. *Int. J. Biol. Macromol.* Vol. 169, 1 February 2021, Pages 428-435, doi.org/10.1016/j.ijbiomac.2020.12.117.
4. S. Vittorio, L. Ielo, S. Mirabile, R. Gitto, A. Fais, **S. Floris**, A. Rapisarda, M. P. Germanò, L. De Luca. 4-(Fluorobenzyl)piperazine-Containing Derivatives as Efficient Inhibitors of Mushroom Tyrosinase. *Chem. Med. Chem.* 2020, 15, 1757–1764, doi.org/10.1002/cmdc.202000125.
5. L. Ielo, B. Deri, M. P. Germanò, S. Vittorio, S. Mirabile, R. Gitto, A. Rapisarda, S. Ronsisvalle, **S. Floris**, Y. Pazy, A. Fais, A. Fishman, De Luca. Exploiting the 1-(4-fluorobenzyl)piperazine fragment for the

- development of novel tyrosinase inhibitors as anti-melanogenic agents: design, synthesis, structural insights and biological profile. *Eur. J. Med. Chem.* 2019 Sep 15;178:380-389, doi:10.1016/j.ejmech. 2019.06.019. Epub 2019 Jun 6.
6. **S. Floris**, A. Fais, A. Rosa, A. Piras, H. Marzouki, R. Medda, A. M. González-Paramás, A. Kumar, C. Santos-Buelga, B. Era. Phytochemical composition, cholinesterase and xanthine oxidase inhibitory properties of seed extracts from *Washingtonia filifera* palm fruit. *RSC Adv.*, 2019, 9, 21278 – 21287, doi: 10.1039/c9ra02928a.
 7. A. Fais, B. Era, A. Di Petrillo, **S. Floris**, D. Piano, P. Montoro, C. I. G. Tuberoso, R. Medda, F. Pintus. Selected enzyme inhibitory effects of *Euphorbia characias* extracts *Res. Int.* 2018, 1–11, 2018, doi: 10.1155/2018/1219367.

Conference paper

1. B. Era, **S. Floris**, S. Porcedda, H. Marzouki, F. Pintus, R. Medda, A. Piras, A. Fais. Inhibitory effect of *Washingtonia filifera* extracts on cholinesterase activities. XVI Congress of the Italian Society of Phytochemistry jointly with 2nd International Congress on Edible, Medicinal and Aromatic Plants (ICEMAP 2019), 19 – 21 Giugno 2019.
2. B. Era, A. Fais, A. Rosa, R. Medda, H. Marzouki, A. Piras, A. Kumar, C. Santos-Buelga, **S. Floris**. Evaluation of biological activities and chemical composition of *Washingtonia filifera* seeds. XVI Congress of the Italian Society of Phytochemistry jointly with 2nd International

- Congress on Edible, Medicinal and Aromatic Plants (ICEMAP 2019), 19 – 21 Giugno 2019.
3. S. Mirabile, S. Vittorio, M. P. Germano, R. Gitto, A. Rapisarda, **S. Floris**, A. Fais, A. Fishman, L. De Luca. Exploiting The 1-(4-fluorobenzyl)piperazine fragment for the development of novel tyrosinase inhibitors. Società Chimica Italiana, Congresso Congiunto delle Sezioni Sicilia e Calabria 2019, Palermo, 1 - 2 marzo 2019.
 4. B. Era, **S. Floris**, S. Porcedda, H. Marzouki, R. Medda, A. Piras, A. Fais. Inhibition of α -Amylase and α -Glucosidase by *Washingtonia filifera* Extracts. 7th International Congress on Medicinal and Aromatic Plants., Toulouse, France, 25 – 28 June 2018.
 5. **S. Floris**, A. Piras, C. Santos-Buelga, R. Medda, A. Fais, B. Era. Inhibitory activity of *Washingtonia filifera* extracts. 30° Edizione Riunione Nazionale “A.Castellani” dei Dottorandi di Ricerca in Discipline Biochimiche Brallo, 4 – 8 Giugno 2018.
 6. R. Medda, D. Piano, **S. Floris**, C. De Sousa Mota, D. De Sanctis, F. Pintus. Crystallization of *Euphorbia characias* latex peroxidase. 59° Congresso della Società Italiana di Biochimica e Biologia Molecolare (SIB), Caserta, 20 – 22 Settembre 2017.
 7. A. Fais, G. L. Delogu, B. Era, A. Di Petrillo, A. Kumar, P. Caria, **S. Floris**, F. Pintus. Butyrylcholinesterase Inhibitors: Structure-Activity Relationships of 2-phenylbenzofuran derivatives. 59° Congresso della Società Italiana di Biochimica e Biologia Molecolare (SIB), Caserta, 20 – 22 Settembre 2017.

List of Abbreviations

ABTS: 2,2'-Azinobis-(3-Ethylbenzothiazoline-6-Sulfonic Acid)

ACh: acetylcholine

AChE: acetylcholinesterase

AD: Alzheimer's disease

AE: aqueous extract

APP: amyloid precursor protein

ATCI: acetylthiocholine iodide

A β : amyloid-beta

BChE: butyrylcholinesterase

BTCl: S-butyrylthiocholine iodide

CAT: catalase

ChEs: cholinesterases

CNPG3: 2-chloro-4-nitrophenyl- α -D-maltotrioside

DCFH-DA: 2',7'-dichlorofluorescein diacetate

DMEM: Dulbecco's Modified Eagle's Medium

DMSO: dimethyl sulfoxide

DTNB: 5,5'-dithiobis-(2-nitrobenzoic acid)

dw: dry weight

ECM: extracellular matrix

EE: ethanol extract

EGCG: epigallocatechin gallate

FALGPA: N-(3-[2-Furyl]-acryloyl)-Leu-Gly-Pro-Ala

FAME: fatty acid methyl esters

FBS: fetal bovine serum

FID: flame ionisation detector

G: Gabés

GAE: gallic acid equivalents

GPx: glutathione peroxidase

HaCaT: Human skin keratinocyte cell line

HE: hexane extract

HFIP: hexafluorisopropanol

HPLC-DAD: liquid chromatograph with a diode array detector

IAPP: islet amyloid polypeptide

L-DOPA: 3,4-dihydroxyphenylalanine

ME: methanol extract

MS: mass spectrometer

MTT: 3-(4,5-dimethylthiazol-2-yl)- 2,5-diphenyltetrazolium bromide

MUFA: monounsaturated fatty acid

pNPG: α -D-glucopyranoside

PUFA: polyunsaturated fatty acid

QE: quercetin equivalents

ROS: reactive oxygen species

S: Sousse

SANA: N-succinyl-(Ala)³-nitroanilide

SD: standard deviation

SOD: superoxide dismutase

T2D: type 2 diabetes mellitus

TEM: Transmission Electron Microscopy

ThT: thioflavin-T

UFA: unsaturated fatty acid

XO: xanthine oxidase

1. INTRODUCTION

1.1 Natural bioactive compounds

Plants have been widely used as food and medicine, since they provide, not only essential nutrients required for human life, but also bioactive compounds and their derivatives, called secondary metabolites. Secondary plant metabolites are numerous chemical compounds produced by the plant cell through metabolic pathways (Hussein and El-Anssary, 2018). They are commonly known as phytochemicals, which play important roles in health promotion and disease prevention. In view of this, nature is a valuable reservoir of novel bioactive compounds. A compound having some biological activity in living organisms is considered bioactive (Mushtaq et al., 2018). Therefore, it can be defined as a substance which could have the ability to interact with one or more component(s) of the living tissue by presenting a wide range of effects (Guaadaoui et al., 2014).

Secondary metabolites have shown to possess various biological effects, which provide the scientific base for the use of plants in the traditional medicine. Plant-based systems continue to play an essential role in healthcare, in fact, according to an estimate, about 67% of the medications validated from 1981-2014 have natural origins (Chang et al., 2019). Many drugs that are available in market today were discovered from natural sources. An important example is the analgesic activity of aspirin, which is so far the world's best known and most universally used medicinal

agent. It originates from the plant genera *Salix* spp. and *Populus* spp. and it is related to salicin. Another good example is serendipitous discovery of the antibiotic penicillin in the laboratory from the fungus *Penicillium notatum* (Koparde et al., 2019).

Inspired by the discoveries of penicillin, resveratrol, lovastatin and many other natural products, researchers worldwide continuously devote effort to find natural bioactive compounds by different sources. In the recent years, researchers have been attempting to better valorise flora as a natural source of bioactive products since they provide unlimited opportunities for new drug discoveries because of the unmatched availability of chemical diversity (Cos et al., 2006).

Moreover, the impact of lifestyle and dietary choices for human health has increased the interest in fruits and vegetables, as well as in foods enriched with bioactive compounds and nutraceuticals. In fact, epidemiological studies have consistently shown that a diet characterized by the daily consumption of fruits and vegetables, is strongly associated with reduced risk of developing a wide range of chronic diseases, such as diabetes, neurodegenerative and cardiovascular diseases (Boeing et al, 2012). The health benefits are attributed to the additive and synergistic interaction between phytochemicals (Liu, 2003).

There is a huge list of medicinal plants reported to have extensive health potentials. One of the most beneficial effects from these natural sources is due to their antioxidant properties. Researchers have focused their studies to explore the most potential sources along with their active components.

The major ingredients from the natural sources are polyphenolic compounds, which are reported to have a high degree of antioxidant activity (Anwar et al., 2018).

1.1.1 Antioxidants

One of the most beneficial effects from natural sources is due to their potential antioxidant properties. Antioxidants are substances that may protect cells against reactive oxygen species (ROS) that are free radicals formed as products under normal physiological conditions due to the partial reduction of molecular oxygen. ROS namely superoxide anion (O_2^-), hydroxyl radical (OH^\bullet) and hydrogen peroxide (H_2O_2), arise in many ways, as a product of the respiratory chain in mitochondria, in photochemical and enzymatic reactions, as a result of the exposure to UV light, ionizing radiation, or heavy metal ions. Superoxide is generated directly from the reduction of oxygen and then dismutated to hydrogen peroxide. Hydrogen peroxide is a molecule with low reactivity, but it can readily penetrate cell membranes and generate the most reactive form of oxygen, the hydroxyl radical (Nita and Grzybowski, 2016). Low levels of ROS production are required to maintain physiological functions, including proliferation, host defence, signal transduction, and gene expression. However, the formation of ROS, as a result of oxidative processes taking place in human organism, could be precursor of systemic cells and tissues damage. Free radical contains one or more unpaired electrons in valency shell or outer orbit and it is capable of independent

existence. Thus, the biomolecule involved in this reaction, loses its electron and becomes a free radical itself, beginning a chain reaction cascade which finally damages the living cell. The concentration of free radicals is determined by the balance between their rates of production and their rates of clearance by various antioxidant compounds and enzymes. It is well known that free radicals and ROS, play a major role in the development of oxidative stress that can lead to many illnesses, including Type 2 Diabetes Mellitus (T2D), inflammation, and Alzheimer's diseases (AD) (Phaniendra et al., 2015). Thus, therapies based on antioxidants can be an effective approach in preventing or treating many diseases (Rani, 2017).

Antioxidants can be divided in enzymatic and non-enzymatic (Figure 1) (Shalaby and Shanab, 2013). Non-enzymatic antioxidants include vitamins such as A, E, C, as well as enzyme cofactors (Q10), peptides, some minerals (zinc and selenium) and the group of polyphenols. Enzymatic antioxidants primarily include glutathione peroxidase (GPx), catalase (CAT), and superoxide dismutase (SOD) (Anwar et al., 2018).

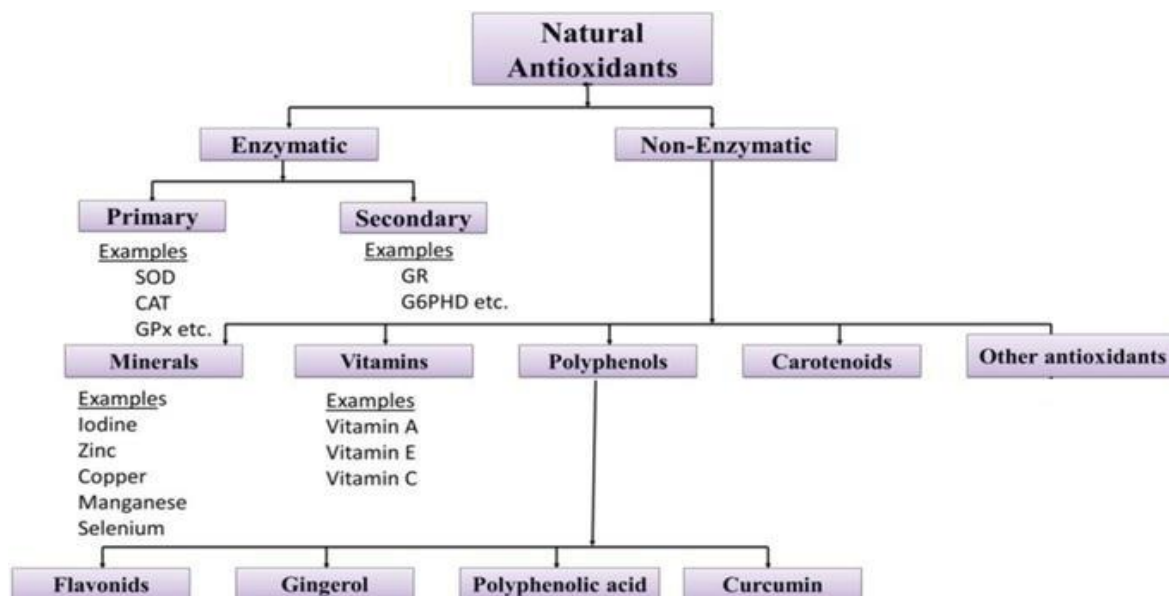


Figure 1. Classification and subclassification of antioxidants found in natural sources. (Anwar et al., 2018).

An important enzyme that has been reported to proliferate during oxidative stress is xanthine oxidase (XO, EC 1.17.3.2, Figure 2), which catalyses the oxidation of hypoxanthine to xanthine and xanthine to uric acid. In both steps, molecular oxygen is reduced, forming the superoxide anion, followed by the generation of hydrogen peroxide.

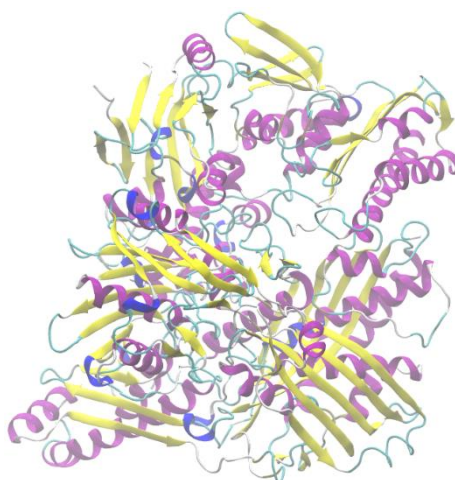


Figure 2. 3D structure of XO.

Overproduction or reduced excretion of uric acid leads to abnormal amounts of uric acid in the body, causing hyperuricemia and gout (Emmerson, 1996). Therefore, compounds that can inhibit XO may reduce both the circulating levels of uric acid and the production of ROS. Allopurinol is a clinically useful XO inhibitor used in the treatment of gout. It is a substrate for XO, which converts it to oxypurinol, which in turn inhibits XO (Burns and Wortmann, 2012). However, allopurinol has serious side effects; thus, new alternatives with increased therapeutic activity and lesser side effects are desired. Several phenolics and flavonoids from natural origin have been described as inhibitors of the XO enzyme, such as ferulic acid, gallic acid, caffeic acid and *p*-coumaric acid (Nile et al., 2016).

Moreover, oxidative stress is associated with photo-induced skin aging since exposure to solar UV radiation represents one of the most significant external stress-inducing factors. One of the main characteristics of skin aging is the loss of structure of the extracellular matrix (ECM) which comprises numerous proteins (Lu et al., 2011). Eighty percent of skin is composed by collagen which is the protein responsible for the tensile strength of the skin, while elasticity is due to the elastin fibre network making up two–four percent of the ECM. Collagen and elastin fibres are produced by fibroblasts and are primarily affected by photoaging resulting in visible changes in the skin such as wrinkles, pigmentation and changes in thickness. ROS induced by UV irradiation can initiate complex molecular pathways including the activation of enzymes that degrade

ECM that is characterized by proteins in the dermis altering skin integrity (Madan and Nanda, 2018). Elastase (EC 3.4.21.36) is a proteolytic enzyme involved in the physiological degradation of elastin, the ECM protein responsible for skin elasticity. An increased elastase activity has been found in several diseases as for instance psoriasis, dermatitis, inflammatory processes and premature skin aging. Collagenase (EC 3.4.24.3) belongs to the family of matrix metalloproteinases and it can degrade the triple-helical region of collagen under physiological conditions providing structural support for bones, tendons, ligaments and blood vessels.

A physiological process which plays a crucial role in preventing UV-induced skin damage by absorbing UV sunlight is the synthesis of melanin pigments. However, excess production or abnormal accumulation of melanin, causes skin problems such as the typical age spots that are the major changes associated with aging. They are directly associated with uneven pigmentation due to the activity of another aging-related enzyme named tyrosinase. Tyrosinase (EC 1.14.18.1) is the rate-limiting enzyme in the metabolism of melanin. It catalyzes the hydroxylation of L-tyrosine to 3,4-dihydroxyphenylalanine (L-DOPA) and the following oxidation of L-DOPA to dopaquinone. Oxidative polymerization of dopaquinone derivatives gives rise to melanin (Slominski et al., 2012).

Thus, inhibitors of all the enzymes described above, represent increasingly important ingredients in cosmetics and medications to

prevent skin aging (Thi Be Tu and Tawata, 2015). The inhibition of these enzymatic activities by natural plant compounds might be a promising approach to prevent skin aging. In view of this, epigallocatechin gallate (EGCG) has been shown to stabilize collagen and protect the chains from collagenase degradation (Jackson et al., 2010), while, pentacyclic triterpenes, such as oleanolic acid, seems to be good inhibitors of elastase (Feng et al., 2013).

Many reports on the potential effectiveness of phenolic compounds in the prevention or attenuation of skin disorders have been published. In fact, they reveal to possess inhibitory activity against collagenase and elastase, such as gallic acid (Wittenauer et al., 2015).

The most intensively studied inhibitor of tyrosinase is kojic acid, a fungal metabolite currently used as a cosmetic skin-whitening agent and as a food additive for preventing enzymatic browning (Chang, 2009). In fact, tyrosinase is also responsible for browning in fruits and vegetables, and thus, inhibitors of this enzyme are frequently applied to plant-based foods. However, concerns over the toxicity and side effects of kojic acid have led to a search for new safe and effective tyrosinase inhibitors. The largest category of phytochemicals that act as potent tyrosinase inhibitors belongs to the group of phenolic compounds. In particular, some flavonoids from plant origin, such as kaempferol, quercetin, and morin, show good inhibitory activity against tyrosinase (Gonçalves and Romano, 2017).

Owing to their wide range of biological effects, plant phenolic compounds are one of the most studied families of natural products.

1.1.2 Polyphenols

Plant polyphenols are divided into two major groups: flavonoids and non-flavonoids.

Non-flavonoids include phenolic acids, tannins, stilbenes and lignans (Figure 3).

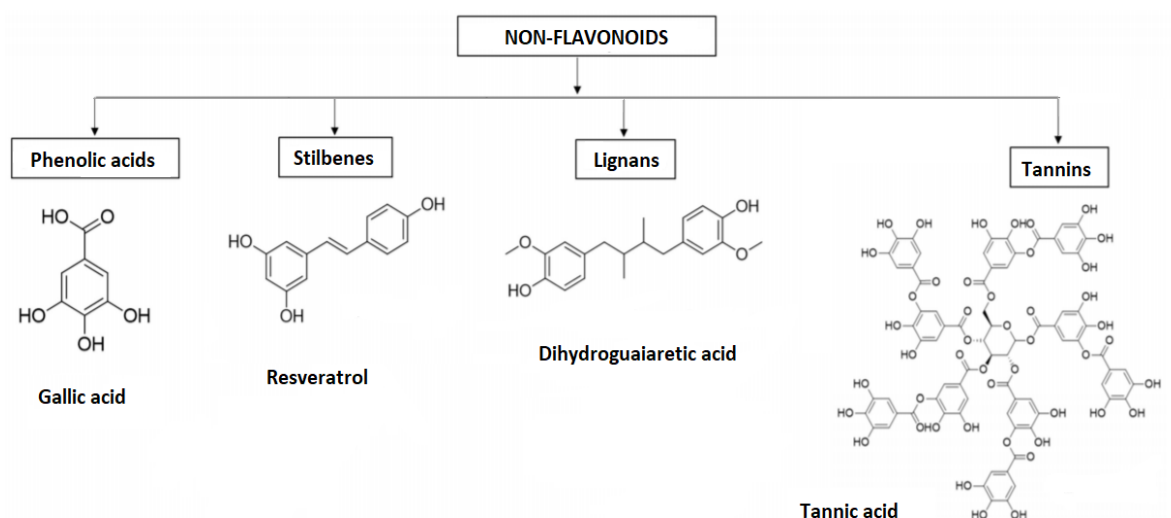


Figure 3. Non-flavonoids classification.

Phenolic acids, such as gallic acid, are found in seeds of different plants, skins of fruits and leaves of vegetables, typically present as amides, esters, or glycosides and rarely in free form. Phenolic acids possess much higher in vitro antioxidant activity than well-known antioxidant vitamins (Kumar and Goel, 2019). Tannins are water-soluble phenolic compounds

with high molecular weights, usually found commonly in the bark of trees, wood, leaves, buds, stems, fruits, seeds, roots, and plant galls. Stilbenes contain two phenyl moieties connected by a two-carbon methylene bridge. The most extensively studied stilbene is resveratrol that is known to be produced by several plant species such as vine plant, peanut and berries. Lignans, such as dihydroguaiaretic acid, are phytoestrogens present in seeds, vegetable oils, cereals, legumes, fruits and vegetables as aglycones, glycosides, esterified glycosides or as bio-oligomers (De Lacerda De Oliveira et al., 2014).

Flavonoids are the major class of the secondary metabolites widely distributed throughout the plant kingdom and are commonly found in fruits, vegetables and certain beverages. Chemically flavonoids are based upon a fifteen-carbon skeleton consisting of two benzene rings (A and B as shown in Figure 4) linked via a heterocyclic pyran ring (C).

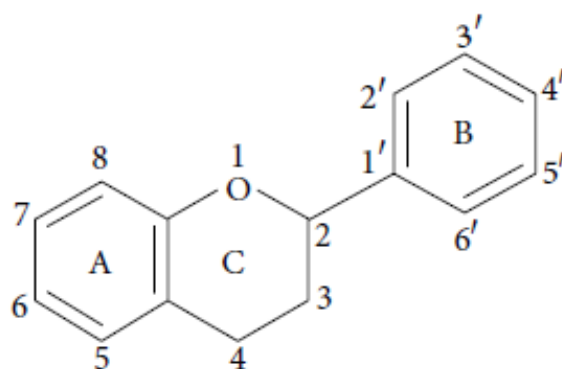


Figure 4. Basic flavonoid structure (Kumar and Pandey, 2013).

The chemical nature of flavonoids depends on their structural class, degree of hydroxylation, other substitutions and conjugations, and degree

of polymerization. They are grouped together into subclasses based on their basic chemical structures; the most common ones are flavanols, flavones, flavonols, isoflavones, flavanones, anthocyanins (Figure 5).

The various classes of flavonoids differ in the level of oxidation and pattern of substitution of the C ring, while individual compounds within a class differ in the pattern of substitution of the A and B rings (Kumar and Pandey, 2013).

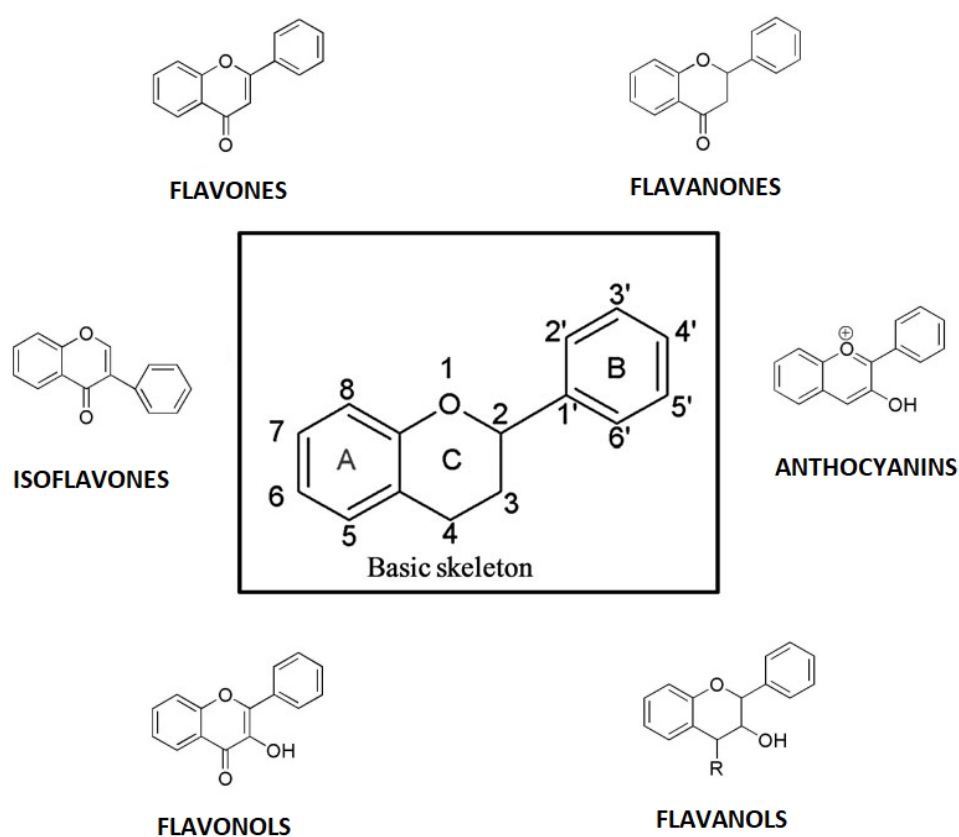


Figure 5. Basic chemical structures of flavonoids.

Flavones are very similar structurally to flavonol compounds, the latter having an extra hydroxyl substitution at the carbon 3-position. The major flavones are apigenin and luteolin. Isoflavones are distinctive and very

important subclass of flavonoid compounds. Flavonols (3-hydroxyflavones) are one the most analysed subgroup of flavonoids due to the importance referring to their antioxidant properties and other biological activities. Quercetin, kaempferol and myricetin are the most representative flavonols. Flavanones are extensively disseminated in larger plant families. Among them, naringenin and hesperetin aglycones seem to be of interest due to the high spread of flavanones in foods and their antioxidant potential. Anthocyanins are a group of phytochemicals, as natural pigments that are responsible for blue, red, purple and orange colours present in many fruits and vegetables. The most common anthocyanidins occurring in fruits and vegetables are cyanidin and delphinidin. Flavanols constitute a greatly complex group of polyphenols in the range from the monomeric flavan-3-ols (e.g. catechin, epicatechin, gallic catechin) to polymeric procyanidins known as condensed tannins. Catechin is the most important representative of the group of flavanols. Several types of catechins can be distinguished: catechin, gallic catechin, catechin 3-gallate, gallic catechin 3-gallate, epicatechin, epigallic catechin, epicatechin 3-gallate, epigallic catechin 3-gallate (Figure 6) (Brodowska, 2017).

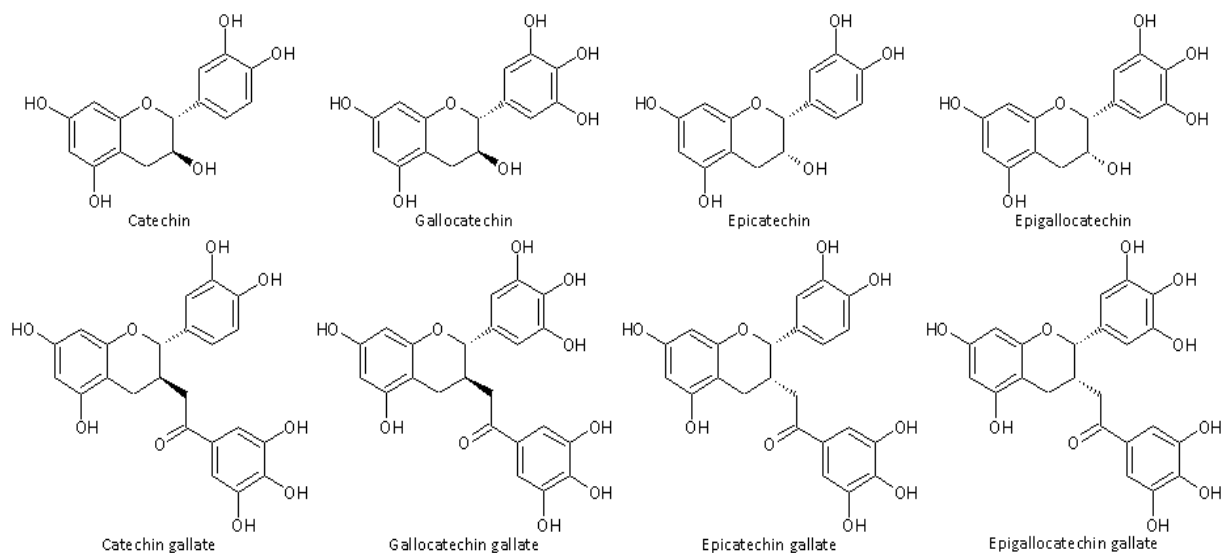


Figure 6. Structures of catechins.

Procyanidins are oligomers and polymers of flavan-3-ols units, mainly found in grape seeds and red wine. Procyanidins are also called proanthocyanidins because they produce coloured anthocyanidins when heated under acidic conditions. Most common flavan-3-ols units of procyanidins are catechin and epicatechin (Jeong et al., 2009).

Procyanidins can be categorized into A-type and B-type depending on the stereo configuration and linkage between monomers: B-type procyanidins are characterized by a single interflavan bond between carbon-4 of the B-ring and either carbon-8 or carbon-6 of the C-ring (Figure 7). B-type procyanidins are the most abundant, with procyanidins B1, B2, B3 and B4 occurring most frequently (Rue et al, 2018).

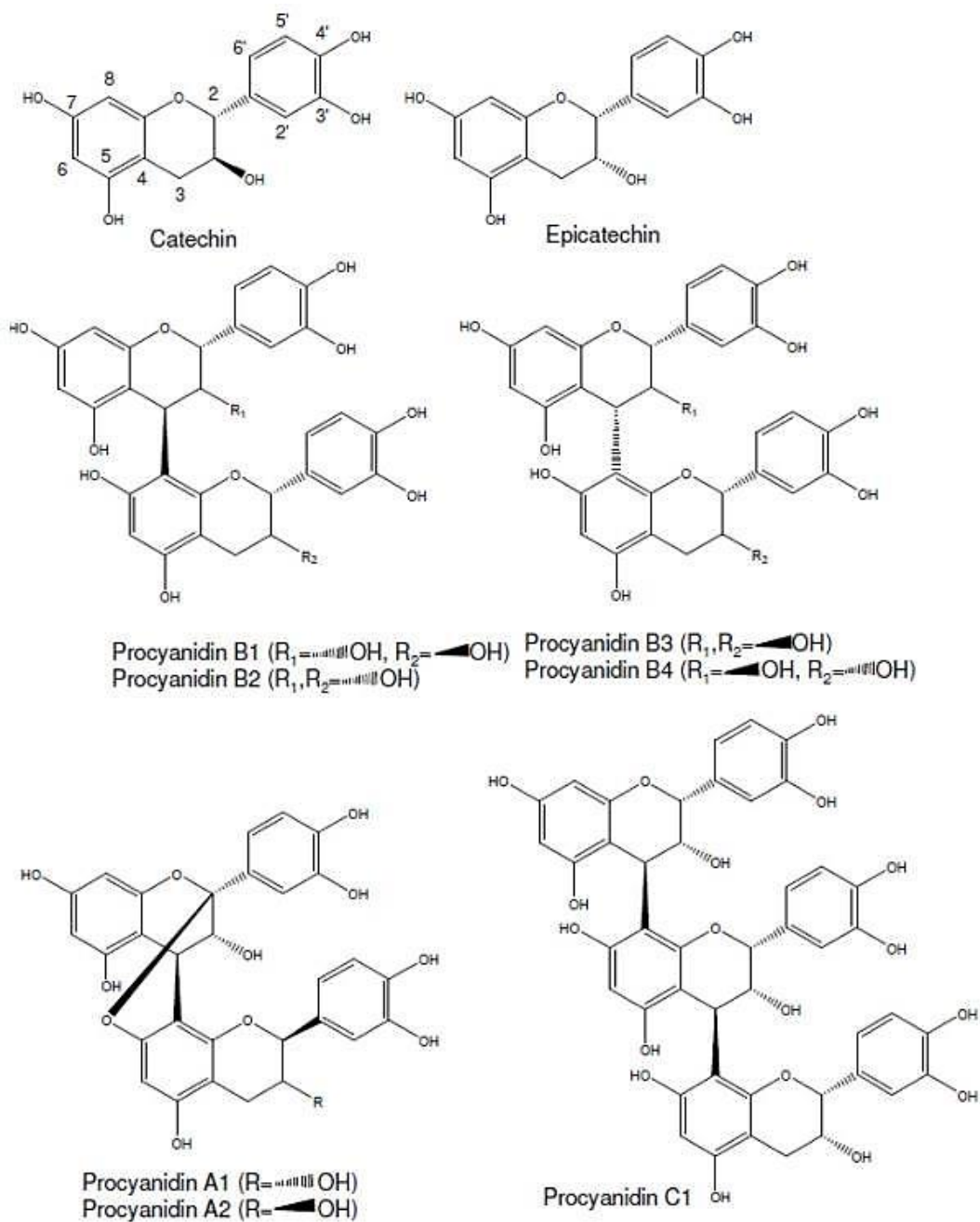


Figure 7. Chemical structures of monomeric and polymeric procyanidins.

Recent interest in flavonoids has been stimulated by the potential health benefits arising from the antioxidant activities of these compounds. The number and position of hydroxyl groups, within of the structure, influence their antioxidant properties.

The two classical antioxidant structural features of flavonoids are the presence of a B-ring catechol group and the presence of a C2-C3 double bond in conjugation with an oxo group at C4 (Kumar and Pandey, 2013). Because luteolin and some of its glycosides fulfil these two structural requirements, it is not surprising that many luteolin-containing plants possess antioxidant properties. The antioxidant activity of luteolin has not only been observed *in vitro* but also *in vivo* (López-Lazaro et al., 2009). The greatest antioxidant activity appears to be exhibited by the flavanol class, in particular the procyanidin group (Wood et al., 2002). Flavonoids are also known to have anti-inflammatory properties and inhibitory capacity on hyperglycaemia key enzymes (Thouri et al., 2017). Their activity as inhibitors has also been demonstrated and correlated with their structure and could be useful for treatment of AD (Xie et al., 2014) and T2D (Moukette et al., 2017).

1.2 Alzheimer's disease

AD is an age-related neurodegenerative disease that results from the synaptic dysfunction and death of neurons in specific brain regions and circuits, specifically the populations of nerve cells sub-serving memory and cognition (Shankar and Walsh, 2009). 36 million people have dementia all over the world and AD represents the most common neurodegenerative dementia amounting to 50-75 per cent of all dementias and is expected to become threefold more by 2050 (Chandra, 2017).

A pathological hallmark of AD is amyloid aggregation of amyloid-beta ($A\beta$). This peptide can self-assemble into amyloid fibrils and accumulate in human tissues as amyloid deposits. In the brain, deposits of beta-amyloid in the cortex and blood vessels are characteristic findings in AD. $A\beta$ is a small piece of a larger protein called “amyloid precursor protein” (APP). When APP is cutted by other proteins into separate, smaller sections that stay inside and outside cells. One of the peptides produced by this proteolytic cleavage is $A\beta$. It accumulates in stages into microscopic amyloid plaques that are considered a hallmark of a brain affected by AD. The peptides first form small clusters called oligomers, then chains of clusters called fibrils, then “mats” of fibrils in beta-sheet structures. The final stage is plaques, which contain clumps of beta-sheets and other substances. According to the amyloid hypothesis, these stages of beta-amyloid aggregation disrupt cell-to-cell communication and activate immune cells. These immune cells trigger inflammation, and ultimately, the brain cells are destroyed (Ali et al., 2011).

Early studies performed on patients suffering from AD found an altered cholinergic activity, which result in cognitive and functional symptoms. The cholinergic system directly contributes to regulation and memory process, thus represents a suitable target for the AD drug design. In the cholinergic system disruption in the levels of acetylcholine (ACh) is caused by hydrolytic action of cholinesterases (ChEs). Acetylcholinesterase (AChE, EC 3.1.1.7, Figure 8A) and Butyrylcholinesterase (BChE, EC 3.1.1.8, Figure 8B) belong to ChEs family

of enzymes and play a role in ACh regulation and in the cholinergic signaling. AChE consists of a ~120-kDa unit and is responsible for the hydrolysis that converts the neurotransmitter ACh to acetate and choline in cholinergic synapses.

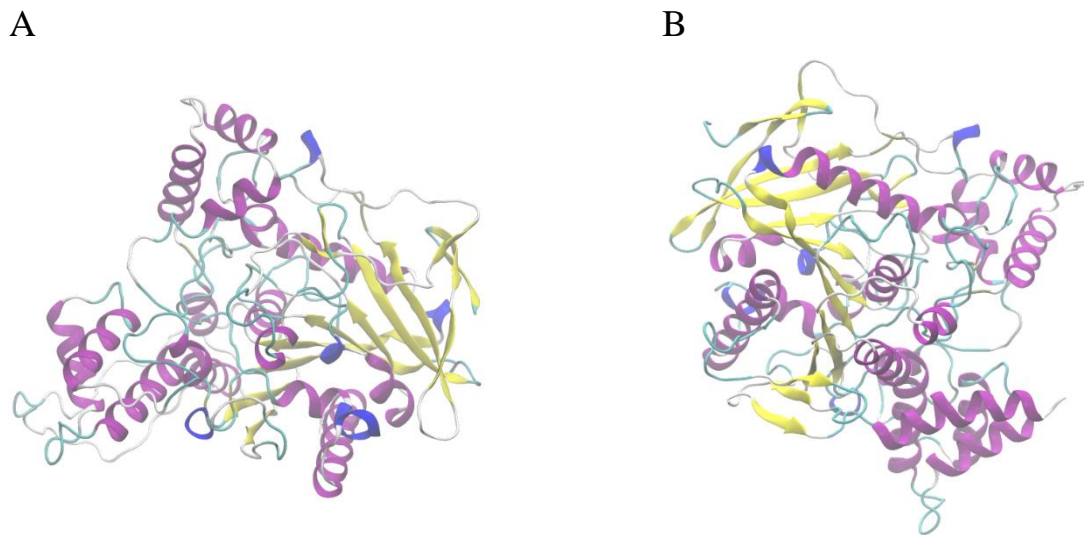


Figure 8. 3D structures of AChE (A) and BChE (B).

AChE has a high specific catalytic activity that hydrolyzes about 25000 molecules of ACh per second. BChE consists of a 62-kDa unit and is a non-specific cholinesterase enzyme, acting on butyrylcholine, ACh, and various choline esters. Therefore, this enzyme is recognized as a co-regulator of cholinergic neurotransmission. ChEs share 65% of their full amino acid sequence, and their molecular forms and active sites are structurally similar (Kim et al., 2016). AChE is substrate specific in nature and is found in high concentrations in the brain, while BChE is non-specific and is distributed throughout the body. In a healthy brain, the

AChE enzyme dominantly degrades ACh while BChE plays only a supportive role. However, several studies have shown the importance of BChE within the nervous system to be pivotal in the late stages of AD. Indeed, in patients with AD, BChE activity progressively increases, while AChE activity remains unchanged.

A well-documented strategy towards an effective management of AD is developing inhibitors that suppress the ChEs enzymes from breaking down ACh and therefore increasing both the level and duration of the neurotransmitter action (Anand and Singh, 2013). Several studies have been conducted to discover new substances based on plant products that can inhibit the action of ChEs and mitigate the effects of AD, while also with fewer side effects than the drugs currently available. The phenomena related to AD are mainly initiated and enhanced by oxidative stress. Oxidative damage is known to play an important role in neuronal damage, due to the neurodegeneration promoted by highly reactive compounds. Since brain tissue is particularly sensitive to ROS mediated cell damage, ROS build up may lead to lipid peroxidation. This process inhibits neurotransmitter production, such as that of ACh, which is deeply involved in memory and learning (de Oliveira et al., 2018). Galantamine represent a treatment for AD. It is a tertiary alkaloid isolated from *Galanthus nivalis* L. (Amaryllidaceae). Galantamine increases the availability of ACh in the cholinergic synapse by competitively inhibiting AChE. Galantamine has more than a 10-fold selectivity for AChE relative to BChE (Coyle and Kershaw, 2001). Several polyphenols individually or

in combination has been reported for their potential against AD, such as quercetin, resveratrol, curcumin, gallic catechins, cinnamic acid, caffeine, and caffeic acid (Jabir et al., 2018).

1.3 Diabetes mellitus

Diabetes mellitus is a progressive metabolic disorder of glucose metabolism. Type 1 diabetes is an autoimmune disease leading to β -cell destruction and insufficient synthesis of insulin, while T2D is characterized by insulin resistance and β -cell dysfunction.

Islet amyloid can be found in islets of Langerhans in almost all patients with T2D. Islet amyloid is made up of islet amyloid polypeptide (IAPP), which is derived from its precursor proIAPP (Paulsson et al., 2006). IAPP is a 37-residue peptide hormone that aggregates to form amyloid fibrils in the pancreatic islets (Godin 2019). Aggregated IAPP has cytotoxic properties and is believed to be of critical importance for the loss of β -cells in T2D, therefore the inhibition of its formation has therapeutic potential. In physiological conditions IAPP is co-secreted with insulin from β -cells, therefore, the formation and accumulation of amyloid fibrils occur on β -cells, leading to their death. IAPP is believed to play a role in the control of food intake, in controlling gastric emptying and in glucose homeostasis (Westermarck et al., 2011). Several studies support the hypothesis that IAPP may play a role in the development of hyperglycaemia (Verchere et al., 1996).

The early stage of T2D is associated with postprandial hyperglycemia due to impaired after meal insulin secretion. Therefore, a therapeutic approach to treat diabetes is to decrease postprandial hyperglycemia. This can be achieved by the inhibition of carbohydrate hydrolyzing enzymes like α -amylase and α -glucosidase that break down starch and disaccharides to glucose, thereby moderating the postprandial blood glucose elevation. α -Amylase (EC 3.2.1.1) catalyzes the endohydrolysis of α -D-1,4-glycosidic bonds in starch, producing maltose and various oligosaccharides. α -Glucosidase (EC 3.2.1.3) catalyzes the hydrolysis of terminal 1,4-linked α -D-glucose residues from nonreducing ends of isomaltose oligosaccharides, yielding free D-glucose. Inhibitors of these enzymes slow down carbohydrate digestion thus prolong overall digestion time, causing a reduction in glucose absorption and consequently blunting postprandial plasma glucose. Currently there are several antidiabetic drugs such as acarbose that act by inhibiting α -amylase and α -glucosidase. Acarbose is an oligosaccharide of microbial origin (Actinoplanes) that potently inhibits *in vitro* and *in vivo* such brush-border enzymes. Acarbose inhibits α -amylase significantly more than it inhibits α -glucosidase activity and this could be the cause of some side effects of this drug, due to an abnormal bacterial fermentation of undigested carbohydrates in the colon. For this reason, there is a need for other natural α -glucosidase and α -amylase inhibitors from plants. In this context, flavonoids showed high α -glucosidase and α -amylase inhibitory effect,

such as apigenin and scutellarin found in some plant extracts (Li et al., 2018).

1.4 Enzyme inhibition

Enzyme inhibitors are molecules that interfere with catalysis by slowing down or blocking enzyme-catalyzed reactions. A first major subdivision must be made between reversible and irreversible inhibitors. Irreversible inhibitors combine with the enzyme with strong bonds usually covalent, or the mutual affinity is so high to prevent the release of the inhibitor. The consequence is that the enzyme is completely deactivated. The deactivation process grows with the time of interaction between enzyme and inhibitor.

Reversible inhibitors bind to the enzyme by weak bonds very similar to those that substrate establishes with the enzyme, so they can be easily dissociated, and the inhibited enzyme can then resume its normal catalytic activity. To produce an inhibitory effect on enzymatic catalysis the inhibitor can bind to the enzyme (E) and/or to the enzyme-substrate (ES) complex or it can subtract the substrate (S) of the reaction. On this basis, four types of inhibition can be distinguished: competitive, non-competitive, uncompetitive and mixed inhibition.

1.4.1 Competitive inhibition

Competitive inhibition refers to the case of the inhibitor binding exclusively to the free enzyme and not at all to the ES binary complex. In competitive inhibition the two ligands (inhibitor and substrate) compete for the same site and generally bind in a mutually exclusive fashion; that is, the free enzyme binds either a molecule of inhibitor or a molecule of substrate, but not both simultaneously. Most often competitive inhibitors function by binding at the enzyme active site, hence competing directly with the substrate for a common site on the free enzyme. The presence of a competitive inhibitor in the enzyme sample has the kinetic effect of raising the apparent K_m of the enzyme for its substrate without affecting the value of V_{max} . This kinetic behaviour is diagnostic of competitive inhibition. Because of the competition between inhibitor and substrate, a hallmark of competitive inhibition is that it can be overcome at high substrate concentrations; that is, the apparent K_i of the inhibitor increases with increasing substrate concentration.

1.4.2 Mixed and non-competitive inhibition

Mixed and non-competitive inhibition refers to the case in which an inhibitor displays binding affinity for both the free enzyme and the enzyme-substrate binary complex. These inhibitors do not compete with substrate for binding to the free enzyme; hence they bind to the enzyme at a site distinct from the active site. Because of this, the inhibition cannot be overcome by increasing substrate concentration. Thus, the effect of a

mixed and non-competitive inhibitor is to decrease the value of V_{\max} without affecting the apparent K_m for the substrate. The term “non-competitive inhibition” is used exclusively for the situation in which the inhibitor displays equal affinity for both the free enzyme and the ES complex. When the inhibitor displays finite but unequal affinity for the two enzyme forms this corresponds to a mixed inhibition.

The dissociation constants for [E] and [ES] is defined by separate symbols, such as K_I and K_{IS} .

1.4.3 Uncompetitive inhibition

Uncompetitive inhibitors bind exclusively to the ES complex, rather than to the free enzyme form. The apparent effect of an uncompetitive inhibitor is to decrease V_{\max} and to decrease K_m (i.e., increase the affinity of the enzyme for its substrate).

Uncompetitive inhibitor would have no affinity for the free enzyme; hence the value of K would be infinite. The inhibitor would, however, have a measurable affinity for the ES complex, so that K would be finite.

1.4.4 Graphic determination of inhibition type

Several graphic methods have been described for determining the mode of inhibition of a molecule. Of these, the double reciprocal, or Lineweaver-Burk, plot is the most straightforward means of diagnosing inhibitor modality. The double reciprocal plot graphs the value of reciprocal

velocity as a function of reciprocal substrate concentration to yield a straight line. Overlaying the double-reciprocal lines for an enzyme reaction carried out at several inhibitor concentrations will yield a pattern of lines that is characteristic of an inhibitor type. In the presence of a competitive inhibition, the velocity is measured as a function of substrate concentration in the absence of inhibitor and at a single, fixed values of [I], as illustrated in Figure 9.

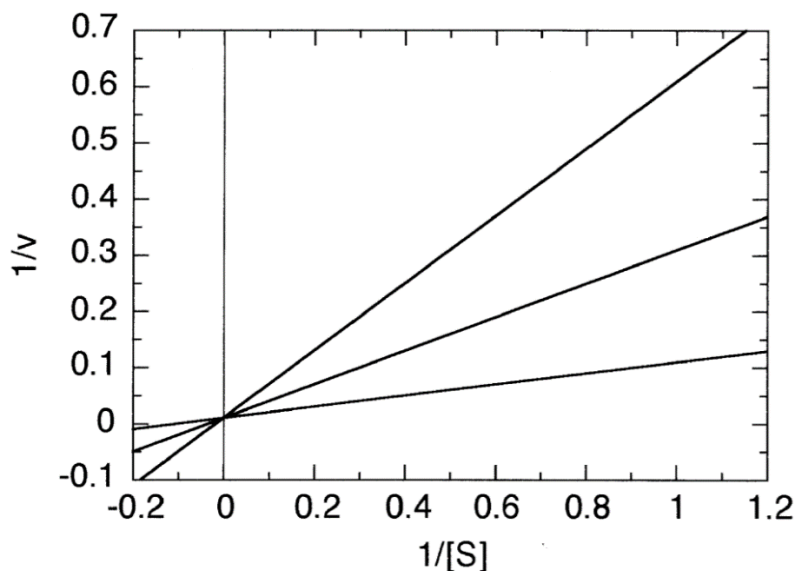


Figure 9. Double-reciprocal plot for the effects of a competitive inhibitor.

The pattern of straight lines with intersecting y intercepts seen in Figure 9 is the characteristic signature of a competitive inhibitor. The lines intersect at their y intercepts because a competitive inhibitor does not affect the apparent value of V_{max} , which is defined by the y intercept in a double-reciprocal plot.

A common approach to determining the K_I value of an inhibitor is to replot the kinetic data obtained in Lineweaver-Burk plots such as the apparent K_m values as function of inhibitor concentration. The x intercept of such a “secondary plot” is equal to the negative value of the K_I , as illustrated in Figure 10.

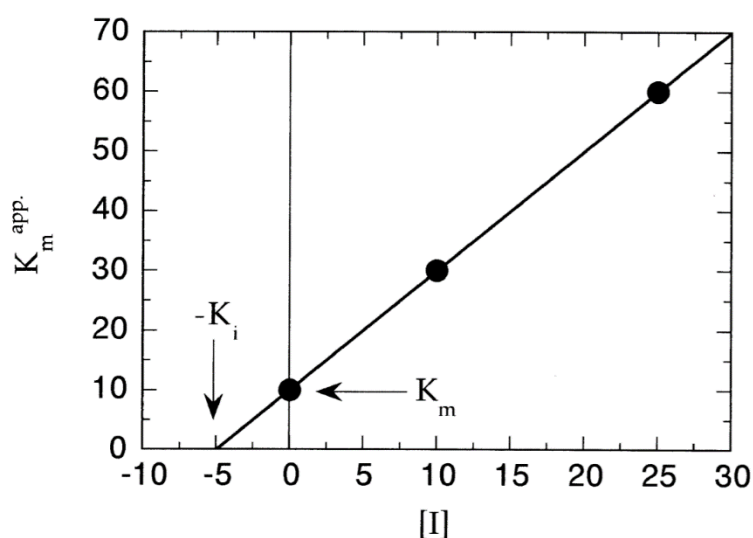


Figure 10. Secondary plot for a competitive inhibitor.

Another common method for determining the K_I value of an inhibitor suggested by Dixon (1953), one measures the initial velocity of the reaction as a function of inhibitor concentration at two or more fixed concentrations of substrate. The data are then plotted as $1/V$ as a function of $[I]$ for each substrate concentration, and the value of $-K_I$ is determined from the x-axis value at which the lines intersect, as illustrated in Figure 11.

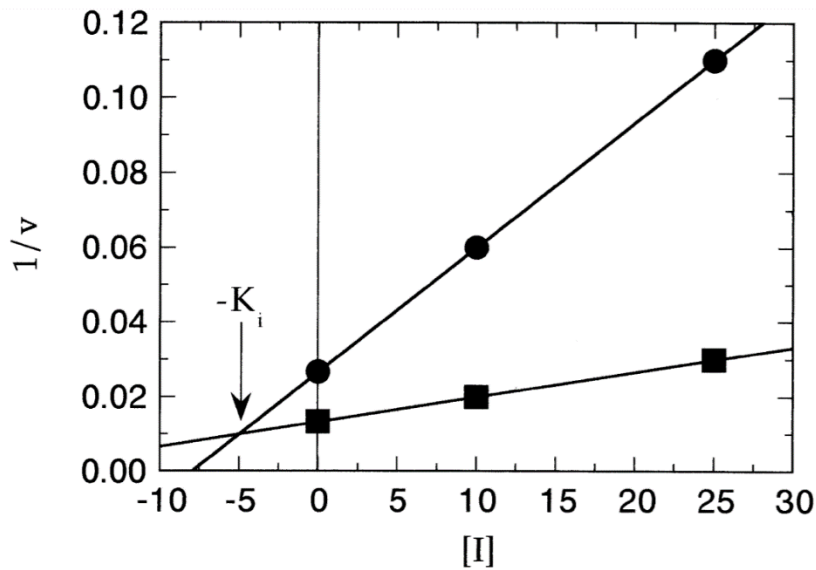


Figure 11. Dixon plot ($1/v$ as a function of $[I]$) for a competitive inhibitor.

A non-competitive or mixed inhibitor has affinity for both the free enzyme and the ES complex; hence the dissociation constants from each of these enzyme forms must be considered in the kinetic analysis of these inhibitors.

Both the slope and the y intercept of the double-reciprocal plot will be affected by the presence of a non-competitive and mixed inhibitors. The pattern of lines seen when the plots for varying inhibitor concentrations are overlaid and the lines will intersect at a value of $1/[S]$ less than zero and a value of $1/v$ greater than zero (Figure 12.A), or the lines will intersect below the x and y axes, at negative values of $1/[S]$ and $1/v$ (Figure 12.B) the inhibition mode is mixed. If the lines converge at $1/[S]$ less than zero on the x axis the inhibition mode is pure non-competitive (Figure 12.C).

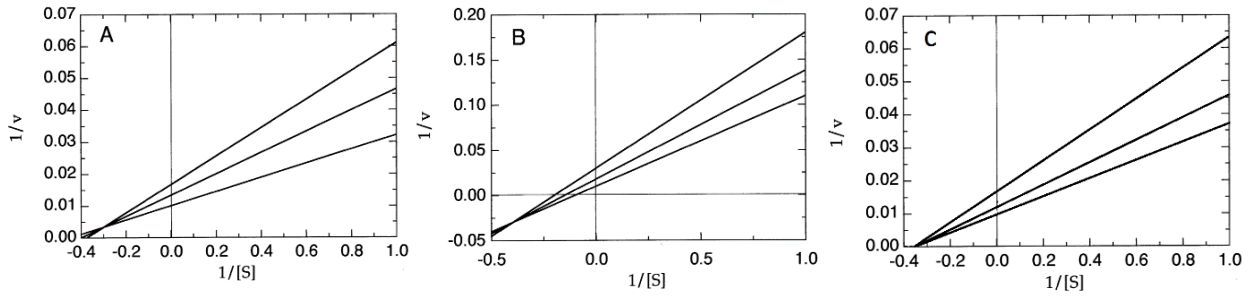


Figure 12. Patterns of lines in the double-reciprocal plots for mixed and non-competitive inhibitors.

Both V_{\max} and K_m are affected by the presence of an uncompetitive inhibitor. The slope of the double-reciprocal plot is independent of inhibitor concentration and that the y intercept increases steadily with increasing inhibitor. Thus, the overlaid double-reciprocal plot for an uncompetitive inhibitor at varying concentrations appears as a series of parallel lines that intersect the y axis at different values, as illustrated in Figure 13.

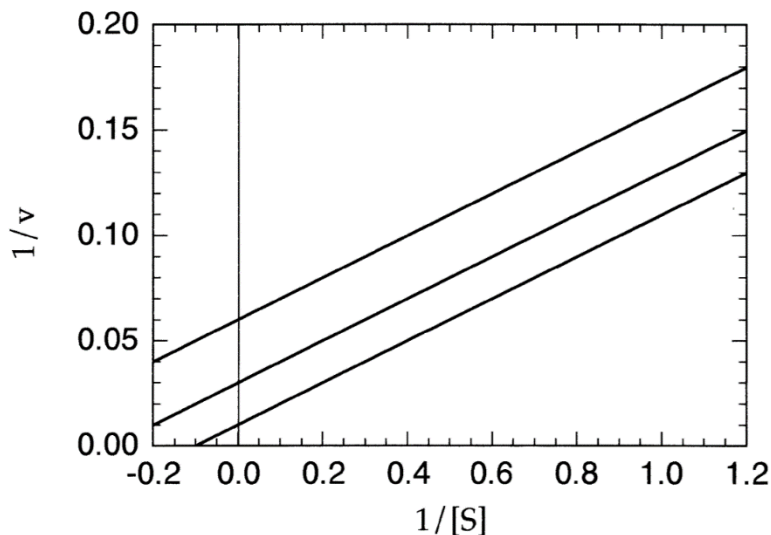


Figure 13. Pattern of lines in the double-reciprocal plot of an uncompetitive inhibitor.

1.5 *Washingtonia filifera*

The palm family includes a range of plant species with wide application in human food, some of which may also be of pharmacological interest (Geavlete et al., 2011). Few studies, however, exist on *Washingtonia* palms, a genus belonging to the Arecaceae family and Coryphoideae subfamily that includes two species: *W. filifera* and *W. robusta* (Benahmed-Bouhafsoun et al., 2015). They differ in subtle characteristics, and even palm experts have trouble to distinguish them. *Washingtonia filifera* (Linden ex André) H.Wendl. ex de Bary known as California fan palm, desert fan palm, or Washington palm is the only palm native to California and considered as the largest one in the United States but has been cultivated in Egypt and elsewhere (Hemmati et al., 2015).



Figure 14. *Washingtonia filifera* (left) and its fruits (right) where pulp and seeds are well visible.

Fruits, including the seeds, of *W. filifera* have been analysed for their nutritional composition, with the conclusion that they possess a higher concentration of carbohydrates than proteins (Cornett, 1987). *W. filifera* fruits and seeds are also relevant sources of dietary oils and the percentage composition of the *W. filifera* seeds is: ash 1.37%, oil 16.30%, protein content 3.46%, total carbohydrate 77.19% and moisture 3.22%. The major nutrients (mg/100 g of seeds) found in the seeds are: potassium, magnesium, calcium and phosphorus (Nehdi, 2011). Previous phytochemical investigation of this species detected lipids, trisaturated and unsaturated glycerides, proteins, leucoanthocyanins, flavonols, C-glycosylflavones and flavonoid sulfates. While the latter compounds, the flavonoid sulfates, are not widely distributed in the plant kingdom, they occur in many members of the Palmae, especially in such important palm genera as *Washingtonia* (El-Sayed et al., 2006). In particular, previously authors have studied the antioxidant activities of the aerial part of *W. filifera* and reported the presence of eight known flavonoids, luteolin 7-O-glucoside, luteolin 7-O-glucoside 2''-sulfate, tricetin 7-O-glucoside, tricetin 7-O-rhamnopyranoside (1''→6'') glucopyranoside, orientin, isoorientin, vitexin and isovitexin 7-O-methyl ether, together with two newly described compounds, luteolin 7-O-glucoside 4''-sulfate and 8-hydroxyisoscoparin (*i.e.*, 8-hydroxychrysoeriol 6-C-glucoside). C-glycosylation at different positions of luteolin significantly affects its antioxidant, anti-AD, anti-diabetic, and anti-inflammatory activities. The differences among these bioactivities of luteolin and its C-glycosylated

derivatives are due to the nature as well as the position of the glycosylation (Choi et al., 2014).

1.6 Objective of this thesis

Plant materials represent a great source of antioxidant and bioactive compounds which are different in their chemical composition and biological properties. There has been a remarkable increment in scientific articles dealing with research of antioxidant molecules because of their protective action from the damage induced by oxidative stress. It causes serious cell and tissue damage leading it to be the major cause of aging process and the pathogenesis of several disease like cancer, diabetes, cardiovascular and neurodegenerative diseases. Fruits are receiving more attention, as they contain different phytochemicals that manifest many biological activities. Despite many reports of commonly consumed fruits on their phenolic content and antioxidant capacity, little information is available for underused fruits (Kolar et al., 2011).

However, previous phytochemical investigation of *W. filifera* detected the presence of different polyphenolic compounds that are known to possess antioxidant properties and several biological activities.

The objective of this thesis was to find novel sources of bioactive molecules with antioxidant potential and beneficial effects on aging process and diseases such as AD and T2D. In this context, the phenolic composition, total polyphenol and flavonoid contents, as well as the

antioxidant activity, anti-cholinesterase, anti-XO, anti-hyperglycaemic properties, of seed extracts from *W. filifera* have been analysed.

2. MATERIAL AND METHODS

2.1 Chemicals

All chemical reagents were obtained as pure commercial products from Sigma Chemical Co (St. Louis, Missouri, USA), unless otherwise indicated, and used without further purification.

2.2 Plant material

The fruits of *W. filifera* were collected in Tunisia in the areas of Gabès (G) (33.880444 N, 10.082222 E) and Sousse (S) (35.855727 N, 10.567089 E) in August 2013. The plant was identified by Dr Marzouki Hanene, Laboratory of Transmissible Diseases and Biologically Active Substances, Faculty of Pharmacy, University of Monastir, Tunisia. The plant materials were washed with deionized water, frozen at -20 °C and then lyophilized. Lyophilization was carried out overnight, using an LIO-5P Freeze Dryer apparatus. The dried material was stored at -20 °C until required.

The fruits of *W. filifera*, separated as pulp and seeds, were crushed separately and then macerated in different solvent systems to compare the bioactivity of the extracts. The lyophilized plant materials (25 g) were extracted in 100 mL of water (AE, aqueous extract), ethanol (EE, ethanol extract) or methanol (ME, methanol extract) for 72 h at room temperature in continuous stirring. After filtration and centrifugation at 10000 rpm, the ethanol and methanol extracts were concentrated, using a rotary evaporator under reduced pressure at 60-70 °C, while the obtained

aqueous extracts were then lyophilized for further analysis. For fatty acid analysis, the seeds were also extracted with *n*-hexane (HE, hexane extract) in a conventional Soxhlet extraction apparatus, and the samples were further concentrated under vacuum on a rotary evaporator. Soxhlet extractions were performed using 15 g of each sample. The powder plant was transferred into a cellulose extraction thimble and inserted into a Soxhlet assembly fitted with a 100 mL flask. A 50 mL portion of *n*-hexane was added, and the whole assembly was heated for 6 h using a heating mantle at 60 °C. The extracts were concentrated using a rotary evaporator at 40 °C, and the dry extracts obtained were stored at -20 °C for chemical and biological assays.

2.3 Fatty acid analysis of *n*-hexane extracts

Dried aliquots of seed HE (3 mg) were dissolved in ethanol solution to be subjected to a mild saponification process at room temperature in the dark with the mixture Desferal/ascorbic acid/10 N KOH as previously described (Rosa et al., 2017). Dried saponified fractions were injected into an Agilent Technologies 1100 liquid chromatograph equipped with a diode array detector (HPLC-DAD system) (Agilent Technologies, Palo Alto, CA) for the quantification of unsaturated fatty acids (UFAs). The separation was carried out on an Agilent Technologies XDB-C18 Eclipse column (150 x 4.6 mm, 3.5 µm particle size) (at 37 °C), equipped with a Zorbax XDB-C18 Eclipse guard column (12.5 x 4.6 mm, 5 µm particle size); a mixture of CH₃CN/H₂O/CH₃COOH (75/25/0.12, v/v/v) was used as

mobile phase at a flow rate of 2.3 mL/min, and detection was performed at 200 nm. UFAs were identified using standard compounds and conventional UV spectra. Quantification of UFAs was made from peak area ratio, which was based on a calibration curve (in the amount range of 0.5-6 µg on column for polyunsaturated fatty acids (PUFA) and 1-10 µg for monounsaturated fatty acids (MUFA), respectively) generated from standard compounds in CH₃CN solution. Calibration curves of all the compounds were found to be linear, with correlation coefficients > 0.97, as previously reported (Rosa et al., 2019). An Agilent OpenLAB Chromatography data system was employed for recording and integration of the results. A portion of dried fatty acids after saponification was methylated with 1 mL of methanolic HCl (3 N) for 30 min at room temperature as previously described. Fatty acid methyl esters (FAME) were analysed using a gas chromatograph Hewlett-Packard HP-6890 (Hewlett-Packard, Palo Alto, USA) with a flame ionisation detector (FID) and equipped with a cyanopropyl methyl-polysiloxane HP-23 FAME column (30 m × 0.32 mm × 0.25 µm) (Hewlett-Packard). Nitrogen was used as a carrier gas at a flow rate of 2 mL/min. The oven temperature was set at 175 °C; the injector temperature was set at 250 °C; and the detector temperature was set at 300 °C. FAME were identified by comparing the retention times with those of standard compounds and quantified as a percentage of total amount of fatty acids (g%) using the Hewlett-Packard software.

2.4 Total polyphenols content

Total polyphenols content was determined by the Folin-Ciocalteu reagent in accordance with the method described by Singleton and Rossi, 1965, with slight modifications. 10 μL of the extracts was dissolved in 50 μL of the Folin-Ciocalteu reagent and 790 μL of distilled water. The solutions were mixed and incubated at room temperature for 1 min. Subsequently, 150 μL of 20% sodium carbonate solution was added. The solution was shaken and then incubated for 45 min in the dark at room temperature. The absorbance of all samples was measured at 750 nm. A calibrating curve was plotted using gallic acid as standard. Results were expressed as mg of gallic acid equivalents (GAE) per g of dry weight (dw).

2.5 Total flavonoids content

The flavonoids content in extracts was determined by aluminium nitrate colorimetric method described by Zhishen et al., 1999, with some modifications. An aliquot of 10 μL of sample solution was mixed with 20 μL of 10% (w/v) aluminium nitrate, 20 μL of 1 M sodium acetate and 850 μL of 80% ethanol. After incubation at room temperature for 40 min, the absorbance of the reaction mixture was measured at 415 nm. Different concentrations of quercetin solution were used for calibrations and results were expressed as mg of quercetin equivalents (QE) per g of dw.

2.6 HPLC–DAD–ESI/MS analyses

The methanolic and ethanolic extracts of *W. filifera* fruits were analysed using a Hewlett–Packard 1200 chromatograph (Agilent Technologies, Waldbronn, Germany) equipped with a quaternary pump and a diode array detector (DAD) coupled to an HP Chem Station (rev. A.05.04) data-processing station. The HPLC system was connected via the DAD cell outlet to an API 3200 Qtrap (Applied Biosystems, Darmstadt, Germany) mass spectrometer (MS) consisting of an ESI source and a triple quadrupole-ion trap mass analyzer, which was controlled by the Analyst 5.1 software.

Pulp analysis. An Agilent Poroshell 120 EC-C18 (2.7 μm , 150 \times 4.6 mm I.D.) thermostated at 35 $^{\circ}\text{C}$ was used. The solvents were: (A) 0.1% formic acid, and (B) acetonitrile. The elution gradient was performed according to the method previously reported (Di Petrillo et al., 2016). Double online detection was carried out in the DAD using 280, 330 and 370 nm as preferred wavelengths and in the MS operated in the negative ion mode. Spectra were recorded between m/z 100 and 1000. Zero grade air served as the nebulizer gas (30 psi) and as turbo gas (400 $^{\circ}\text{C}$) for solvent drying (40 psi). Nitrogen served as the curtain (20 psi) and collision gas (medium). Both quadrupoles were set at unit resolution and EMS and EPI analyses were also performed. The EMS parameters were: ion spray voltage -4500V, DP -50 V, EP -6 V, CE -10 V and cell exit potential (CXP) -3 V, whereas EPI settings were: DP -50 V, EP -6 V, CE -30 V and CES 10 V.

Seed analysis. An Agilent Poroshell 120 EC-C18 (2.7 μm , 150 \times 4.6 mm I.D.) at 25 $^{\circ}\text{C}$ was used. The solvents were: (A) 0.1% formic acid, and (B) acetonitrile. The elution gradient established was isocratic 0–10% B over 3 min, 10–14% B over 34 min, 14–15% B over 53 min, 15–60% B over 15 min, isocratic 60% B for 5 min and re-equilibration the column, using a flow rate of 0.5 mL/min. Double online detection was carried out as in the DAD using 280, 330 and 370 nm as preferred wavelengths and in the MS operated in the negative ion mode. Spectra were recorded between m/z 100 and 1000. Zero grade air served as the nebulizer gas (50 psi) and as turbo gas (500 $^{\circ}\text{C}$) for solvent drying (40 psi). Nitrogen served as the curtain (25 psi) and collision gas (medium). Both quadrupoles were set at unit resolution and EMS and EPI analyses were also performed. The EMS parameters were: ion spray voltage -3500V, DP -65 V, EP -10 V, CE -20 V and cell exit potential (CXP) -3 V, whereas EPI settings were: DP -40 V, EP -8 V, CE -50.

The phenolic compounds present in the samples were identified according to their UV and mass spectra and by comparison with commercial standards when available.

2.7 UHPLC-ESI-QqTOF-MS analyses

Kinetex 150 \times 2.1 mm ID 2.6 μm , options: 1) F5 (pentafluorophenyl) 2) C18 was used (injection volume 5 μL , 0.5mg/mL). The elution gradient established was isocratic 0–10% B over 0.8 min, 10–14% B over 14 min, 14–15% B over 23.5 min, 15–60% B over 28.7 min, 60%-100% over 37 min and

re-equilibration of the column, where the elution buffers were formic acid 0.1% on aqueous solution (A) and formic acid 0.1% on acetonitrile solution (B). Double online detection was carried out as in the DAD using 210, 280, 330 and 370 nm as the preferred wavelengths. Compact QqTOF-MS (Bruker Daltonics) were operated in negative and positive mode and calibrated with the sodium formate clusters. Calibration segment was introduced at the beginning of every run. The main MS parameters were following: scan range 50–1400 m/z, nebulizer pressure 1.5 bar, dry gas (N₂) 7.0 L/min, temperature 200 °C, capillary voltage 2.2 kV (negative mode) 4.5kV (positive mode), ion energy 53 eV, collision energy 8 eV. The analysis of the obtained mass spectra was carried out using Data Analysis software (Bruker Daltonics).

2.8 Biological activities

2.8.1 ABTS^{•+} radical scavenging activity

2,2'-Azinobis-(3-Ethylbenzothiazoline-6-Sulfonic Acid (ABTS) radical-scavenging activity was evaluated with the method as reported by Delogu et al. (2016), using Trolox (6-hydroxy-2,5,7,8-tetramethylchroman-2-carboxylic acid) as a standard. The free radical ABTS^{•+} was produced by reacting 7 mM ABTS with 2.45 mM potassium persulfate (final concentration) in aqueous solution and kept in the dark at room temperature for 24 h before use. Subsequently, an aliquot of this mixture was diluted to obtain an absorbance of approximately 0.700 ± 0.05 (mean

± SD). Samples of each extract (10 µL) were added to 1 mL of ABTS⁺ and the absorbance at 734 nm was recorded after 1 min incubation. Afterwards the decrease in A₇₃₄ was calculated and compared to the Trolox standard curve. The results were expressed as concentration of sample necessary to give a 50% reduction in the original absorbance (EC₅₀).

2.8.2 Xanthine oxidase assay

The inhibitory effect of *W. filifera* extracts on XO activity was determined spectrophotometrically by monitoring the formation of uric acid at 295 nm. XO activity was measured according to the method previously reported (Fais et al., 2018). The reaction mixture contained 879 µL of 100 mM phosphate buffer pH 7.5, 50 µL of an aqueous solution of XO (0.5 U/mL) from cow milk and 10 µL of extract sample solution or control sample solution. After mixing, 61 µL of xanthine solution 0.82 mM was added and the enzyme activity was determined at 295 nm, for 3 min at 25 °C. Allopurinol was used as standard XO inhibitor. Spectrophotometric determinations were made in an Ultrospec 2100 spectrophotometer (Biochrom Ltd, Cambridge, England) using a 1 cm length path cells and with a plate reader FLUOstar OPTIMA (BMG Labtech, Offenburg, Germany).

2.8.3 Tyrosinase assay

The inhibition of tyrosinase activity by *W. filifera* extracts was determined by using L-DOPA as substrate (Di Petrillo et al, 2019). The reaction mixture contained 25 mM phosphate buffer (pH 6.8), mushroom tyrosinase (100 U/mL, final concentration), with or without plant extract solution. Then, L-DOPA (0.5 mM) was added into the mixture and the activity was determined by following the increase in absorbance at 475 nm resulting from the formation of the dopachrome product. The concentration range of extract used for the mushroom tyrosinase inhibition assay was 0–0.3 mg/mL. In the assays performed without plant extracts, DMSO was added to the reaction mixture as blank control. Kojic acid was used as a positive control.

2.8.4 Elastase assay

Elastase inhibition was assayed monitoring the release of *p*-nitroaniline during cleavage of the substrate N-succinyl-(Ala)³-nitroanilide (SANA) by the action of the enzyme by the method described (Chompoo et al., 2012) with slight modifications. The assay was performed in 0.1 M Tris-HCl buffer (pH 8.0). Porcine pancreatic elastase (3.3 µg/mL) was incubated with or without the extracts for 20 minutes and, after incubation, the substrate (1.6 mM) was added and the enzyme activity was monitored at 410 nm. Controls were performed with DMSO while oleanolic acid was used as a positive control.

2.8.5 Collagenase assay

Collagenase from *Clostridium histolyticum*, was prepared in Tricine buffer 0.05 M, pH 7.5, containing 0.4 M NaCl and 0.01 M CaCl₂, and incubated (1 U/mL) with test samples at different concentrations for 15 minutes. The synthetic substrate N-(3-[2-Furyl]-acryloyl)-Leu-Gly-Pro-Ala (FALGPA), prepared in the same buffer solution, was then added to start the reaction (final concentration of 0.8 mM). Absorbance was monitored at 340 nm (Chompoo et al., 2012). Controls were performed with DMSO while epigallocatechin gallate was used as a positive control.

2.8.6 *In Vitro* determination of Sun Protection Factor

Sun protection factor of *W. filifera* extracts was determined using UV absorbance method according to the methodology described by Mansur et al. (1986). The absorbance of extracts (0.1 mg/mL) were measured in the range of 290–320 nm, with 5 nm increments and three determinations were made at each point. The SPF was calculated by applying the Mansur equation:

$$\text{SPF} = \text{CF} \times \sum_{290}^{320} \text{EE}(\lambda) \times \text{I}(\lambda) \times \text{Abs}(\lambda)$$

Where: CF = correction factor (10); EE (λ) = erythemogenic effect of radiation with wavelength λ ; I(λ) = solar intensity spectrum; Abs(λ) = spectrophotometric absorbance values at wavelength λ . The values of

EE(λ) \times I(λ) are constant. They were determined by Sayre et al. (1979) and are showed in Table 1.

Table 1. E (λ) and I (λ) values used for SPF calculation.

Wavelength (nm)	EE \times I
290	0.0150
295	0.0817
300	0.2874
305	0.3278
310	0.1864
315	0.0837
320	0.0180

2.8.7 Cholinesterase assays

Kinetic assays of cholinesterase activity were performed using the Ellman's method (Ellman's et al., 1961) with slight modifications (Kumar et al., 2018) using a plate reader. The reaction mixture contained 70 μ L phosphate buffer (0.1 M, pH 8.0), enzyme solution (acetylcholinesterase from *Electrophorus electricus* 0.3 U/mL, butyrylcholinesterase, from equine serum, 0.15 U/mL), 100 μ L of 5,5'-dithiobis-(2-nitrobenzoic) acid (DTNB) (1.5 mM final concentration) and inhibitor, dissolved in DMSO at the desired concentrations or DMSO alone (2%). Further, acetylthiocholine iodide (ATCI) or S-butyrylthiocholine iodide (BTCl) (20 μ L) was added as the substrate to the reaction mixture for AchE and BChE assays respectively and the absorbance monitored at 405 nm (37 °C) for 4 minutes. Each extract was evaluated at six concentrations (ranging from 5 to 50 μ g/mL). Galantamine was used as standard cholinesterase inhibitor.

2.8.8 α -Amylase assay

To assay α -amylase activity, a reaction mix containing 60 μ L of 50 mM sodium phosphate buffer at pH 7.0, 20 μ L of 1 M NaCl and 40 μ L of α -amylase from porcine pancreas (1 mg/mL) was used. The solution was incubated in absence or presence of extract at 37 °C for 10 min. After incubation, 80 μ L of a 2.5 mM 2-chloro-4-nitrophenyl- α -D-maltotriose (CNPG3) solution was added as substrate and the amount of 2-chloro-nitrophenol released by the enzymatic hydrolysis was monitored at 405 nm. Different concentration ranges were used for the assays: 0-12 μ g/mL for alcoholic extracts and 0-40 μ g/mL for aqueous extracts. Acarbose was used as a reference inhibitor.

2.8.9 α -Glucosidase assay

α -Glucosidase assay was performed as described by Fais et al., 2018. The enzyme (0.125 U/mL) solution was dissolved in 0.1 M sodium phosphate buffer (pH 6.8). Twenty microliters of test samples at various concentrations (0-2 μ g/mL) were mixed with the enzyme solution in microplate wells and incubated for 15 min at 37 °C. Subsequently, 20 μ L of 5 mM *p*-nitrophenyl α -D-glucopyranoside (pNPG) solution in 0.1 M phosphate buffer was added. After incubation at 37 °C for 15 min, the reaction was terminated by the addition of 50 μ L of 0.2 M sodium carbonate solution. α -Glucosidase activity was determined spectrophotometrically at 405 nm on 96-well microplate reader by

measuring the amount of *p*-nitrophenol released. DMSO control was used whenever required and the final concentration of DMSO was maintained below 8% v/v, which was found that it is not affecting the enzyme activity. Acarbose was used as a reference inhibitor.

Kinetic of all enzyme inhibition was determined by the Lineweaver-Burk double reciprocal plot. The assays were performed increasing the concentration of the respective substrate in the absence and presence of the extracts at different concentrations.

The inhibition potency for all enzymes was expressed as IC₅₀ values, which represent the inhibitor concentration giving 50% inhibition of enzyme activity, calculated as $[1-(B/A)] \times 100$, where A is the change in absorbance of the assay without the plant extract, and B is the change in absorbance of the assay with the plant extract.

IC₅₀ values were calculated by interpolation in dose-response curves. IC₅₀ values displayed represent the mean \pm standard deviation for three independent assays.

The equilibrium constants for binding with the free enzyme (K_I) and with the enzyme-substrate complex (K_{IS}) were obtained either from the slope or the vertical intercepts plotted versus inhibitor concentration, respectively.

2.8.10 ThT binding assay

Extrinsic fluorescence of the benzothiazole dye, thioflavin T (ThT), is widely used for the identification and quantification of amyloid fibrils, such as IAPP, *in vitro*, and has become the premier technique used to monitor fibrillation kinetics in real-time. When ThT is added to samples containing β -sheet-rich deposits, such as the cross- β sheet quaternary structure of amyloid fibrils, it displays enhanced fluorescence and a characteristic blue shift with excitation and emission maxima at approximately 440 and 490 nm, respectively. As there is a stoichiometric and saturable interaction between ThT and amyloid fibrils, fluorescence from the amyloid–ThT complex provides accurate quantification of amyloid fibril formation. The corresponding spectra are measured, and the fluorescence intensities of the dye are plotted as a function of time. Any deviation from the control sample along the time scale, that is, peptide aggregation in the absence of any additive, could be indicative of inhibition or acceleration of the aggregation processes (Hudson et al., 2009).

IAPP stock solutions were prepared by dissolving 2 mg of synthetic amylin in 250 μ L (2 mM) of hexafluoroisopropanol (HFIP). This stock solution was stored at -20 °C. All solutions for these studies were prepared by adding a PBS buffered (1 mM) ThT solution to IAPP peptide (in lyophilized dry form) immediately before the measurement. The final concentration of IAPP solution was 40 μ g/mL. When compounds were present, the IAPP to compound ratio was at 1:10, 1:5, 1:1, 1:0.1 and 1:0.01

by weight (400 $\mu\text{g}/\text{mL}$, 200 $\mu\text{g}/\text{mL}$, 40 $\mu\text{g}/\text{mL}$, 4 $\mu\text{g}/\text{mL}$, 0.4 $\mu\text{g}/\text{mL}$) and 0.5% DMSO was present in the solution. ThT fluorescence was monitored at 480 nm with 440 nm excitation at 37 °C on a FLUOstar Omega microplate reader. The experiments performed as sextuplicates were repeated three times.

2.8.11 Congo red stain

Congo red staining was performed to visualize the presence of amyloid fibrils. The cotton dye Congo red binds to amyloid fibrils, that appear red-orange. When observed with crossed polarizers in the polarization microscopy, stained amyloid exhibits bright green birefringence, often referred to as “apple green birefringence”.

Droplets (5 μL) of the peptide solutions were placed three times on the same spot (15 μL) on a glass slide. When dried, the slides were put in Congo B solution for 5 min, twice in absolute ethanol for 10 s, twice in xylene for 1 min and then mounted.

2.8.12 Negative stain

Negative staining was made for analysis by Transmission Electron Microscopy (TEM), a useful technique for assessing the morphology of *in vitro* formed amyloid fibrils from proteins or peptides that allows researchers to see structural features at the nanometer scale that cannot be visualized by light microscopy. Negative staining typically generates the

sample with good contrast and well-preserved morphology. The stain forms a coating over the sample that appears light and the outlining appears dark.

A drop of 5 μL of the samples from the plate suspended in 15 μL of distilled water was applied on to the grids strengthened with a carbon coating. The excess was then drawn off with filter paper and the grid was air dried. A drop of 50% uranyl acetate and 50% absolute ethanol was applied to the grids for 30 seconds. The excess was again drawn off with filter paper and the grid finally was air dried.

2.9 Cell culture

Human skin keratinocyte cell line HaCaT (CLS Cell Lines Service, Germany) cells were cultured in Dulbecco's Modified Eagle's Medium (DMEM) containing 10% fetal bovine serum (FBS, Gibco, NY, USA) and 1% penicillin/streptomycin at 37 °C in a humidified atmosphere with 5% CO₂.

2.9.1 Cell viability

Cell viability was detected by the colorimetric 3-(4,5-dimethylthiazol-2-yl)-2,5-diphenyltetrazolium bromide (MTT) assay as previously described with minor modification (Pintus et al., 2015). MTT is reduced by metabolically active cells, in part by the action of dehydrogenase enzymes, to generate reducing equivalents such as NADH and NADPH. The

resulting intracellular purple formazan can be solubilized and quantified by spectrophotometric means.

Cells were plated in 96-well plates (2×10^4 cells/well). After 48 h incubation with DMSO or extracts at different concentrations (0–100 $\mu\text{g/mL}$), cells were labelled with MTT solution for 3 h at 37 °C. The resulting violet formazan precipitates were dissolved in DMSO and the absorbance of each well was determined at 590 nm using a microplate reader with a 630 nm reference.

2.9.2 Intracellular ROS levels

The cellular ROS levels were determined with the 2',7'-dichlorofluorescein diacetate (DCFH-DA) method (Fais et al., 2018). HaCaT were treated with various concentrations of extract (0–50 $\mu\text{g/mL}$) for 24 h. Then, the cells were incubated with DCFH-DA (10 μM) at 37 °C for 30 min. After incubation, 1 mM H_2O_2 was added to the wells, and the fluorescence intensity of DCF was immediately measured using a fluorescent plate reader at excitation wavelength of 485 nm and emission wavelength of 530 nm, taking readings at intervals of 5 min for 50 min.

2.10 Data analysis

All experiments were performed in triplicates and the data were expressed as mean \pm standard deviation (SD). Statistical differences were evaluated using GraphPad Prism software version 8 (San Diego, CA,

USA). Comparison between groups was conducted by one-way analysis of variance (ANOVA) followed by the Tukey Multiple Comparisons Test and Student's unpaired t-test with Welch's correction. A P value of less than 0.05 was considered statistically significant.

2.11 Molecular docking

The crystal structure of XO (PDB ID: 1FIQ) enzyme was considered as modeled protein structure for computational investigation. The protein-ligand binding sites were predicted using COACH-D server, which is an enhanced version of the COACH server. The COACH algorithm predicts ligand poses by using a consensus of five methods. The first four are template-based methods: TM-SITE, S-SITE, COFACTOR and FINDSITE. The fifth method is a template-free that performs binding site prediction by examining both sequence conservation and structural geometry of the cavity (region). The results obtained from the five individual methods are then combined to consensus predictions by the COACH algorithm. These ligands are then clustered based on the spatial distance between their geometric centres (average linkage clustering algorithm with a cut-off distance 4 Å). The final step in the protocol consists of docking the ligand from the user input or the templates into the predicted binding pockets to build their complex structures employing molecular docking algorithm AutoDock Vina. For each predicted binding pocket, up to 10 binding poses are generated and the one that matches the best with the consensus prediction of binding residues is selected.

Moreover, the three-dimensional (3D) structure of IAPP (PDB id: 2L86) and α -amylase (PDB id: 1DHK) were obtained from protein data bank. However, due to the unavailability of the experimental 3D structure of an α -glucosidase protein from *Saccharomyces cerevisiae*, we performed a template-based homology modelling using Swiss-model web server with 3D reference structure of isomaltase from *Saccharomyces cerevisiae* (PDB id: 3AJ7) having 72% sequence identity with the target protein structure. The predicted protein tertiary structure model was evaluated by local quality estimates and Ramachandran plot of the dihedrals. The 3D structures of the ligands were obtained using open-babel software; the details of ligand preparation have been described by Fais et al. (2018). The docking experiment to generate and predict best protein-ligand complex pose was performed using a COACH-D server.

3. RESULTS AND DISCUSSION

3.1 Fatty acid analysis of *n*-hexane extracts

Quali-quantitative information on the individual fatty acids (FA) that compose *W. filifera* *n*-hexane extracts was obtained by GC-FID and HPLC-DAD analyses. Table 2 shows the FA composition by GC-FID analysis (expressed as % of total FA, g/100 g) of HE obtained from seeds of *W. filifera* collected in the areas of Sousse and Gabès.

Table 2. Fatty acids composition (% of total fatty acids) obtained by GC-FID analysis of *n*-hexane extracts (HE) obtained from seeds of *W. filifera* collected in the areas of Sousse and Gabès.

Fatty acid	g/100 g	
	HES	HEG
8:0	1.06 ± 0.17	1.01 ± 0.23
10:0	1.55 ± 0.24	1.61 ± 0.25
12:0	36.11 ± 4.23	33.50 ± 2.70
14:0	12.26 ± 0.58	10.40 ± 0.45 ^a
16:0	6.23 ± 0.29	6.32 ± 0.37
16:1	2.23 ± 0.42	3.07 ± 0.33 ^b
18:0	2.62 ± 0.45	3.05 ± 0.05
18:1 <i>n</i> -9	25.09 ± 2.17	25.47 ± 1.39
18:2 <i>n</i> -6	8.40 ± 0.63	9.95 ± 1.36
18:3 <i>n</i> -3	0.04 ± 0.01	0.06 ± 0.00
18:3 <i>n</i> -6	0.02 ± 0.01	0.05 ± 0.00
20:0	0.33 ± 0.43	0.08 ± 0.01
20:1	0.31 ± 0.06	0.26 ± 0.19
SFA	60.16 ± 4.03	55.97 ± 2.92
MUFA	27.63 ± 2.45	28.80 ± 1.58
PUFA	8.47 ± 0.62	10.06 ± 1.35

Abbreviations: SFA, saturated fatty acids; MUFA, monounsaturated fatty acids; PUFA, polyunsaturated fatty acids. Oil analysis was performed in quadruplicate and all data are expressed as mean values ± standard deviations (SD); (n = 4). Evaluation of the statistical significance of differences between the two groups was performed using Student's unpaired t-test with Welch's correction; ^a = $p < 0.01$; ^b = $p < 0.05$.

The HE Sousse (HES) showed a proportion of approximately 60% saturated FA (SFA) (mainly lauric acid 12:0, myristic acid 14:0, and palmitic acid 16:0, respectively 36, 12, and 6%), 28% monounsaturated FA (MUFA) (mainly oleic acid 18:1 *n*-9 and palmitoleic acid 16:1 *n*-7, 25 and 2% respectively), and 8% of polyunsaturated FA (PUFA), essentially constituted by the essential FA linoleic acid (18:2 *n*-6), with traces (0.04%) of α -linolenic acid (18:3 *n*-3). The absolute content of main UFA was determined by HPLC as follows (Table 3): 304.3 ± 10.9 mg/g, 102.3 ± 4.2 mg/g and 0.8 ± 0.04 mg/g of *n*-hexane extract, for the acids 18:1 *n*-9, 18:2 *n*-6 and 18:3 *n*-3, respectively. The HE Gabès (HEG) was characterized by a similar FA profile, with a high level of SFA (56%, with 34% of 12:0), followed by MUFA (29%) and PUFA (10%). HEG showed a slight lower level of SFA and higher amounts of UFA than HES. Significant differences were only observed in the levels of myristic acid (14:0), with 12% and 10% for HES and HEG, respectively ($p < 0.01$), and palmitoleic acid (16:1 *n*-7), with 2% and 3% for HES and HEG, respectively ($p < 0.05$). Absolute values of the main UFA determined by HPLC (Table 3) for HEG were 275.4 ± 13.3 mg/g, 108.2 ± 6.3 mg/g and 0.9 ± 0.1 mg/g, for acids 18:1 *n*-9, 18:2 *n*-6 and 18:3 *n*-3, respectively. Both HES and HEG contained lauric acid (12:0) as the majority fatty acid (34–36%), but also exhibited a high content of oleic acid (18:1 *n*-9; 25%). Thus, the *W. filifera* seed oil can be regarded as a lauric-oleic oil because of the abundance of these two fatty acids. The FA composition of HEG and HES oil extracts determined herein was slightly different from that of *W. filifera* seed oil obtained previously from a

Tunisian sample (Nehdi, 2011). Specifically, like HEG and HES, the major FA were SFA (43%), followed by MUFA (41%) and PUFA (16%), however, the Tunisian seed oil showed oleic acid as the most abundant fatty acid (41%), followed by lauric acid (18%), linoleic acid (16%), myristic acid (11%) and palmitic acid (9%). This result could be ascribable to several factors, for example differences in the FA metabolism due to the impact of the harvesting location such as climate, soil, and water availability.

Table 3. Main unsaturated fatty acids (expressed as mg/g extract), obtained by HPLC analysis, of n-hexane extracts (HE) obtained from seeds of *W. filifera* collected in Sousse and Gabès areas.

Fatty acids	HES	HEG
18:1 n-9	304.33 ± 10.93	275.41 ± 13.26
18:2 n-6	102.31 ± 4.21	108.19 ± 6.26
18:3 n-3	0.84 ± 0.04	0.88 ± 0.06

Oil analysis was performed in quadruplicate and all data are expressed as mean values ± standard deviations (SD); (n = 4).

3.2 Total polyphenols, total flavonoids content and antioxidant activity

Very low amounts of phenolic compounds, as well as low antioxidant activity, were detected in the pulp extracts (Table 4).

Table 4. Total phenolic and flavonoid contents, ABTS radical scavenging activity in *W. filifera* pulp extracts.

	Total Phenolic mg GAE/g dw	Flavonoid mg QE/g dw	ABTS EC₅₀ µg/mL
EEG	10.5±1.7	10.81±2.6	>150
EES	9.19±1.2	9.48±1.1	>150
MEG	25.2±3.6	14.7.9±6.4	>150
MES	26.37±3.2	10.79±5.5	>150
AEG	1.7±0.1	-	>150
AES	180.3±10.3	-	>150
Trolox			3.4 ± 0.3

Total phenolic and flavonoid contents in the analysed seed extracts are shown in Table 5.

Table 5. Total phenolic and flavonoid contents, ABTS radical scavenging activity in *W. filifera* seed extracts.

	Total Phenolic mg GAE/g dw	Flavonoid mg QE/g dw	ABTS EC₅₀ µg/mL
EEG	325.96 ± 32.20 ^{a,b}	215.43 ± 98.61 ^a	11.11 ± 1.15 ^{a*}
EES	412.30 ± 115.78 ^{a,b}	308.33 ± 137.23 ^a	9.06 ± 0.35 ^{a*}
MEG	708.83 ± 169.10 ^a	591.98 ± 386.14 ^a	5.52 ± 0.84 ^b
MES	637.4 ± 275.11 ^{a,c}	462.60 ± 294.20 ^a	9.71 ± 1.21 ^{a*}
AEG	133.54 ± 30.0 ^b	§-	22.64 ± 0.14 ^{c*}
AES	233.06 ± 33.68 ^{b,c}	§-	17.78 ± 0.45 ^{d*}
Trolox			3.4 ± 0.3

Each value is the mean \pm SD of three independent measurements (n = 3). § Below limit of detection.

a, b, c, d Different letters within the same column denote statistically significant differences between extracts ($p < 0.05$). * Values of EC_{50} of EEG, EES, MES, AEG and AES compared to Trolox are significantly different ($p < 0.01$).

The highest total phenolic content was found in the ME, followed by EE and AE. MEG showed a total phenolic content two times higher than the corresponding EEG. A positive correlation was found between total phenolic content versus flavonoid content ($r = 0.98$, $r^2 = 97\%$), determined in the alcoholic seed extracts, whereas hardly flavonoids were found in the aqueous extracts.

The antioxidant activity of the extracts was assessed by their ability to scavenge the ABTS radical. The results obtained for the seed extracts are included in the Table 5. As for total phenolic content, the aqueous extracts showed lower antioxidant capacity (higher EC_{50} values) than alcoholic extracts. The correlation of the total phenol content and ABTS radical scavenging activity was also shown in Figure 15.

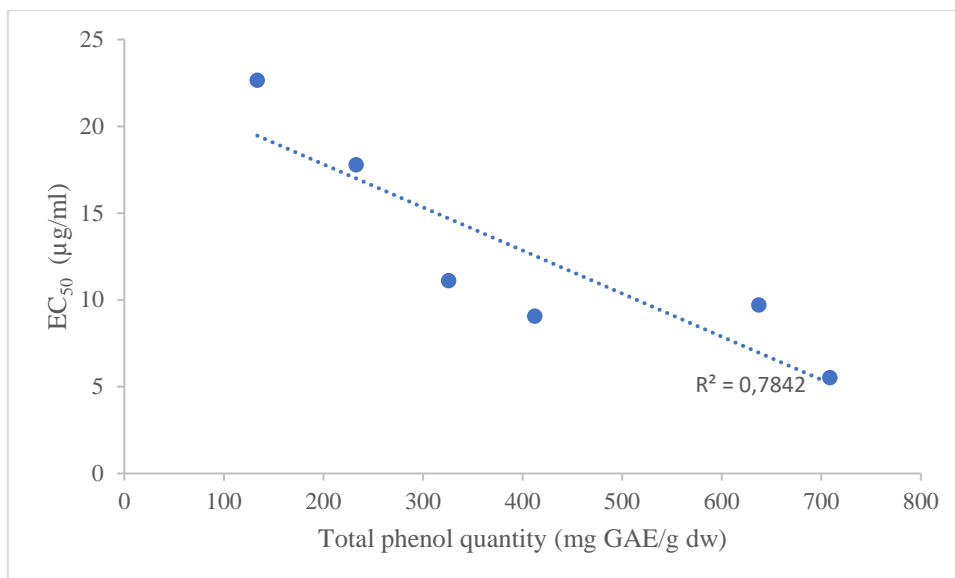


Figure 15. Correlation coefficient (R^2) of total phenol content in *W. filifera* seed extracts with their antioxidant activity (ABTS assay).

This correlation seems logical considering that the Folin–Ciocalteu reagent measures the reducing capacity of a sample rather than being specific for phenolics. Pulp extracts presented much lower antioxidant capacity than seeds, with EC_{50} value for ABTS radical scavenging ability higher than $150 \mu\text{g/mL}$, which is in line with their low levels of phenolic compounds.

3.3 HPLC/UHPLC–DAD–ESI/MS analyses

The characterization of individual phenolic compounds was performed by HPLC-DAD/ESI-MS. Data of the retention time, λ max, pseudomolecular ions, main fragment ions in MS^2 , and tentative identification are presented in Table 6. As it can be seen, the composition

of the sample was mostly consisting of flavan-3-ols (i.e., catechins and proanthocyanidins). Epicatechin and procyanidin B1 were identified by comparison with standards, whereas the identities of the procyanidin dimers B2-B4 and trimer C2 were tentatively assigned by comparison with data available in our data library. The identities of the remaining compounds were established based on their molecular weights. A point to highlight is the presence of some proanthocyanidins containing possible (epi)afzelechin units as well as A-type linkages. B-type procyanidin dimers (B1-B4) were the main phenolic compounds in the extracts of *W. filifera* seeds. In a previous study was reported the antioxidant activity of procyanidin dimer B1-B4 (Ling et al., 2005). Minority amounts of other flavonoids, mainly quercetin and isorhamnetin derivatives possessing sulfate residues were also detected. Although flavonoid sulfates are not very common in plants, they have been reported to occur in species of the Palmae family (Harborne 1975). As far as we know, no previous reports have been published on the phenolic profile of *W. filifera* seeds.

Table 6. Retention time (Rt), wavelengths of maximum absorption (λ_{\max}), mass spectral data, and tentative identification of phenolic compounds detected in *W. filifera* seeds.

Peak	Rt (min)	λ_{\max} (nm)	Pseudomolecular ion [m-H] ⁻ (m/z)	MS ² (m/z)	Tentative identification
1	12.0	260, 293	331		Galloylglucose
2	16.3	280, 307	451		(Epi)catechin glucoside
3	20.2	279	577	451, 425, 407, 289	B-type procyanidin dimer (B3)
4	20.7	279	577		B-type procyanidin dimer (B1)
5	21.1	278	865	695, 577, 425, 407, 287	B-type procyanidin trimer (C2)
6	22.5		577		B-type procyanidin dimer (B4)
7	22.9		577		B-type procyanidin dimer (B2)
8	23.7		863		A-type procyanidin trimer
9	25.4		1153	849, 577, 407, 287	B-type procyanidin tetramer
10	27.5	278	289	245, 203, 179, 109	Epicatechin
11	28.4		561	435, 407, 289	(Epi)catechin-(epi)afzelechin dimer
12	29.4	283	449	287, 269	Dihydrokaempferol hexoside
13	30.9		863	711, 575, 423	A-type procyanidin trimer
14	32.6		865		B-type procyanidin trimer

15	34.1		865		B-type procyanidin trimer
16	38.3		865		B-type procyanidin trimer
17	39.1		1153		B-type procyanidin tetramer
18	40.5		865		B-type procyanidin trimer
19	41.4		849	697, 577, 407, 287	B-type proanthocyanidin trimer containing one afzelechin unit
20	43.3	254, 353	689	301	Quercetin rutinoside sulfate
21	43.8		1441		B-type procyanidin pentamer
22	45.3	256, 358	703	315	Isorhamnetin rutinoside sulfate
23	45.3		577		B-type procyanidin dimer
24	46.5		849		B-type procyanidin trimer containing one afzelechin unit
26	50.4		557	315	Isorhamnetin glucoside sulfate
28	61.8	255, 353	463	301	Quercetin glucoside
29	65.1		577		B-type procyanidin dimer
30			865		B-type procyanidin trimer

Through UHPLC-DAD-ESI/MS analysis, three phenolic compounds have been identified, catechin, protocatechuic acid, and *p*-hydroxybenzoic acid, in addition to those identified in the previous HPLC-DAD-ESI/MS analyses.

HPLC-DAD/ESI-MS analyses was also performed on pulp extracts. The results obtained showed a phenolic composition mainly characterized by the presence of flavones, such as luteolin, especially in glycosylated and sulphated forms.

3.4 Biological activities

3.4.1 Xanthine oxidase inhibition

It was encouraging to observe that only pulp extracts were inactive against the XO enzyme, while all seed extracts displayed inhibitory activity at 150 $\mu\text{g/mL}$, ranging between 36.7 ± 0.1 and 74.6 ± 0.2 %, as reported in Table 7. The alcoholic seed extracts showed an IC_{50} values for the XO inhibitory activity between 75.2 ± 17.0 $\mu\text{g/mL}$ and 95.8 ± 5.9 $\mu\text{g/mL}$ range, higher than those of the standard drug allopurinol calculated in the same experimental conditions ($\text{IC}_{50} = 2.0 \pm 0.4$ $\mu\text{g/mL}$).

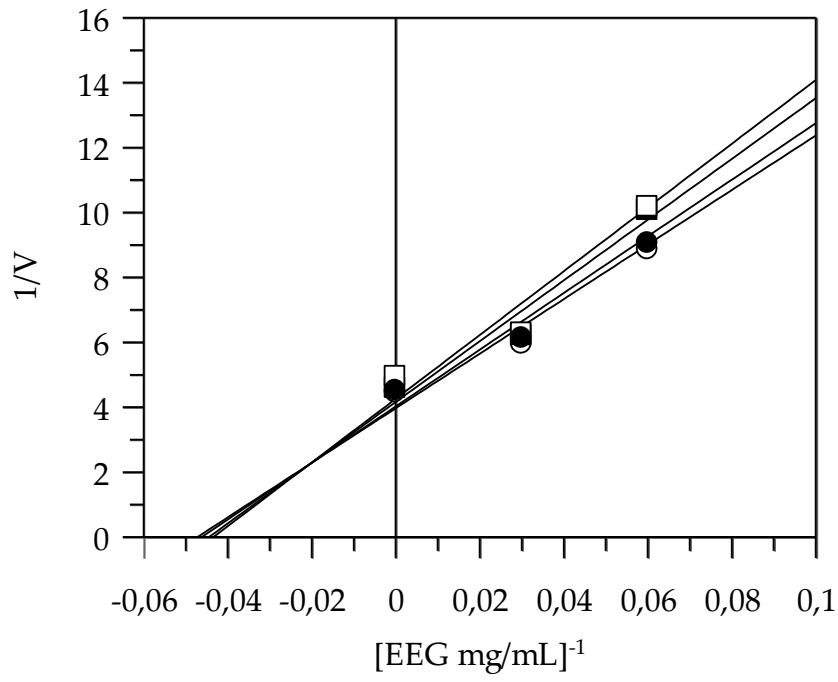
Table 7. Percentage of inhibition (% I) at 150 µg/mL, IC₅₀ value (µg/mL) and inhibition type of *W. filifera* seeds extracts against xanthine oxidase.

Extracts	% I	IC₅₀	Inhibition type
EEG	52.4±0.8	95.8±5.9*	mixed
EES	63.9±0.1	87.0±0.5*	mixed
MEG	72.8±0.3	75.2±17.0*	mixed
MES	74.6±0.2	76.1±5.2*	mixed
AEG	36.7±0.1	n.d	n.d
AES	37.7±0.1	n.d	n.d
Allopurinol		2.0 ± 0.4	

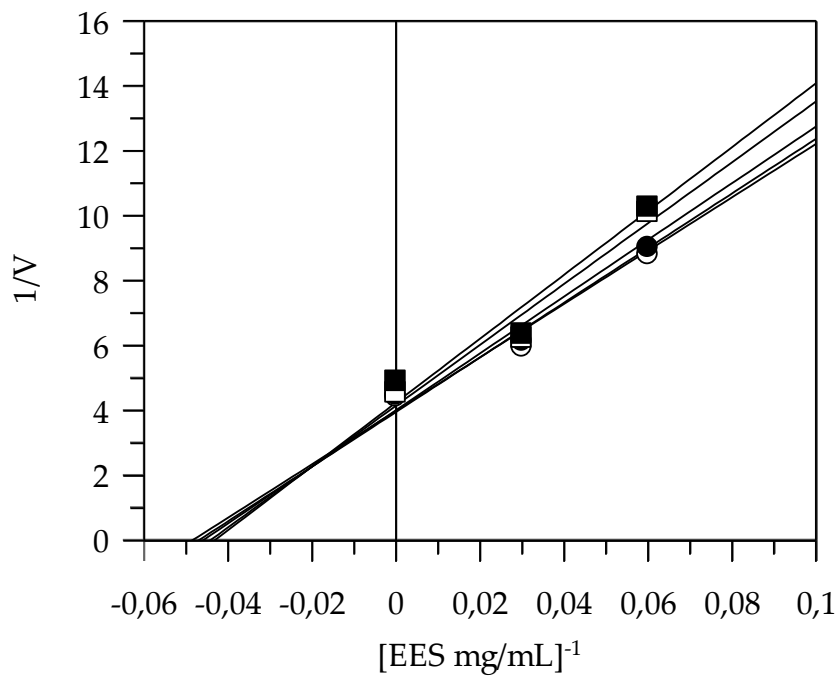
n.d.: not determined because the inhibition at highest screened concentration (150 µg/mL) was less than 40%. Values were expressed as mean ± SD (n = 3). * Values of IC₅₀ for alcoholic extracts compared to allopurinol significantly different (p < 0.05).

The Dixon plots of alcoholic extracts showed a mixed type of inhibition characteristics, since different concentration of substrate resulted in a family of straight lines which intersected in the second quadrant (Figure 16). This kinetic analysis indicates that these extracts can bind not only with the free enzyme but also with the enzyme-substrate complex. The data are plotted as 1/V as a function of [I] for each substrate concentration.

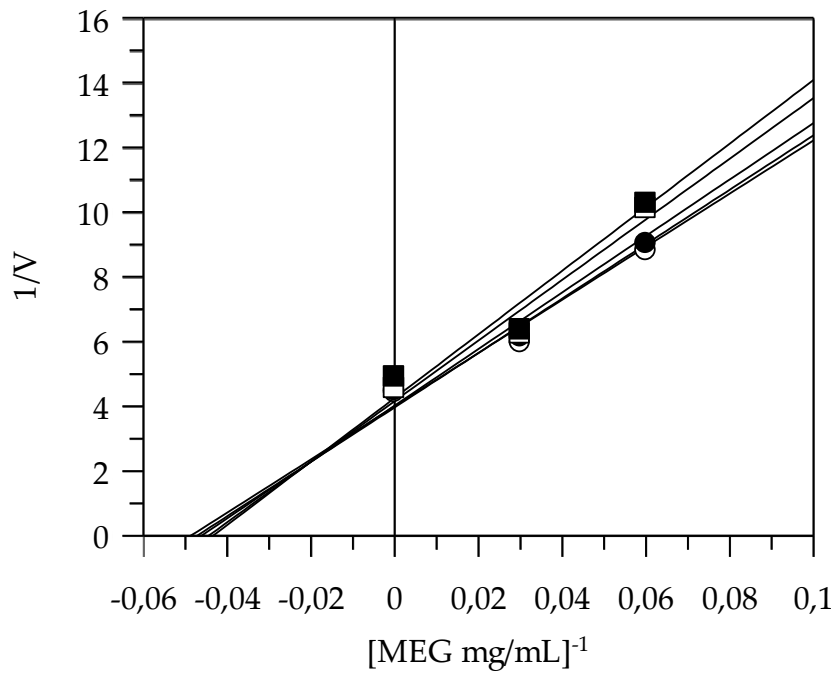
A



B



C



D

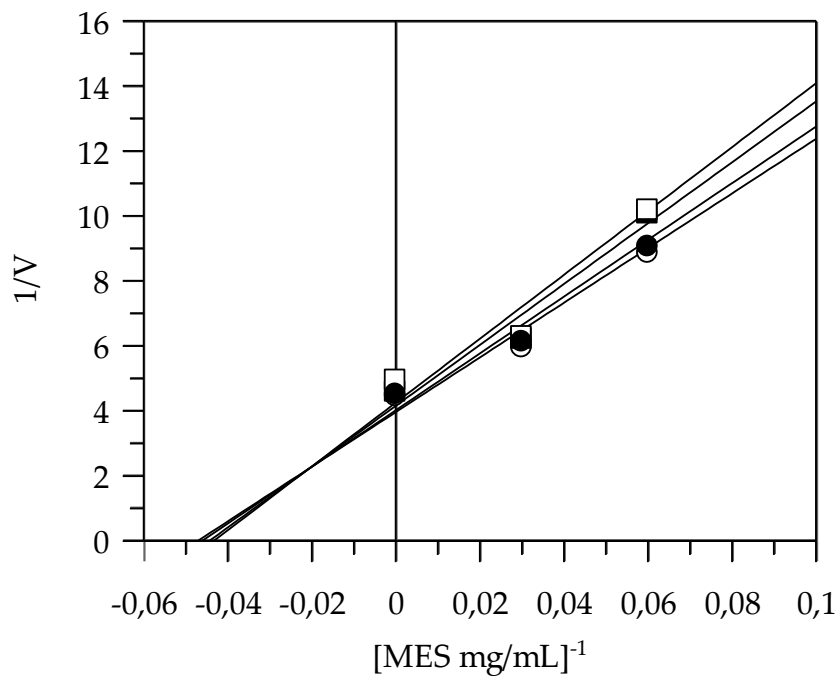


Figure 16. Dixon plots analysis of EEG (A), EES (B), MEG (C) and MES (D) against XO. The concentration of the substrate xanthine was 0.05 mM (○), 0.045 mM (●), 0.03 mM (□) and 0.025 mM (■).

Flavan-3-ols, the major compounds in the seed extracts, have been reported to possess inhibitory XO activity (Moini et al., 2000). Epicatechin behaves as a good XO inhibitor (Di Majo et al., 2014). Procyanidin B1, one of the major components detected herein, also revealed good XO inhibition capacity, showing an IC_{50} value of $53.5 \pm 6.0 \mu\text{g/mL}$. As far as we know, no previous reports exist on XO inhibition by this procyanidin.

3.4.2 Tyrosinase, elastase and collagenase inhibition

All the extracts weakly inhibit tyrosinase activity, with IC_{50} values higher than that of the standard, kojic acid. A better inhibition was observed against elastase and collagenase activities and ethanolic (EEG and EES) and methanolic (MEG and MES) extracts exerted the best effect.

Alcoholic seeds extracts have shown a good inhibitory effect against elastase, with IC_{50} values ranging between $10.76 \pm 3.38 \mu\text{g/mL}$ and $19.75 \pm 5.55 \mu\text{g/mL}$, comparable to that of the standard inhibitor oleanolic acid calculated in the same experimental conditions ($IC_{50} = 11.75 \pm 0.63 \mu\text{g/mL}$). The best inhibitory effect is given by alcoholic seeds extracts against collagenase, with values of IC_{50} about a half of the standard inhibitor

(EGCG) calculated in the same experimental conditions ($IC_{50} = 126.8 \mu\text{g/mL}$), as showed in Table 8.

Table 8. IC_{50} value ($\mu\text{g/mL}$) of *W. filifera* seeds extracts against tyrosinase, elastase and collagenase.

Plant extracts	IC_{50} ($\mu\text{g/mL}$)		
	Tyrosinase*	Elastase*	Collagenase*
EEG	73.0 ± 5.09^a	17.69 ± 2.81^a	55.2 ± 19.09^a
EES	89.0 ± 3.60^b	19.75 ± 5.55^a	50.04 ± 6.87^a
MEG	89.5 ± 4.35^b	10.76 ± 3.38^a	50.03 ± 1.18^a
MES	139.0 ± 3.34^c	12.47 ± 3.11^a	33.36 ± 13.06^a
AEG	90.0 ± 2.11^b	70.1 ± 4.56^b	ND
AES	70.0 ± 3.17^a	47.66 ± 2.88^c	ND
Kojic acid	17.9 ± 0.98^d	-	-
Oleanoic acid	-	11.75 ± 0.63^a	-
Epigallocatechin gallate	-	-	120.8 ± 6.22^b

Each value is the mean \pm SD of three independent measurements ($n = 3$). *Different letters within the same column denote statistically significant differences between extracts ($p < 0.05$).

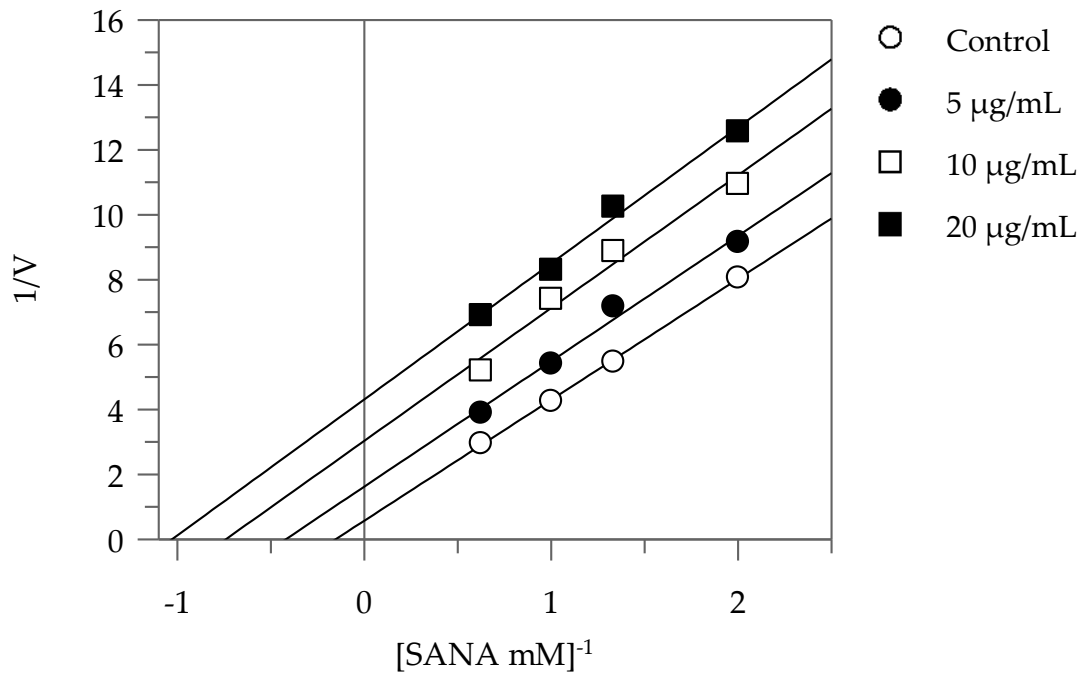
We have focused our attention on ethanol and methanol extracts in order to investigate the mode of inhibition of these enzymes, since they had a better effect against elastase and collagenase activities. The kinetic

parameter and the inhibition type are reported in Table 9. The Lineweaver-Burk plots of ethanolic extracts against elastase showed an uncompetitive type of inhibition characteristics, since increasing the concentration of extracts resulted in a family of parallel straight lines (Figure 17). Methanolic extracts showed a non-competitive inhibition type since increasing the concentration of extracts resulted in a family of straight lines with different slope and y-intercepts, which intersected in the x-axis. The equilibrium constants for binding with the free enzyme (K_I) and with the enzyme-substrate complex (K_{IS}) were obtained from the slope (K_m/V_{max}) or the $1/V_{max}$ values (y-intercepts) versus inhibitor concentration, respectively.

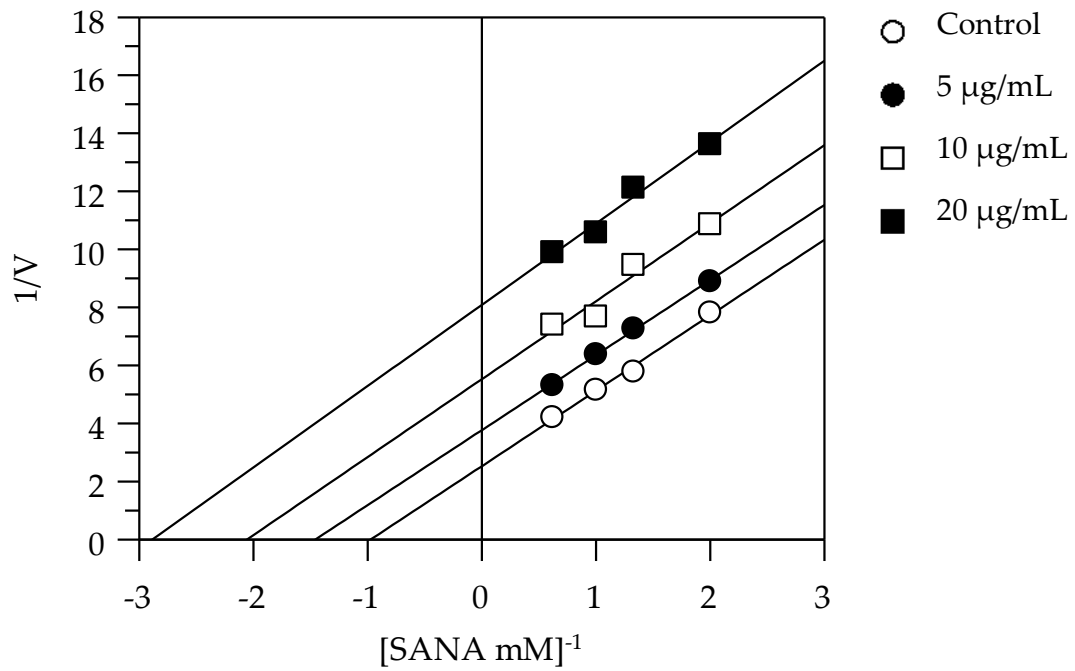
Table 9. Kinetic parameters and inhibition type of *W. filifera* extracts toward elastase and collagenase.

Elastase			
Plant extracts	Inhibition type	K_I ($\mu\text{g/mL}$)	K_{IS} ($\mu\text{g/mL}$)
EEG	uncompetitive	-	3.91
EES	uncompetitive	-	8.89
MEG	noncompetitive	9.66	9.55
MES	noncompetitive	9.48	9.57
Collagenase			
EEG	uncompetitive	-	11.49
EES	uncompetitive	-	9.64
MEG	uncompetitive	-	13.04
MES	uncompetitive	-	7.58

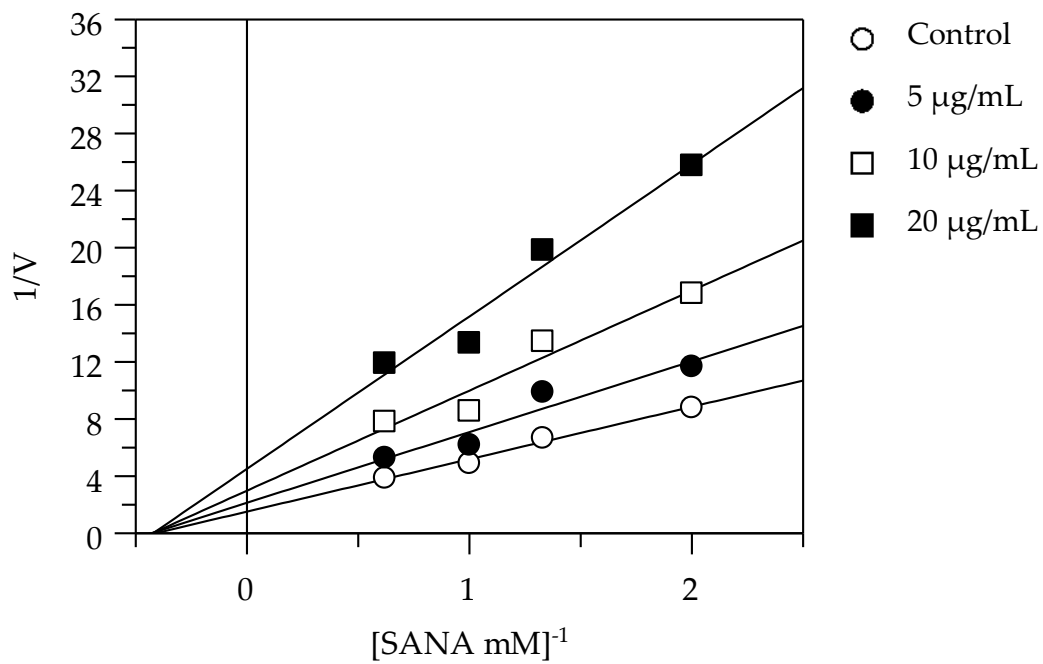
A



B



C



D

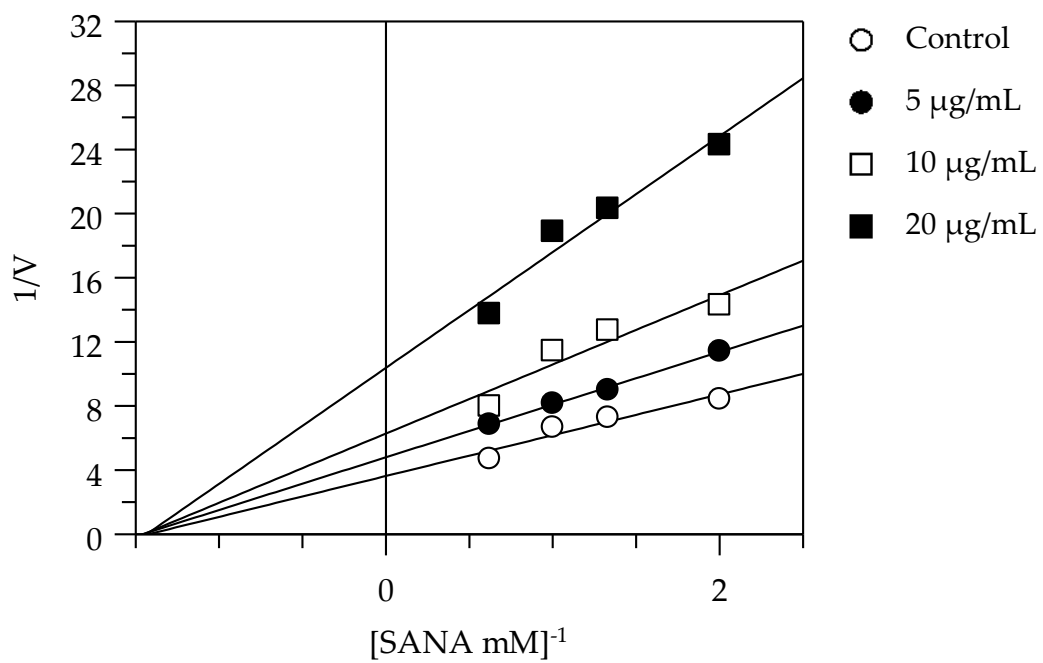
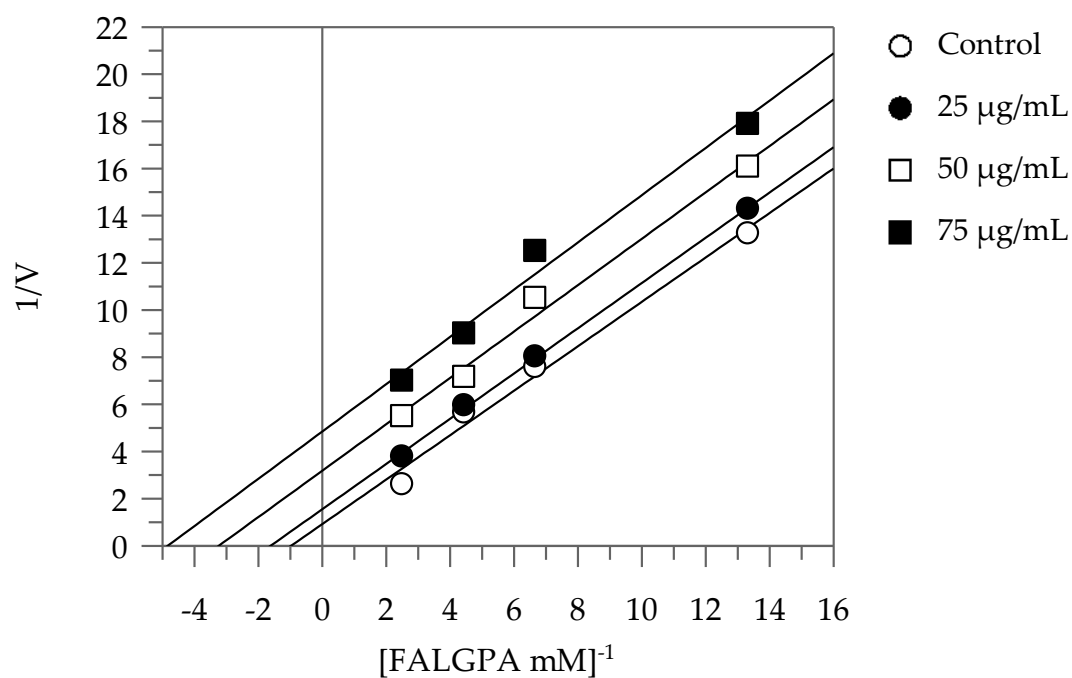


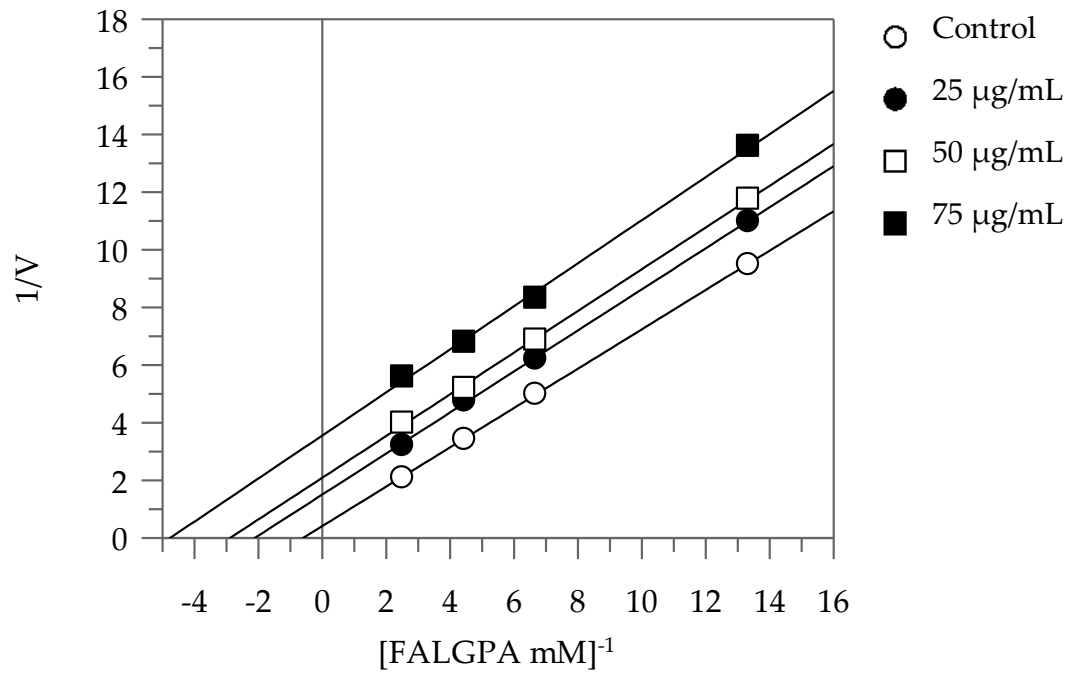
Figure 17. Lineweaver–Burk plots analysis of EEG (A), EES (B), MEG (C) and MES (D) against elastase.

The Lineweaver-Burk plots of all alcoholic extracts against collagenase showed an uncompetitive type of inhibition mode (Figure 18).

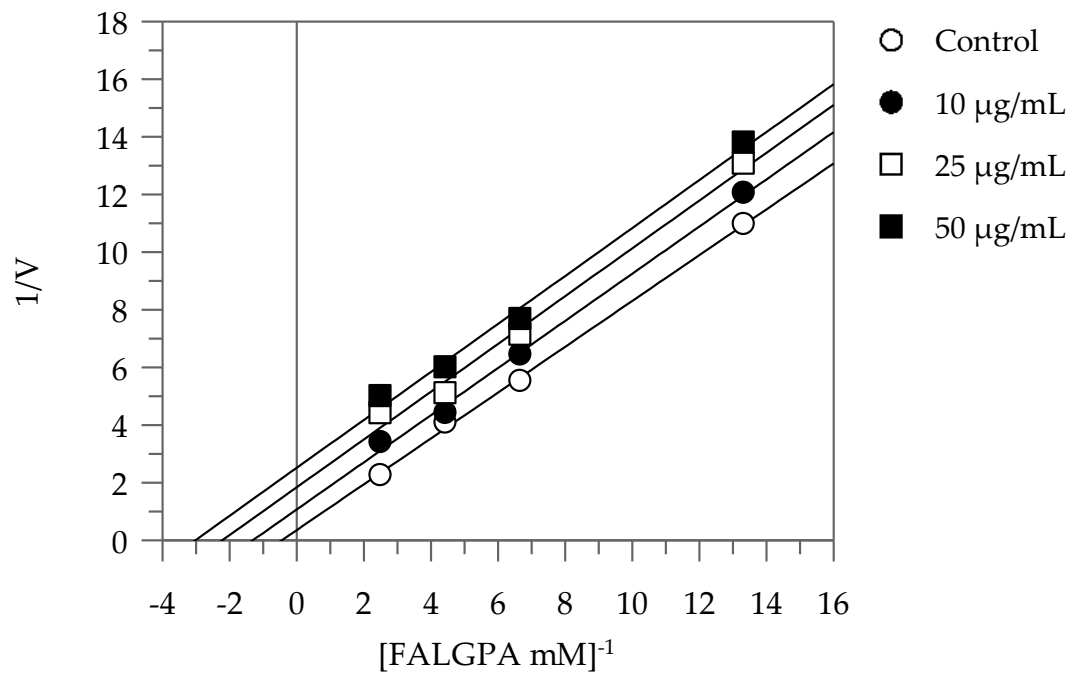
A



B



C



D

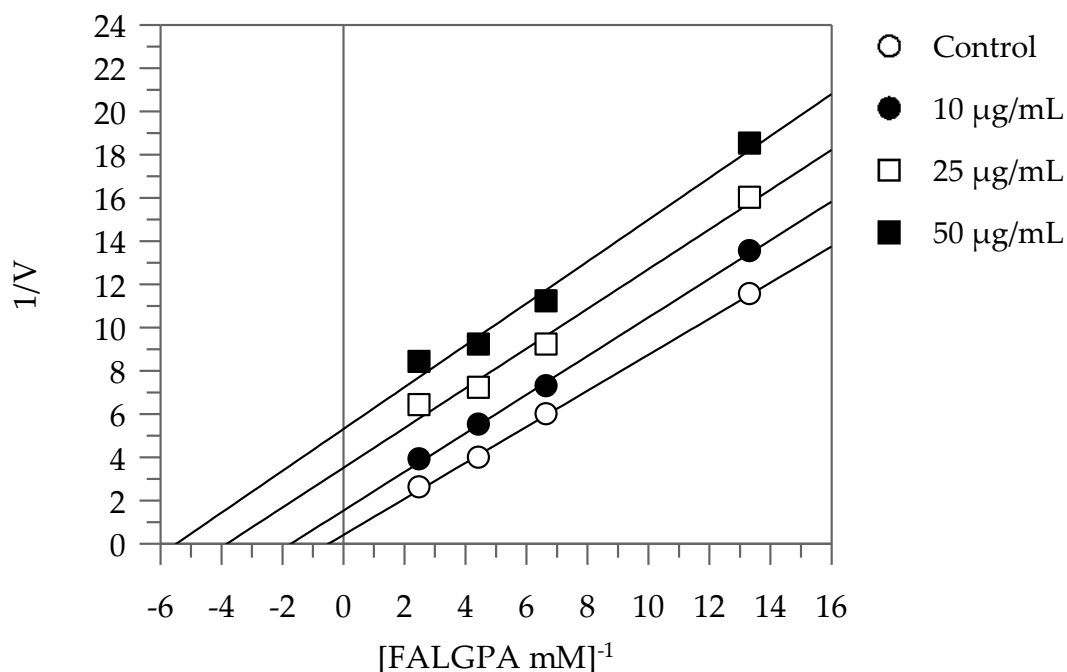


Figure 18. Lineweaver–Burk plots analysis of EEG (A), EES (B), MEG (C) and MES (D) against collagenase.

B-type procyanidins were the main compounds in the extracts of *W. filifera* seeds; a positive relationship between the degree of procyanidin polymerization and the capacity of the procyanidins to inhibit elastase was observed in previous paper (Brás et al., 2010; Brás et al., 2010). Moreover, an inhibitory activity against elastase and collagenase by some procyanidin compounds has been reported (Itoh., et al 2019; Wittenauer et al., 2015). A synergic action of these compounds could contribute to explain the significant inhibition of the *W. filifera* methanolic extract against both the enzymes.

3.4.3 Sun Protection Factor

Photo-protectant activity is very important for compounds with possible skin application; thus, we determined the sun protection factor (SPF) of our extracts. The SPF indicates the ability of a substance to absorb UV rays, protecting the skin from the toxic effects produced by such radiation. Plant-based cosmetics have great potential in absorbing UV-radiation because plant extracts contain polyphenols such as flavonoids or carotenoids. These compounds having aromatic rings can absorb UV rays and therefore act as sun filter. Since alcoholic seed extracts of *W. filifera* contain phenolic and flavonoid compounds, the photo-protective effect of these extracts was evaluated. As shown in Table 10, all the analysed extracts, at the concentration of 100 µg/mL, showed SPF values ranging from 1.52 and 3.35. Methanol extracts revealed to possess the best photo-protective effect. UV rays are responsible of skin diseases and they trigger the processes that result in skin aging, oxidative stress and wrinkles formation. Thus, reducing the absorption of this radiation enhances in an indirect way the antioxidant activities and the inhibition of aging-related enzymes.

Table 10. Absorbance and SPF values of ethanolic and methanolic extracts of *W. filifera*.

Wavelength (nm)	Absorbance			
	EEG	EES	MEG	MES
290	0.377	0.349	0.585	0.829
295	0.202	0.19	0.31	0.445
300	0.156	0.146	0.237	0.345
305	0.145	0.137	0.218	0.319
310	0.135	0.128	0.203	0.298
315	0.123	0.116	0.183	0.269
320	0.108	0.103	0.16	0.238
SPF	1.52	1.43	2.30	3.35

3.4.4 Cholinesterase inhibition

The anticholinesterase activity of all the extracts at a concentration of 20 µg/mL was checked using AChE/BChE assays. Table 11 shows the AChE and BChE inhibitory activities of the of *W. filifera* seeds extracts, compared with those of standard inhibitor galantamine. The IC₅₀ for AChE was not determined because the inhibition at highest screened concentration (20 µg/mL) was less than 40%.

Table 11. Percentage of inhibition (% I) at 20 µg/mL and IC₅₀ value (µg/mL) of *W. filifera* seeds extracts against Cholinesterases.

Extracts	AChE	AChE	BChE	BChE
	% I	IC ₅₀	% I	IC ₅₀
EEG	3.2±0.5	n.d	65.6±0.78	13.73±1.31 ^a
EES	16.5±6.22	n.d	53.9±6.5	27.30±5.37 ^{b*}
MEG	7.7±2.22	n.d	64.5±9.26	15.13±2.05 ^{a,c}
MES	20.9±1.56	n.d	63.1±1.91	22.60±2.72 ^{b,c*}
AEG	28.6±7.78	n.d	45.6±1.06	15.08±1.05 ^{a,c}
AES	38.5±11.6	n.d	48.5±1.06	18.51±0.001 ^{a,c*}
Galantamine		0.895±0.043		7.65±1.78

n.d.: not determined because the inhibition at highest screened concentration (20 µg/mL) was less than 40%. Values were expressed as mean ± SD (n = 3). ^{a, b, c} Different letters within the same column denote statistically significant differences between extracts (p< 0.05).* Values of IC₅₀ of EES, MES and AES compared to galantamine significantly different (p< 0.05).

The IC₅₀ values ranged from 13.73 ± 1.31 µg/mL to 27.30 ± 5.37 µg/mL in the different seed extracts. There was no statistically significant difference between the IC₅₀ values of EEG, MEG and AEG compared to galantamine. In particular, the results obtained revealed that EEG showed very potent BChE inhibitory activity, with IC₅₀ values (13.73 ± 1.31 µg/mL) close to those of the standard drug galantamine (IC₅₀ = 7.65 ± 1.78 µg/mL) calculated in the same experimental conditions. This can be considered a

satisfactory result since the standard inhibitor is a single molecule while a mixture of numerous compounds exists in the plant extracts. The percentage of inhibition activity against BChE of a procyanidin B1 standard at a concentration of 20 $\mu\text{g/mL}$ was also checked obtaining a value of $18.98 \pm 2.52 \%$. Thus, anti-BChE activity observed in seed extracts cannot be mainly attributed to procyanidin B1, even if it is present in high concentration. However, our findings lead us to consider that this compound could contribute to the anti-BChE effect in these extracts. Several studies on plant AChE inhibitors have been performed, however, fewer BChE inhibitors have been identified. No ChE inhibitory activity was found for any of the pulp extracts examined. ChEs inhibition has been extensively used as approach for the treatment of AD. BChE activity progressively increases in patients with AD, while AChE activity remains unchanged or declines. Therefore, the use of molecules selectively interacting with BChE might have a relevant role in treatment of patients with advanced AD.

3.4.5 α -Amylase and α -Glucosidase inhibition

The ability of the extracts of *W. filifera* seeds to restrict α -amylase and α -glucosidase activities was evaluated and the results are reported in Table 12. All extracts exhibited potent inhibitory activity on α -glucosidase. The IC_{50} values are statistically lower than that of the reference inhibitor, ranging from 0.53 ± 0.014 to $1.63 \pm 0.23 \mu\text{g/mL}$. In particular, the α -glucosidase inhibitory activity of the MEG was found to be ~ 170 times

more active than acarbose. As can be observed in Table 12, some extracts inhibited α -amylase with a higher potency than the standard acarbose. MES showed the highest α -amylase inhibitory activity with IC_{50} 2.39 ± 0.23 $\mu\text{g/mL}$. The main compounds identified until now in the extracts of *W. filifera* seeds, i.e. B-type procyanidin dimers (B1-B4), catechin, protocatechuic acid, and *p*-hydroxybenzoic acid, have reveal to possess an inhibitory effect against α -amylase and α -glucosidase. Each compound showed an IC_{50} value higher than that shown by the MES. In fact, the inhibitory activity against α -amylase of compounds mentioned above seems to be in the order of mg/mL, with IC_{50} values of 1.78 ± 0.07 mg/mL for protocatechuic acid, 1.94 ± 0.09 mg/mL for *p*-hydroxybenzoic acid and 2.44 ± 0.11 mg/mL for catechin. The inhibitory activity against α -glucosidase is also lower than that showed by MES, with IC_{50} values of 63.37 ± 4.10 $\mu\text{g/mL}$, 58.68 ± 4.20 $\mu\text{g/mL}$ and 3.89 ± 0.12 $\mu\text{g/mL}$ respectively (Tan et al., 2017).

The synergic action of these compounds could contribute to explain the significant inhibition of the *W. filifera* methanolic extract against α -amylase and α -glucosidase.

Table 12. IC₅₀ values of *W. filifera* extracts against α -glucosidase and α -amylase.

Extracts	IC ₅₀ μ g/mL	IC ₅₀ μ g/mL
	α -glucosidase	α -amylase
EEG	1.54±0.11 ^a	11.33±1.99 ^a
EES	0.72±0.41 ^a	3.73±0.45 ^b
MEG	0.53±0.014 ^a	6.75±0.11 ^{b, c}
MES	0.88±0.028 ^a	2.39±0.23 ^b
AEG	1.63±0.23 ^a	48.32±1.32 ^d
AES	0.82±0.085 ^a	25.82±0.13 ^d
Acarbose	90±7.3 ^b	8.04±0.65 ^{a, c}

Mean values in the same column having different letters are significantly different ($P < 0.05$).

Table 13 shows that EEG acts as a competitive inhibitor against α -glucosidase. In fact, by increasing the concentration of extract, a family of straight lines with different slope, all intersecting on the y-axis, was found (Figure 19A). This kinetic analysis indicates that the extract binds with the free enzyme and the equilibrium constant, $K_i = 0.08 \mu\text{g/mL}$, was obtained from the slope (K_m/V_{max}) versus inhibitor concentration.

Table 13. Enzyme kinetics parameters following α -glucosidase and α -amylase with different *W. filifera* seed extracts.

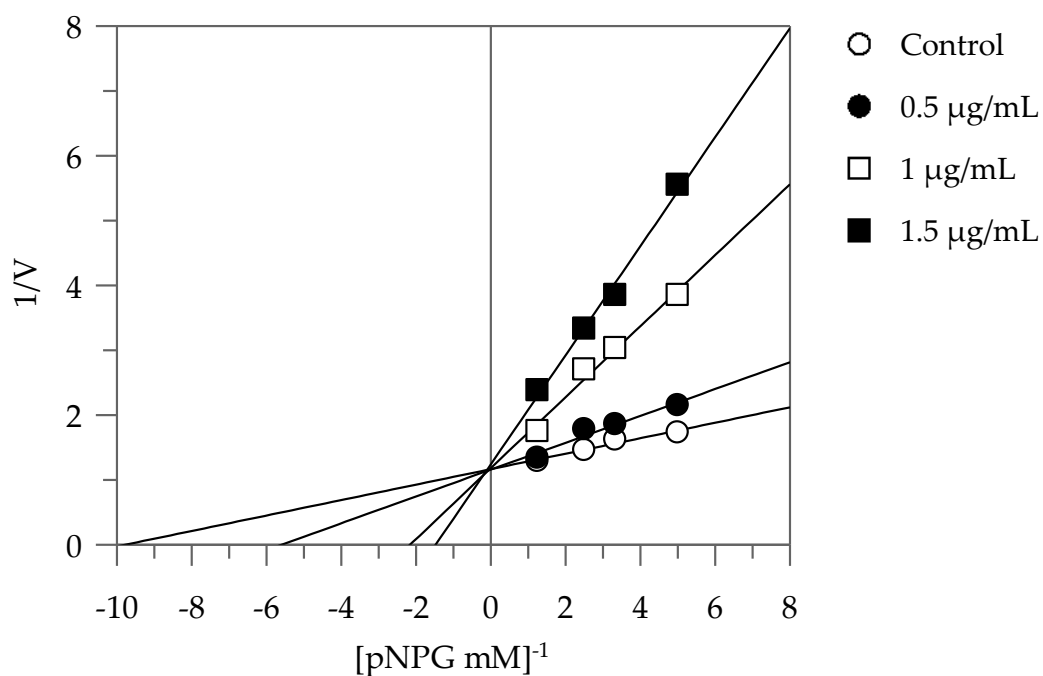
	K_i $\mu\text{g/mL}$	K_{is} $\mu\text{g/mL}$	Inhibition type
<i>α-glucosidase</i>			
EEG	0.08	-	Competitive
EES	0.22	0.41	Mixed
MEG	0.08	1.8	Mixed
MES	0.03	0.48	Mixed
AEG	0.07	0.41	Mixed
AES	0.31	1.74	Mixed
<i>α-amylase</i>			
EES	-	2.47	uncompetitive
MES	-	3.66	uncompetitive

The EES showed a different mode of inhibition if compared to the other alcoholic extract, although the composition of alcoholic extracts of the seeds is the same. The different type of inhibition is probably due to the relative quantity of the compounds in the extract.

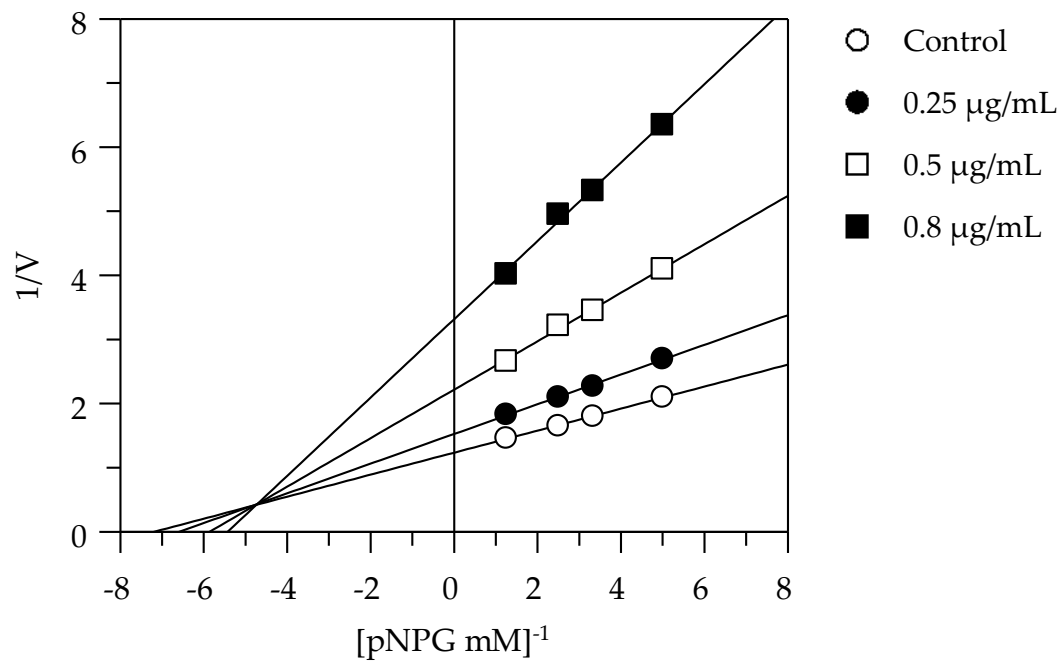
The Lineweaver-Burk plots of the other extracts showed a mixed type of inhibition characteristics, since increasing the concentration of extracts resulted in a family of straight lines with different slope and y-intercepts, which intersected in the second quadrant, as shown in Figure 19 (B-F). This kinetic analysis indicates that these extracts can bind not only with

the free enzyme but also with the enzyme-substrate complex. The equilibrium constants for binding with the free enzyme (K_I) and with the enzyme-substrate complex (K_{IS}) were obtained from the slope (K_m/V_{max}) or the $1/V_{max}$ values (y -intercepts) versus inhibitor concentration, respectively (Table 13).

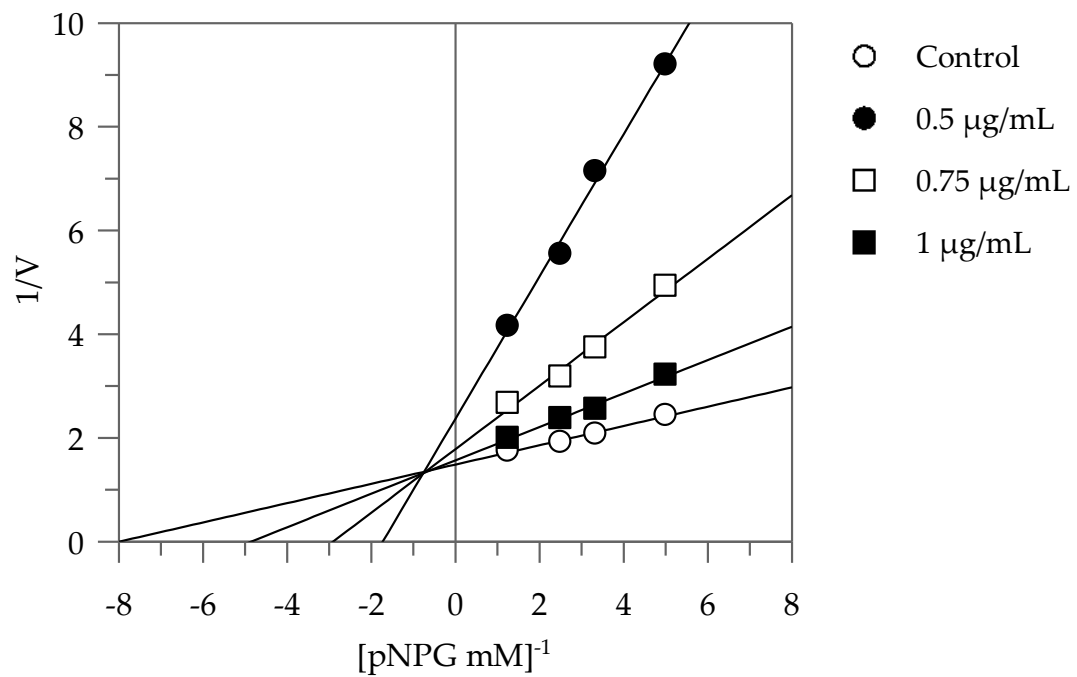
A



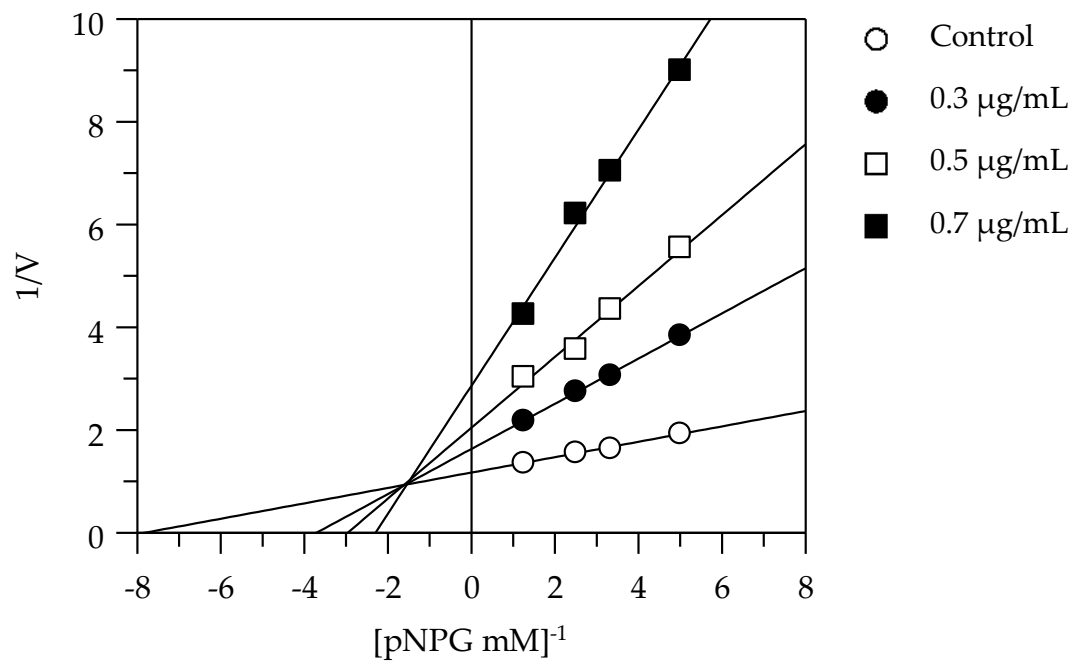
B



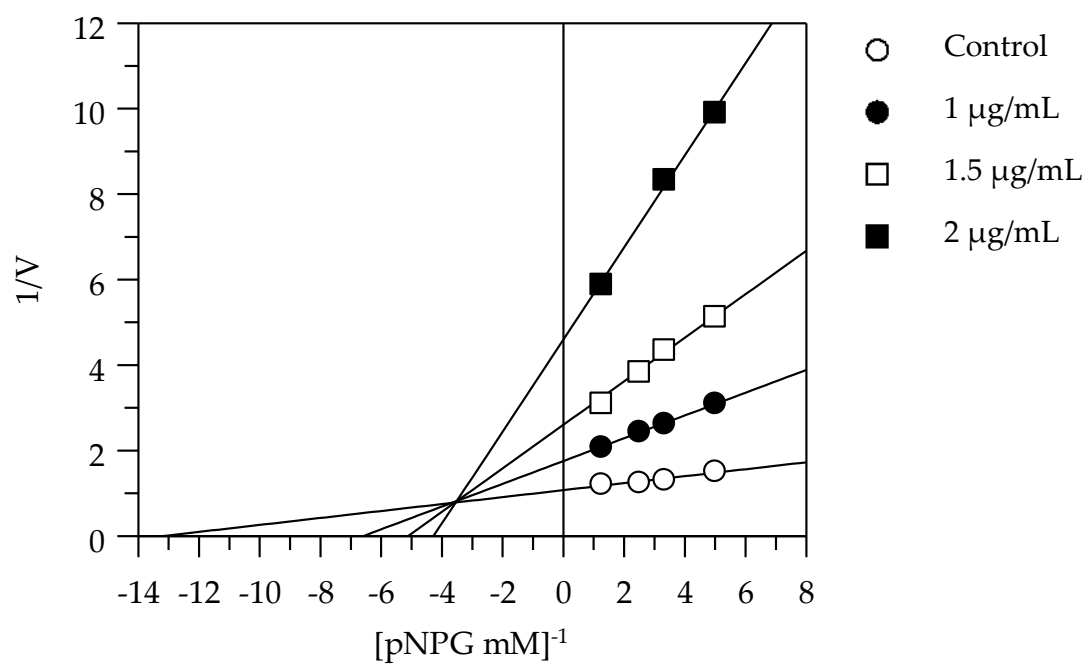
C



D



E



F

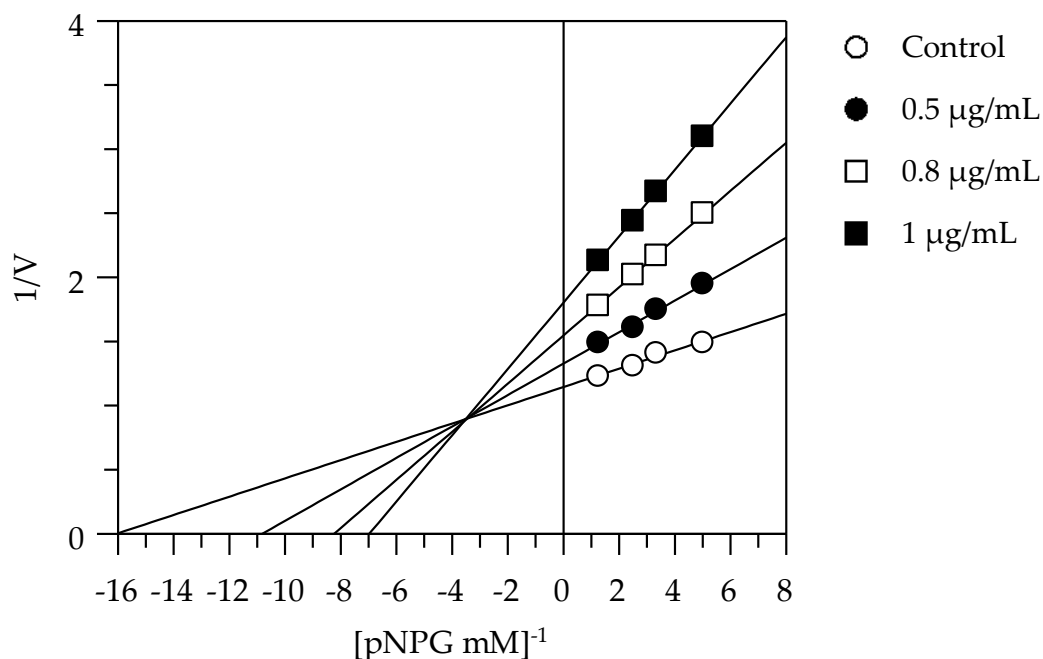
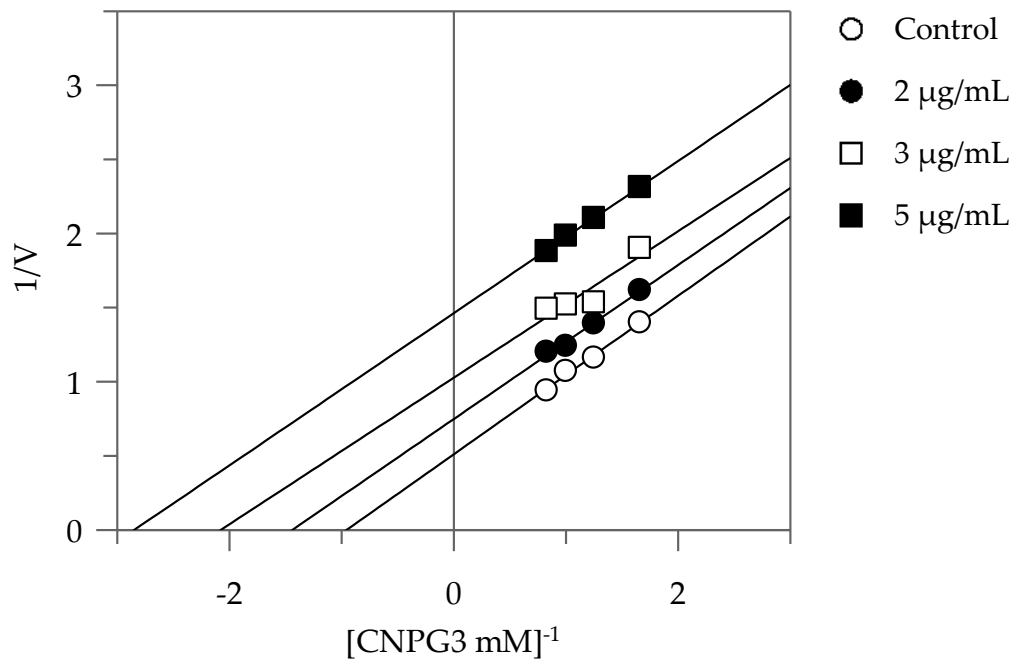


Figure 19. Inhibition of α -glucosidase enzyme. Lineweaver–Burk plots analysis of EEG (A), EES (B), MEG (C), MES (D), AEG (E) and AES (F).

The extracts with higher inhibitory activity against α -amylase, EES, and MES, behave with an uncompetitive inhibition, since the kinetic analysis of these extracts, produces a family of parallel lines for increasing extracts concentration (Figure 20). The equilibrium constant for binding with the enzyme-substrate complex (K_{IS}) was calculated from the replotting of the intercepts ($1/V_{\max}$) versus the inhibitor concentration, resulting in a value of 2.47 and 3.66 $\mu\text{g/mL}$ for EES and MES, respectively (Table 13).

A



B

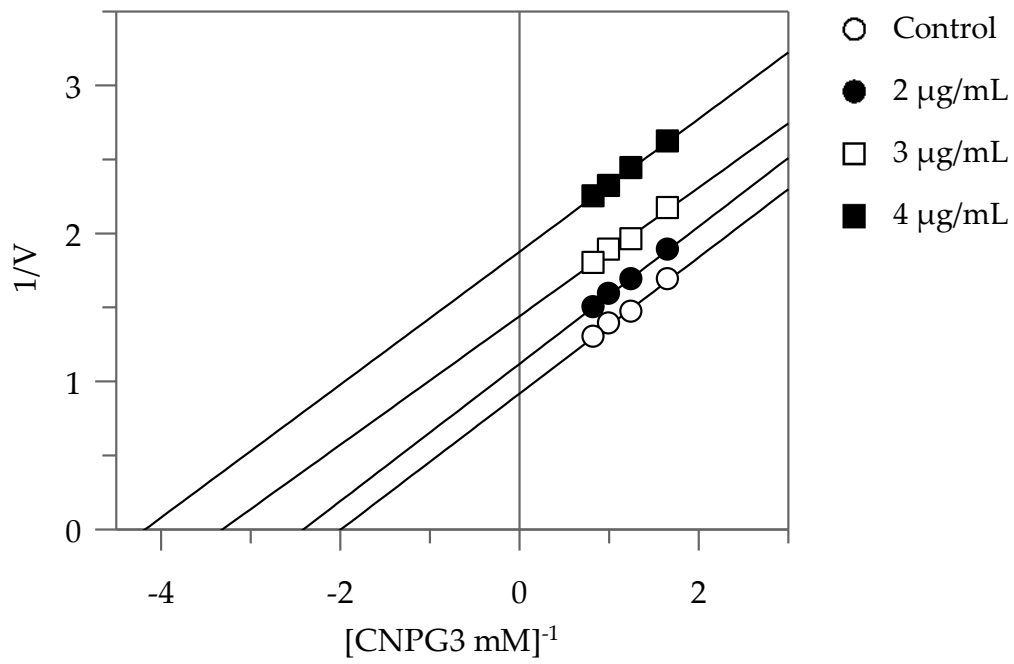


Figure 20. Inhibition of α -amylase enzyme. Lineweaver–Burk plots analysis of EES (A) and MES (B).

W. filifera methanolic seeds extract from Sousse (MES) showed to be as the overall best extract, having the highest inhibitory activity against α -amylase and among the lowest IC₅₀ values for α -glucosidase (100-fold lower than acarbose).

Moreover, acarbose is one of the therapeutic drugs used for the treatment of hyperglycaemia in T2D patients but several side effects generally occur, probably due to a more significant inhibition of α -amylase if compared to α -glucosidase inhibition (Oboh et al., 2016). MES instead showed a better inhibition against α -glucosidase showing also a lower ratio between α -glucosidase and α -amylase inhibition, making this extract as a good candidate for further deeper study.

3.4.6 Inhibition of IAPP aggregate formation

In order to identify and quantify IAPP amyloid fibrils, MES was also tested for the ThT assay. The methanolic extract showed complete inhibition of fibrils formation at 1:5 (IAPP 40 μ g/mL:MES 200 μ g/mL) and 1:10 (IAPP 40 μ g/mL:MES 400 μ g/mL) ratio (Figure 21). In fact, the corresponding curves appear flat and superimposed, meaning that there is no formation of fibrils. There is also a delay at 1:1 (IAPP 40 μ g/mL:MES 40 μ g/mL) ratio on fibril formation, made evident by the shifting of the curve that is smaller by decreasing the concentration of the extract,

highlighting that the inhibition is dose-dependent. The ThT assay was repeated three times and extended up to 150 hours.

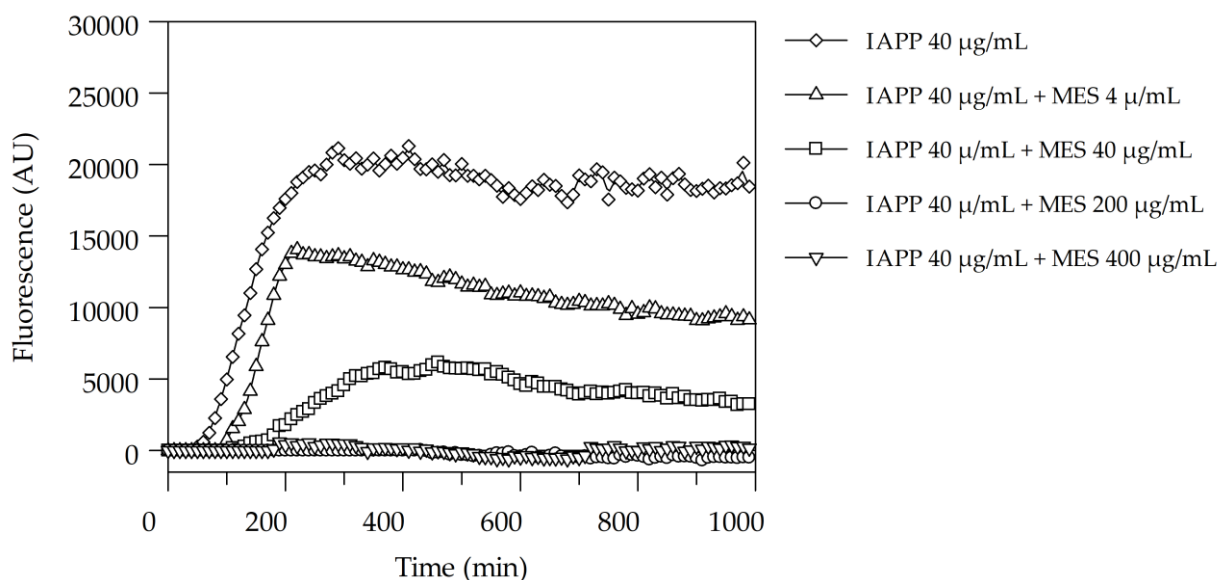


Figure 21. Thioflavin T fluorescence emission plot corresponding to β -sheet formation of IAPP in the presence of *W. filifera* methanolic seeds extract from Sousse.

Congo red staining was performed to visualize the presence of amyloid fibrils. Congo red staining of solution 1:5 (IAPP 40µg/mL:MES 200 µg/mL) was negative and confirmed that inhibition of IAPP fibrillation was inhibited.

In addition, negative staining was made for analysis by TEM. Figure 22 showed that at 1:5 IAPP to extract ratio (MES 200 µg/mL), the formation of IAPP fibrils is inhibited.

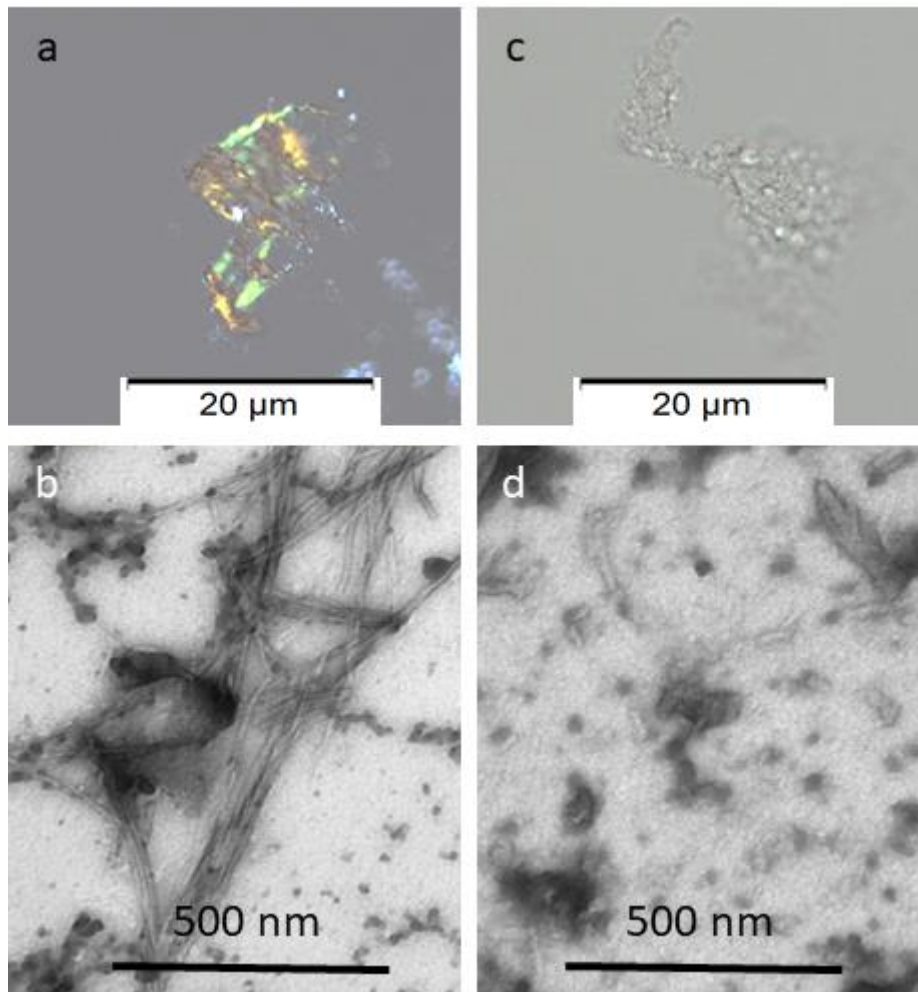


Figure 22. Congo red and Electron microscopy analyses of the material recovered after ThT analysis. In **(a)**, amyloid exhibiting green birefringence after Congo red staining and **(b)** long unbranched amyloid fibrils are present in solution of IAPP 40 $\mu\text{g}/\text{mL}$. In **(c)**, no Congophilic material can be detected and in **(d)** an amorphous material is present in solution containing IAPP 40 $\mu\text{g}/\text{mL}$ with MES 200 $\mu\text{g}/\text{mL}$. Samples in **a** and **c** are stained with Congo red and samples in **b** and **d** are negatively contrasted with 2% Uranyl acetate in 50% ethanol.

3.4.7 Cell viability and intracellular ROS level

The antioxidant activities of extracts using a spectrophotometric method revealed seeds to be good sources of phenolic compounds with antioxidant properties. In particular MEG showed the best activity, indeed, considering its great antioxidant potential and its good inhibitory activity against the enzyme tested, we decided to confirm the antioxidant capacity of MEG in a cellular model.

First, the effects of the *W. filifera* extract on cell viability in HaCaT cells was investigated. HaCaT cells are the immortalized human keratinocytes and has been extensively used to study the epidermal homeostasis (Schurer et al., 1993). In order to determine the safety of this extract, cells were treated with various concentration of sample for 24 h and were examined using MTT test. The results indicated that the extract was not cytotoxic in HaCaT cells and only a little decrease (viability of 80 %) was observed at 100 $\mu\text{g}/\text{mL}$ (Figure 23).

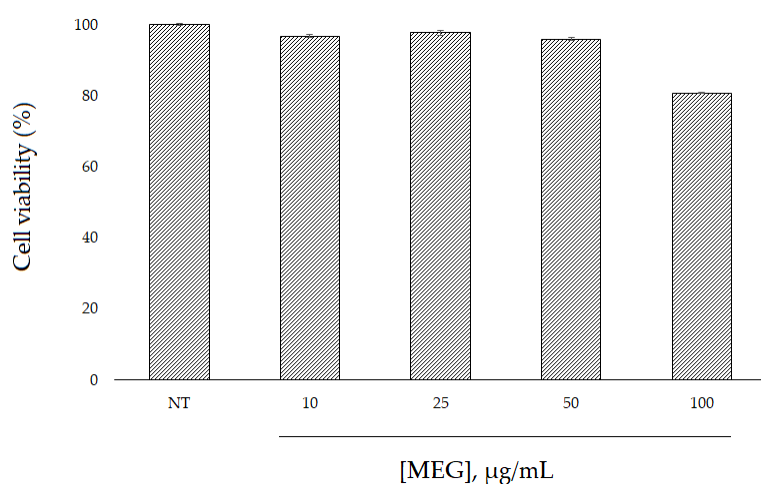


Figure 23. Effect of MEG on HaCat cell viability. After 24 h incubation with the extract at different concentrations, cell viability was determined by MTT assay.

Since the viability was not affected until 50 $\mu\text{g}/\text{mL}$ (viability of 96 %), we decided to perform further cellular experiment using up to this extract concentration. We evaluated ROS levels in cells before and after oxidative stress and after treatment with MEG. The study was conducted using DCFHDA, which easily diffuses through the cell membrane and is hydrolyzed by the endogenous esterases to DCFH. Rapid increases in DCF indicate the oxidation of DCFH by intracellular ROS such as H_2O_2 . As shown in Figure 24, H_2O_2 incubation significantly increased ROS formation in HaCaT cells, but treatment with extract decreased H_2O_2 -induced ROS production in a dose-response manner. Thus, these results confirm the antioxidant assays and suggest that MEG may also reduce the formation of ROS in cells.

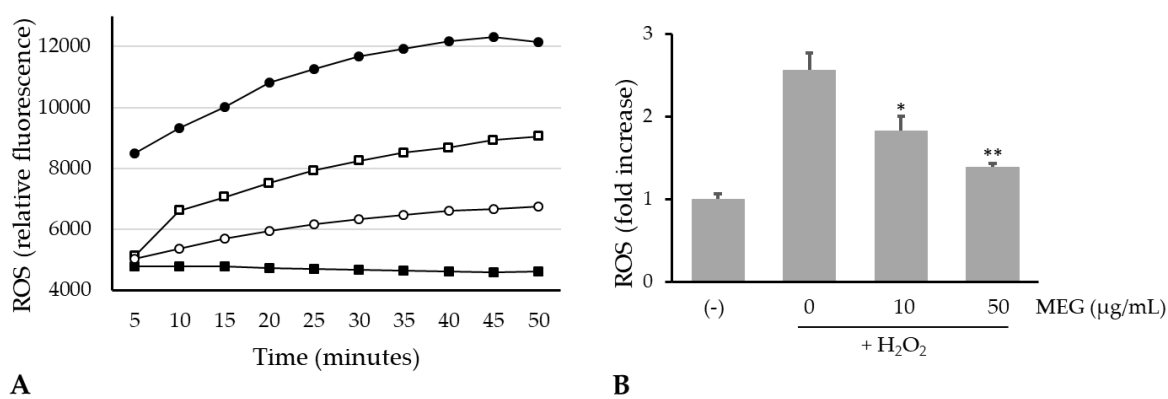


Figure 24. Inhibition of H_2O_2 -induced ROS generation by MEG on HaCaT cells. A) ROS levels (expressed as DCF fluorescence) in HaCaT cells pretreated with MEG and incubated with 1 mM H_2O_2 up to 50 minutes. (■): untreated cells, (●): 1 mM H_2O_2 , (□): 10 $\mu\text{g}/\text{mL}$ MEG + H_2O_2 , (○): 50 $\mu\text{g}/\text{mL}$ MEG + H_2O_2 . B). Effect of MEG on ROS production in HaCaT cells after 30 minutes treatment with 1 mM H_2O_2 . Data (means \pm SE) are normalized to untreated controls. * $p < 0.01$ and ** $p < 0.001$ compared to the H_2O_2 treated group.

B-type procyanidins were the main phenolic compounds identified; these exhibit a wide range of biological, pharmacological and chemoprotective properties against oxygen free radicals (Bagchi et al., 2000; de la Iglesia et al., 2010). Previous study has shown that the anti-radical activity of procyanidins is strong at high concentrations. Antioxidant activity is dependent on the structure of the free radical-scavenging compounds, the substituents present on the rings of the flavanoids and the degree of polymerization. Although there is some debate as to whether the degree of polymerization increases the antioxidant capacity, it appears that epicatechin and epicatechin polymers are better antioxidant than catechin and catechin polymers and the B procyanidins are better antioxidants than the A procyanidins (Wood et al., 2002). Moreover, procyanidins extract are more effective superoxide radical-scavengers than the antioxidant vitamin C and Trolox (Bagchi et al., 1997).

3.5 Molecular docking

Molecular docking is a powerful technique that allows predicting and identifying the most probable binding mode of the ligand to a partner protein. Therefore, to predict the best ligand pose within the XO binding site we performed docking of ligand procyanidin B1 and B2, which consists of catechin and epicatechin units joined in a beta-configuration. For comparison, docking of ligands catechin and epicatechin, which are the elementary flavan-3-ol units in these dimers, was also checked.

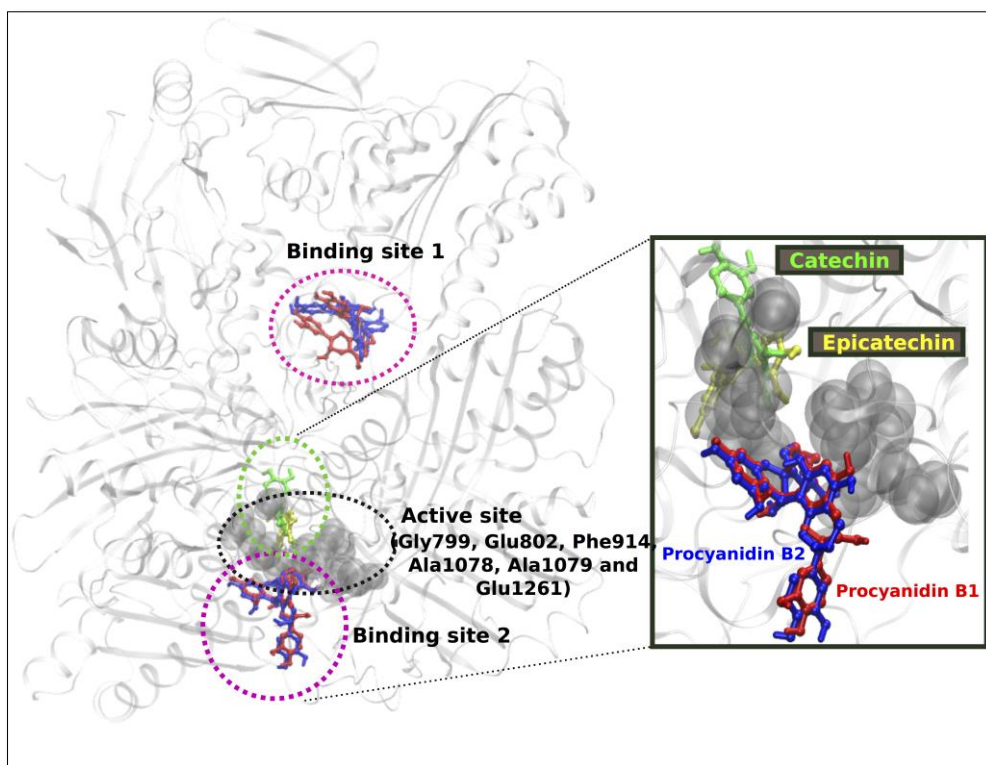


Figure 25. Predicted docked positions for the ligands bound to XO protein. The active site residues are shown as grey Van der Waals sphere (grey). Two probable binding sites 1 and 2 for ligands procyanidin B1 (red) and B2 (blue) are circled in pink, while the binding region for ligands catechin (green) and epicatechin (yellow) within green circle. In the rectangular box, a zoomed representation of the binding region for the ligands close to the active site is shown.

For procyanidin ligands (B1, B2) two most probable binding sites (Figure 25) was observed. Binding site 1, which is located distant from the protein active site exhibits the best docking energy values for both the ligands (Table 14). We observe a reasonable overlap in ligand poses, with procyanidin B1 displaying a favorable docking energy.

Table 14. Summary of predicted docking energies for ligands bound to XO. In column 3 confidence score (C-score) of the predicted binding residues, associated with specific ligand-binding clusters. In column 4, we report the cluster size that represents the population number of ligand structures specific to a binding site.

Protein – Ligand	Docking Energy (kcal/mol)	C-Score	Cluster size
XO – Procyanidin B1	-4.6 (Site 1)	0.12	28
	-2.7 (Site 2)	0.22	41
XO – Procyanidin B2	-3.8 (Site 1)	0.12	28
	-3.0 (Site 2)	0.22	41
XO – Catechin	-8.6 kcal/mol	0.19	30
XO – Epicatechin	-9.2 kcal/mol	0.15	28

On the other hand, binding site 2 (Figure 25) for both procyanidin ligands (B1, B2) was found to be near the XO protein active site. Interestingly, the binding region for the ligands catechin and epicatechin are in the active site and in close vicinity to the binding site 2 of procyanidin ligands.

Experimental data performed on seed extracts indicated a mixed-type inhibition against XO-enzyme. Now, considering that the concentration of procyanidin is pronounced (among the dimers) in the seed extracts, a

plausible explanation for mixed-type inhibition can be established from the spatial location of the predicted binding sites (different from the active site) for the procyanidin ligands.

To delve into the binding mode of the ligands with XO protein, further examination was made using Ligplot software, which revealed a conserved interaction picture regarding XO binding for both procyanidins B1 and B2 (Figure 26) and for catechin and epicatechin (Figure 27).

For the binding site 1 (Figure 26 a-b), we note two additional interactions involving residues Leu 147, Ile 1229 and Pro 1230 and procyanidin B1, thus confirming better docking energy value with respect to procyanidin B2. On the other hand, for binding site 2, a good overlap between the ligands poses is confirmed by a conserved interaction picture (Figure 26 c-d).

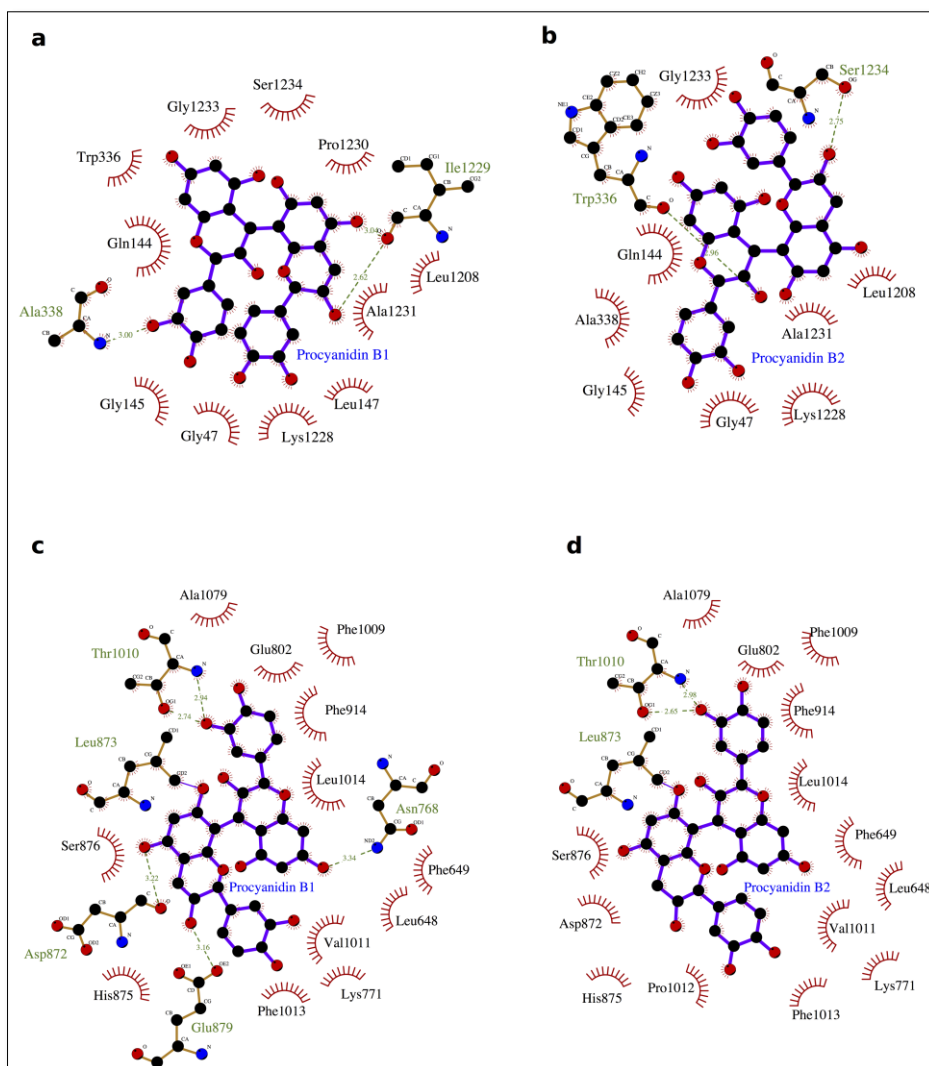


Figure 26. Procyanidin ligands B1 and B2 bound to XO protein. In a) and b) ligand poses in the binding site 1, while in (c), (d) in the binding site 2. Hydrophobic interactions are represented by red spokes radiating towards the interacting ligand atoms, while hydrogen-bonded interaction with dashed green line.

Well-conserved binding regions for ligands catechin and epicatechin (Figure 27) involving interactions with amino acid residues Gly799, Glu802, Phe914, Ala1078, Ala1079 and Glu1261 in the active site confirmed

significantly better docking energy with respect to the procyanidin ligands (B1, B2).

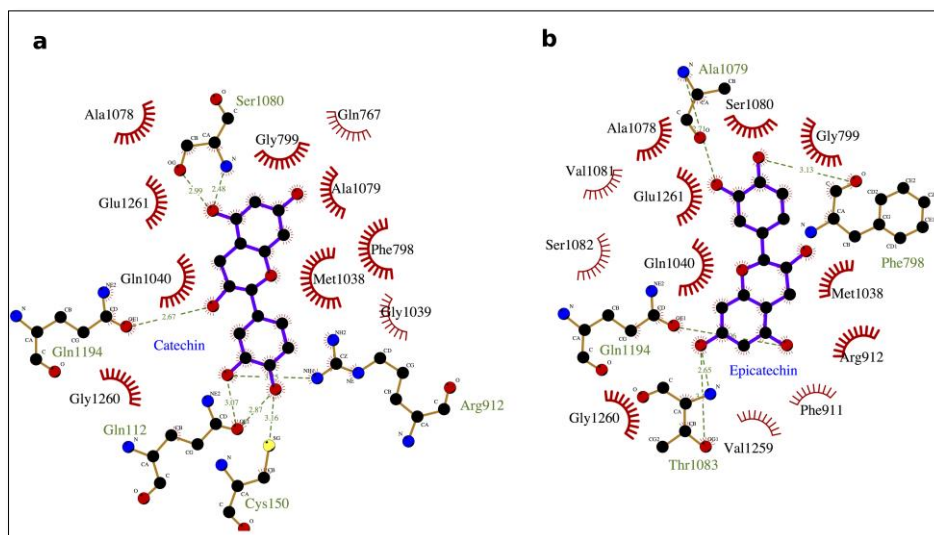


Figure 27. Interaction picture of ligands catechin and epicatechin bound to XO protein. Hydrophobic interactions are represented by red spokes radiating towards the interacting ligand atoms, while hydrogen-bonded interaction with dashed green line.

The main compounds identified in *W. filifera* seeds were also subjected to docking simulations to determine their binding affinities against IAPP, α -amylase and α -glucosidase. The binding affinity data of the compounds are presented in Table 15.

Table 15. Binding energies of identified *W. filifera* compounds against IAPP, α -amylase and α -glucosidase.

	IAPP	α-amylase	α-glucosidase
Catechin	-6.9 kcal/mol	-7.1 kcal/mol	-8.1 kcal/mol
Protocatechuic acid	-4.9 kcal/mol	-5.5 kcal/mol	-5.3 kcal/mol
<i>p</i>-Hydroxybenzoic acid	-4.5 kcal/mol	-5.2 kcal/mol	-5.2 kcal/mol
B type Procyanidin dimer	-7.8 kcal/mol	-8.5 kcal/mol	-4.9 kcal/mol

The binding affinity of the compounds ranges from -4.5 to -7.8 kcal/mol towards IAPP, from -5.2 kcal/mol to -8.5 kcal/mol for the α -amylase and ranging from -4.9 kcal/mol to -8.1 kcal/mol regarding α -glucosidase. Among the four compounds, catechin displayed better binding energy values for all the three protein targets.

An investigation of the physicochemical properties of the main compounds identified in this extract is reported in Table 16.

Table 16. Physicochemical properties of bioactive compounds in the investigated extracts.

	Molecular formula	Molecular Weight (g/mol)	Rotatable bonds	H-bond acceptor atoms	H-bond donor atoms	Polar surface area (Å²)	LogP_{o/w}	Water solubility
Catechin	C ₁₅ H ₁₄ O ₆	290.27	1	6	5	110.38	0.85	Soluble
Epicatechin	C ₁₅ H ₁₄ O ₆	290.27	1	6	5	110.38	0.85	Soluble
Protocatechuic acid	C ₇ H ₆ O ₄	154.12	1	4	3	77.76	0.65	Soluble
<i>p</i>-Hydroxybenzoic acid	C ₇ H ₆ O ₃	138.12	1	3	2	57.53	1.05	Soluble
Procyanidin B-type	C ₃₀ H ₂₆ O ₁₂	578.52	3	12	10	220.76	1.37	Soluble
Procyanidin A-type	C ₃₀ H ₂₄ O ₁₂	576.50	2	12	9	209.76	1.61	Moderately
Quercetin-3-O-glucoside	C ₂₁ H ₂₀ O ₁₂	464.38	4	12	8	210.51	-0.27	Soluble
Dihydrokaempferol 7-glucoside	C ₂₁ H ₂₂ O ₁₁	450.39	4	11	7	186.37	-0.48	Soluble

4. CONCLUSIONS

Natural products from plants provide unlimited opportunities for new drugs because their chemical diversity could give rise to a range of biological activities. *W. filifera* seed extracts appeared to be a good source of phenolics and showed a significant antioxidant activity. The phenolic composition mainly consisted of procyanidin dimers B1–B4. *W. filifera* seeds have been revealed to possess a good antioxidant activity along with inhibitory activity against XO and aging key enzymes. Aging is mainly related to UV-induced damage of the connective tissue of the skin. UV rays cause oxidative stress which is responsible for the activation of the enzymes degrading the ECM and the appearance of wrinkles and age spots. *W. filifera* seeds extracts could act in the prevention of premature aging, acting simultaneously on several fronts: at the beginning of the process via their photoprotective effect and therefore reducing UV-rays absorption; then, they showed a good antioxidant effect with methanol extract preventing ROS formation in cellular system without cell toxicity; finally, all the extracts inhibit collagenase, elastase and tyrosinase, even if the latter with a minor extent.

Moreover, it is well known that free radicals and ROS play a major role in the development of oxidative stress that can lead to many illnesses, including T2D and AD. Indeed, oxidative stress is involved in neuronal damage, due to the neurodegeneration promoted by highly reactive compounds.

In this regard, *W. filifera* seeds showed a good cholinesterase inhibition, selective for butyrylcholinesterase, which is of interest, because in patients with AD, BChE activity progressively increases, while AChE activity remains unchanged.

The production of free radicals and ROS is also believed to be related with increasing hyperglycaemia that is associated with T2D. In this respect, *W. filifera* seed extracts showed significant inhibitory activities against α -amylase and α -glucosidase. In addition to these properties, the methanolic *W. filifera* seed extract showed a complete inhibition of the formation of the toxic IAPP aggregates. Since studies have reported the implication of IAPP in pancreatic β -islet cell death, the inhibition of amyloid aggregation becomes important in the prevention or progression of diabetes.

Considering the effect of *W. filifera* seed extracts on target enzymes for AD and the correlation between AD and T2D, *W. filifera* seeds can emerge as a promising natural source of bioactive compounds for these diseases.

Molecular docking studies allowed us to predict ligand binding sites on the surface of proteins and thus provided a plausible explanation to their type of inhibition. These findings should contribute to valorise *W. filifera* seeds as a source of bioactive compounds. Moreover, the result obtained will encourage further experiments in order to isolate the single active components with nutraceutical and therapeutic potential.

Overall, our results are of interest considering that seeds are an inedible part of the fruit that is discarded.

REFERENCES

- Ali H. S., Al-Omar M. A., Al-Khalifa A. R. S., Abdulla M. M., Ezzeldin E. and Amr A-G. E., Anti-Alzheimer Activity and Structure Activity Relationship of Some Synthesized Terpinoidal Oxaliplatin Analogs, *Am. J. Sci.* (2011); 7(9): 534-542.
- Anand P. and Singh B., A review on cholinesterase inhibitors for Alzheimer's disease, *Arch. Pharm. Res.* (2013); 36(4): 375-99.
- Anwar H., Hussain G. and Mustafa I., Antioxidants from Natural Sources", in *Antioxidants in Foods and Its Applications*, E. Shalaby and G. M. Azzam, Eds., pp. 3–28, IntechOpen, (2018).
- Bagchi D., Bagchi M., Stohs S.J., Das D.K., Ray S.D., Kuszynski C.A., Joshi S.S., Pruess H.G., Free radicals and grape seed proanthocyanidin extract: importance in human health and disease prevention, *Toxicology.* (2000); 148: 187–97.
- Bagchi D., Garg A., Krohn R.L., Bagchi M., Tran M.X., Stohs S.J., Oxygen free radical scavenging abilities of vitamins C and E, and a grape seed proanthocyanidin extract in vitro, *Res. Commun. Mol. Pathol. Pharmacol.* (1997); 95: 179–89.
- Benahmed-Bouhafsoun A., Djebbar H. and Kaid-Harche M., Determination of Polyphenolic Compounds of *Washingtonia robusta* H. Wendl Extracts, *A. Phys. Pol. A.* (2015); Vol.128: B-465.
- Boeing H., Bechthold A., Bub A., Ellinger S., Haller D., Kroke A., Leschik-Bonnet E., Muller M. J., Oberritter H., Schulze M., Stehle P.

- and Watzl B., Critical review: vegetables and fruit in the prevention of chronic diseases, *Eur J Nutr* (2012); 51: 637–663.
- Brás N.F., Gonçalves R., Fernandes P.A., Mateus N., Ramos M.J., de Freitas V., Understanding the binding of procyanidins to pancreatic elastase by experimental and computational methods, *Biochem.* (2010); 49: 5097–108.
 - Brás N.F., Gonçalves R., Mateus N., Fernandes P.A., Ramos M.J., de Freitas V., Inhibition of pancreatic elastase by polyphenolic compounds, *J. Agric. Food Chem.* (2010); 58: 10668–76.
 - Brodowska K. M., Natural flavonoids: classification, potential role, and application of flavonoid analogues, *EJBR* (2017); 7 (2): 108-123
 - Burns C. M. and Wortmann R. L., Latest evidence on gout management: what the clinician needs to know, *Ther Adv Chronic Dis* (2012); 3(6): 271-286.
 - Chandra S. R., Alzheimer's disease and other dementias: An alternative approach, *Indian J Med Res* (2017); 145(6): 723-729.
 - Chang C.-W. T., Takemoto J. Y., and Zhan J. Natural Bioactive Compounds, *Isr. J. Chem.* (2019); 59: 325-326.
 - Chang T.-S., An Updated Review of Tyrosinase Inhibitors *Int. J. Mol. Sci.* (2009); 10: 2440-2475.
 - Choi J. S., Islam Md. N., Ali Md. Y., Kim Y. M., Park H. J., Sohn H. S. and Jung H. A., The effects of C-glycosylation of luteolin on its antioxidant, anti-Alzheimer's disease, anti-diabetic, and anti-inflammatory, *Arch. Pharm. Res.* (2014); 37: 1354-1363.

- Chompoo J., Upadhyay A., Fukuta M., Tawata S., Effect of *Alpinia zerumbet* components on antioxidant and skin diseases-related enzymes, BMC Complement. Altern. Med. (2012); 12: 106.
- Cornett J.W., Nutritional Value of Desert Fan Palm Fruits, Principles, (1987); 31(4): 159-161.
- Cos P., Vlietinck A. J., Berghe D. V. and Maes L. Anti-infective potential of natural products: how to develop a stronger in vitro 'proof-of-concept', J. Ethnopharmacol. (2006); 106(3):290-302.
- Coyle J. and Kershaw P. Galantamine, a Cholinesterase Inhibitor that Allosterically Modulates Nicotinic Receptors: Effects on the Course of Alzheimer's Disease, Biol. Psychiatry (2001); 49: 289-299.
- de la Iglesia R., Milagro F.I., Campión J., Boqué N., Martínez J.A., Healthy properties of proanthocyanidins, Biofactors. (2010), 36, 159–68.
- De Lacerda De Oliveira L., de Carvalho M. V. and Melo L. Health promoting and sensory properties of phenolic compounds in food, Rev. Ceres, Viçosa (2014); 764-779.
- De Oliveira T. S., Vieira Thomaz D., da Silva Neri H. F., Bonancio Cerqueira L., Ferreira Garcia L., Vicente Gil H. P., Pontarolo R., Ramos Campos F., Alves Costa E., Alcantara dos Santos F. C., de Souza Gil E. and Ghedini P. C., Neuroprotective Effect of *Caryocar brasiliense* Camb. Leaves Is Associated with Anticholinesterase and Antioxidant Properties, Oxid. Med. Cell. Longev. (2018; 1-12.

- Delogu G. L., Matos M. J., Fanti M., Era B., Medda R., Pieroni E., Fais A., Kumar A. and F. Pintus, 2-Phenylbenzofuran derivatives as butyrylcholinesterase inhibitors: Synthesis, biological activity and molecular modelling, *Bioorg. Med. Chem. Lett.* (2016); 26(9): 2308-13.
- Di Majo D., La Guardia M., Leto G., Crescimanno M., Flandina C. and Giammanco M., Flavonols and flavan-3-ols as modulators of xanthine oxidase and manganese superoxide dismutase activity, *Int. J. Food. Sci. Nutr.*, (2014); 65(7): 886–892.
- Di Petrillo A., González-Paramás A. M., Era B., Medda R., Pintus F., Santos-Buelga C. and Fais A., Tyrosinase inhibition and antioxidant properties of *Asphodelus microcarpus* extracts, *BMC Complement. Altern. Med.* (2016); 16(1): 453.
- Di Petrillo A.; González-Paramás A.M., Rosa A., Ruggiero V., Boylan F., Kumar A., Pintus F., Santos-Buelga C., Fais A., Era B., Chemical composition and enzyme inhibition of *Phytolacca dioica* L. seeds extracts, *J. Enzyme Inhib. Med. Chem.* (2019); 34: 519-527.
- Ellman G. L., Courtney K. D., Andres V. J and Feather-Stone R. M., A new and rapid colorimetric determination of acetylcholinesterase activity, *Biochem. Pharmacol.* (1961); 7: 88-95.
- El-Sayed N. H., Ammar N. M., Al-Okbi S. Y., Abou El-Kassem L. T. and Mabry T. J., Antioxidant activity and two new flavonoids from *Washingtonia filifera*, *Nat. Prod. Res.* (2006); Vol. 20, No. 1: 57–61.

- Emmerson B., The Management of Gout, N. Engl. J. Med. (1996); 334: 445-451.
- Fais A., Era B., Asthana S., Sogos V., Medda R., Santana L., Uriarte E., Matos M.J., Delogu F, Kumar A. Coumarin derivatives as promising xanthine oxidase inhibitors, Int. J. Biol. Macromol. (2018); 120(Pt A): 1286-1293.
- Fais A., Era B., Di Petrillo A., Floris S., Piano D., Montoro P., Tuberoso C. I. G., Medda R. and Pintus F., Selected Enzyme Inhibitory Effects of *Euphorbia characias* Extracts, Biomed. Res. Int. (2018); 2018: 1219367.
- Feng L., Liu X., Zhu W., Guo F., Wu Y., Wang R., Chen K., Huang C. and Li Y., Inhibition of Human Neutrophil Elastase by Pentacyclic Triterpenes, PLoS One. (2013); 8(12): e82794.
- Geavlete P., Multescu R. and Geavlete B., *Serenoa repens* extract in the treatment of benign prostatic hyperplasia, Ther. Adv. Urol. (2011); 3(4): 193-198.
- Godin E., Nguyen P. T., Zottig X. and Bourgault X. S., Identification of a hinge residue controlling islet amyloid polypeptide self-assembly and cytotoxicity, J. Biol. Chem. (2019); 294(21): 8452–8463.
- Gonçalves S. and Romano A., Inhibitory Properties of Phenolic Compounds Against Enzymes Linked with Human Diseases, in Soto-Hernández, M. (ed), Phenolic Compounds - Biological Activity. IntechOpen (2017), London, pp. 99-118.

- Guaadaoui A., Benaicha S., Elmajdoub N., Bellaoui M., Hamal A., What is a bioactive compound? A combined definition for a preliminary consensus, *Int. J. Food. Sci. Nutr.* (2014); 3(3): 174-179.
- Harborne J. B., Flavonoid sulphates: A new class of sulphur compounds in higher plants, *Phytochem.* (1975); Vol. 14: 1147-1155.
- Hemmati A. A., Kalantari H., Siahpoosh A., Ghorbanzadeh B. and Jamali H., Anti-inflammatory Effect of Hydroalcoholic Extract of the *Washingtonia filifera* Seeds in Carrageenan-Induced Paw Edema in Rats, *Jundishapur J. Nat. Pharm Prod.* (2015); 10(1): e19887.
- Hudson S. A., Ecroyd H., Kee T. W. and Carver J. A., The thioflavin T fluorescence assay for amyloid fibril detection can be biased by the presence of exogenous compounds, *FEBS J.* (2009); 276(20): 5960-72.
- Hussein R. A. and El-Anssary A. A, Plants Secondary Metabolites: The Key Drivers of the Pharmacological Actions of Medicinal Plants, in P. Builders (Ed.), *Herbal Medicine*. Intech Open (2018); pp. 11–30.
- Itoh S., Yamaguchi M., Shigeyama K., Sakaguchi I., The Anti-Aging Potential of Extracts from *Chaenomeles sinensis*, *Cosmetics* (2019): 6: 21.
- Jabir N. R., Khan F. R., Tabrez S., Cholinesterase targeting by polyphenols: A therapeutic approach for the treatment of Alzheimer's disease, *CNS Neurosci Ther.* (2018); 24: 753–762
- Jackson J. K., Zhao J., Wong W. and Burt H. M., The inhibition of collagenase induced degradation of collagen by the galloyl-

- containing polyphenols tannic acid, epigallocatechin gallate and epicatechin gallate, *J Mater Sci: Mater Med* (2010); 21: 1435–1443.
- Jeong W-S and Kong A-N T., Biological Properties of Monomeric and Polymeric Catechins: Green Tea Catechins and Procyanidins, *Pharm. Biol.* (2004); Vol. 42: Supp,84–93.
 - Kim J. H., Lee S-H, Lee H. W., Sun Y. N., Jang W-H., Yang S-Y., Jang H-D. and Kim, Y. H., (-)-Epicatechin derivate from *Orostachys japonicus* as potential inhibitor of the human butyrylcholinesterase, *Int. J. Biol. Macromol.* (2016); 91: 1033-9.
 - Kolar F. R., Kamble V. S. and Dixit G. B., Phytochemical constituents and antioxidant potential of some underused fruits, *Afr. J. Pharm. Pharmacol.* (2011); Vol. 5(18): 2067-2072.
 - Koparde A. A., Doijad R. C. and Magdum C. S., Natural Products in Drug Discovery” in *Pharmacognosy – Medicinal Plants*, IntechOpen (2019), London, UK, pp. 1–20.
 - Kumar A., Pintus F., Di Petrillo A., Medda R., Caria P., Matos M. J., Viña D., Pieroni E., Delogu F., Era B., Delogu G. L. and Fais A., Novel 2-pheynlbenzofuran derivatives as selective butyrylcholinesterase inhibitors for Alzheimer's disease, *Sci. Rep.* (2018); 8(1): 4424.
 - Kumar N. and Goel N., Phenolic acids: Natural versatile molecules with promising therapeutic applications, *Biotechnology Reports* (2019); 24: e00370.

- Kumar S. and Pandey A. K., Chemistry and Biological Activities of Flavonoids: An Overview, *Scientific World Journal*. (2013); 2013: 162750.
- Li K., Yao F., Xue Q., Fan H., Yang L., Li X., Sun L. and Liu Y., Inhibitory effects against α -glucosidase and α -amylase of the flavonoids-rich extract from *Scutellaria baicalensis* shoots and interpretation of structure–activity relationship of its eight flavonoids by a refined assign-score method, *Chem. Cent. J.* (2018); 12(1): 82.
- Ling Z-Q., Xie B-J. and Yang E-L., Isolation, characterization, and determination of antioxidative activity of oligomeric procyanidins from the seedpod of *Nelumbo nucifera* Gaertn, *J. Agric. Food. Chem.* (2005); 53(7): 2441-5.
- Liu R. H., Health benefits of fruit and vegetables are from additive and synergistic combinations of phytochemicals, *Am. J. Clin. Nutr.* (2003);78(suppl):517S–20S.
- López-Lázaro M., Distribution and Biological Activities of the Flavonoid Luteolin, *Mini Rev Med Chem.* (2009); 9(1): 31-59.
- Lu P., Takai K., Weaver V. M, and Werb Z., Extracellular Matrix Degradation and Remodeling in Development and Disease, *Cold Spring Harb. Perspect. Biol.* (2011); 3: a005058.
- Madan K. and Nanda S. In-vitro evaluation of antioxidant, anti-elastase, anti-collagenase, anti-hyaluronidase activities of safranal

- and determination of its sun protection factor in skin photoaging, *Bioorg. Chem.* (2018); 77: 159-167.
- Mansur JS., Breder MNR., Mansur MCA., Azulay RD., Determinação Do Fator De Proteção Solar Por Espectrofotometria, *An. Bras. Dermatol. Rio De Janeiro* (1986); 61: 121-4.
 - Moini H., Guo Q. and Packer L., Enzyme inhibition and protein-binding action of the procyanidin-rich french maritime pine bark extract, pycnogenol: effect on xanthine oxidase, *J. Agric. Food. Chem.* (2000); 48(11): 5630-9.
 - Mosmann T., Rapid colorimetric assay for cellular growth and survival: application to proliferation and cytotoxicity assays, *J. Immunol. Methods* (1983); 65(1-2): 55-63.
 - Moukette B. M., Moor V. J. A., Nya C. P. B., Nanfack P., Nzufo F. Ta., Kenfack M. A., Ngogang J. Y., and Pieme C. A., Antioxidant and Synergistic Antidiabetic Activities of a Three-Plant Preparation Used in Cameroon Folk Medicine, *Int. Sch. Res. Notices.* (2017); 2017: 9501675.
 - Mushtaq S., Abbasi B. H., Uzair B., Abbasi R., Natural Products as Reservoirs of Novel Therapeutic Agents, *EXCLI Journal* (2018); 17: 420-451
 - Nehdi I. A., Characteristics and composition of *Washingtonia filifera* (Linden ex André) H.Wendl. seed and seed oil, *Food Chem.* (2011); 126: 197–202.

- Nile S. H., Ko E. Y., Kim D. H. and Keum Y-S., Screening of ferulic acid related compounds as inhibitors of xanthine oxidase and cyclooxygenase-2 with anti-inflammatory activity, *Rev. Bras. Farmacogn.* (2016);26: 50–55.
- Nita M. and Grzybowski A., The Role of the Reactive Oxygen Species and Oxidative Stress in the Pathomechanism of the Age-Related Ocular Diseases and Other Pathologies of the Anterior and Posterior Eye Segments in Adults, *Oxid. Med. Cell. Longev.* (2016); 3164734.
- Paulsson J. F., Andersson A., Westermark P. and Westermark G. T., Intracellular amyloid-like deposits contain unprocessed pro-islet amyloid polypeptide (proIAPP) in beta cells of transgenic mice overexpressing the gene for human IAPP and transplanted human islets, *Diabetologia* 49 (2006); 1237–1246.
- Phaniendra A., Jestadi D. B. and Periyasamy L., Free Radicals: Properties, Sources, Targets, and Their Implication in Various Diseases, *Ind. J. Clin. Biochem.* (2015); 30(1): 11–26.
- Pintus F., Spanò D., Corona A. and Medda R., Antityrosinase activity of *Euphorbia characias* extracts *Peer J.* (2015); 3: e1305.
- Rani K., Role of antioxidants in prevention of diseases, *Appl. Biotechnol. Bioeng.* (2017); 4(1): 495–496.
- Rosa A., Caprioglio D., Isola R., Nieddu M., Appendino G. and Falchi A. M., Dietary zerumbone from shampoo ginger: new

- insights into its antioxidant and anticancer activity, *Food Funct.* (2019); 10(3): 1629-1642.
- Rosa A., Maxia A., D. Putzu, A. Atzeri, B. Era, A. Fais, C. Sanna and A. Piras., Chemical composition of *Lycium europaeum* fruit oil obtained by supercritical CO₂ extraction and evaluation of its antioxidant activity, cytotoxicity and cell absorption", *Food Chem.*, (2017); 230: 82–90.
 - Rue E. A., Rush M. D., van Breemen and R. B., Procyanidins: a comprehensive review encompassing structure elucidation via mass spectrometry, *Phytochem Rev.* (2018); 17(1): 1–16.
 - Sayre R.M., Agin P.P., Levee G.J., Marlowe E., Comparison of in vivo and in vitro testing of sunscreens formulas, *Photochem. Photobiol.* (1979); 29: 559-566.
 - Schurer N., Kohne A., Schliep V., Barlag K., Goerz G., Lipid composition and synthesis of HaCaT cells, an immortalized human keratinocyte line, in comparison with normal human adult keratinocytes. *Exp. Dermatol.* (1993); 2: 179–185.
 - Shalaby E. A. and Shanab S. M. M., Antioxidant compounds, assays of determination and mode of action, *Afr. J. Pharm. Pharmacol.* (2013); Vol. 7(10): pp. 528-539.
 - Shankar G. M. and Walsh D. M., Alzheimer's disease: synaptic dysfunction and A β , *Mol Neurodegener.* (2009); 4: 48.

- Singleton V. L. and Rossi J. A., Colorimetry of Total Phenolics with Phosphomolybdic-Phosphotungstic Acid Reagents, *Am J Enol Vitic.* January (1965); 16: 144-158.
- Slominski A., Zmijewski M., and Pawelek J., L-tyrosine and L-DOPA as hormone-like regulators of melanocytes functions, *Pigment Cell Melanoma Res.* (2012); 25(1): 14–27.
- Tan Y., Chang S. K. C. and Zhang Y., Comparison of α -amylase, α -glucosidase and lipase inhibitory activity of the phenolic substances in two black legumes of different genera, *Food Chem.* (2017); 214: 259-268.
- Thi Be Tu P. and Tawata S., Anti-Oxidant, Anti-Aging, and Anti Melanogenic Properties of the Essential Oils from Two Varieties of *Alpinia zerumbet*, *Molecules* (2015); 20: 16723-16740.
- Thouri A., Chahdoura H., El Arem A., Hichri A. O., Hassin R. B. and Achour L., Effect of solvents extraction on phytochemical components and biological activities of Tunisian date seeds (var. Korkobbi and Arehti), *BMC Complement Altern Med.* (2017); 17: 248.
- Verchere C. B., D'Alessio D. A., Palmiter R. D., Weir G. C., Bonner-Weir S., Baskin D. G. and Kahn S. E., Islet amyloid formation associated with hyperglycemia in transgenic mice with pancreatic beta cell expression of human islet amyloid polypeptide, *Proc. Natl. Acad. Sci. USA* (1996); 93(8): 3492-6.

- Westermark P., Andersson A. and Westermark G. T., Islet Amyloid Polypeptide, Islet Amyloid, and Diabetes Mellitus, *Physiol. Rev.* (2011); 91(3): 795-826.
- Wittenauer J., Mäckle S., Sußmann D., Schweiggert-Weisz U. and Carle R., Inhibitory effects of polyphenols from grape pomace extract on collagenase and elastase activity, *Fitoterapia* (2015); 101: 179-87
- Wood J. E., Senthilmohan S. T. and Peskin A. V., Antioxidant activity of procyanidin-containing plant extracts at different pHs, *Food Chem.* (2002); 77: 155–161.
- Xie Y., Yang W., Chen X. and Xiao J., Inhibition of flavonoids on acetylcholine esterase: binding and structure–activity relationship, *Food Funct.* (2014); 5(10): 2582-9.
- Zhishen J., Mengcheng T. and W. Jianming, The determination of flavonoid contents in mulberry and their scavenging effects on superoxide radicals, *Food Chem.* (1999); 64: 555-559.